AN EXPERIMENTAL AND THEORETICAL STUDY OF THE ENERGY ABSORPTION FROM HIGH VOLTAGE RADIATION BY MEANS OF IONIZATION MEASUREMENTS WITH AN EXTRAPOLATION TYPE CHAMBER

A Thesis submitted to the university of London
for the Degree of Ph.D. in physics

by

ALY ABDEL KERIM IBRAHIM.

A B S T R A C T

This experimental and theoretical study aims at further investigation, by means of an extrapolation type of ionization chamber, of the ionization measurement of energy absorption from high-voltage radiations within a medium. Wavelengths ranging between 0.08 and 0.5 A^{o} were used.

The walls of the ionization chamber were made of simple elements (graphite, aluminium and copper) or pressed bakelite - graphite mixtures which were loaded with cerium oxide in order to control the effective atomic number of the mixtures.

A distinct advantage of the experimental arrangement used is the possibility of measuring the ionization per unit spacing when the air space is vanishingly small which thus eliminates the variable effects of chamber size. The results of earlier workers with chambers of fixed finite dimensions have been difficult to interpret in terms of theoretical considerations because of these effects. Furthermore, by varying the thickness of the upper plane electrode of the chamber, correction could be made for absorption of radiation in this electrode, which, at long wavelengths, maybe considerable in the media of higher atomic number.

The results obtained with a chamber of graphite walls show that graphite behaves approximately as air walled material, the ionization per unit volume is constant i.e. the ionization I_o being proportional to V where V is the air volume. With walls of atomic number greater than that of air the ionization per unit spacing increases slightly as the spacing decreases up to a certain threshold spacing blow which it increases very rapidly. The ionization per unit spacing and the threshold spacing both depends upon the material of the electrodes and the wavelength of the radiation.

The ionization per unit spacing at zero dimensions may be measured in two ways. Firstly, by drawing at the origin a tangent to the ionization - spacing curve and secondly by extrapolation to zero dimensions of the ionization per unit spacing - spacing curve.

It was thus possible to compare these experimental observations with expectations based upon the Bragg - Gray theory of ionization within a cavity.

This comparison suggests that the Bragg - Gray theory may be ragarded as a satisfactory description of the facts for the range of wavelengths studied, at least for elements of atomic number up to that of

aluminium (Z = 13). For copper (Z = 29) and the mixtures (depending upon the electron emission from Ce of Z = 58) the experimental results disagree with the theory except for the shortest wavelengths, and the disagreement increases with increase of wavelength.

Suggestions are advanced and a modification made to Gray's equation in an attempt to correct for this disagreement. These are based upon a consideration of the sources and the energy of the photoelectrons emitted from the wall materials.

AN EXPERIMENTAL AND THEORETICAL STUDY OF THE ENERGY ABSORPTION FROM HIGH VOLTAGE RADIATION BY MEANS OF IONIZATION MEASUREMENTS WITH AN EXTRAPOLATION TYPE CHAMBER

A Thesis submitted to the university of London

for the Degree of Ph.D. in physics

by

ALY ABDEL KERIM IBRAHIM.

CONTENTS

IV. DISCUSSION AND CONCLUSIONS

(a) The Ionization - Volume Curves.

(b) The Ionization per Unit Spacing as the volume tends to zero $\frac{I}{d}\ d = o$

(i) First Method.

(ii) Second Method.

(c) The Absorption Factor (f)

(d) The Ratio of Ionization between chambers of high atomic Number and Air walled material.

(e) Comparison between Theoretical and Practical values.

(f) Electron Range and Ionization - Electrode spacing curve.

(i) Relative numbers of Recoil and Photoelectrons.

(ii) The absolute value of the range.

(iii) The mean Range of the electrons in air.

(g) A Modification to Grays theory.

I. INTRODUCTION

The ionization produced in an air filled cavity by high voltage radiation within a medium has been a subject of considerable theoretical and experimental investigation for the last thirty years or so. Provided that certain conditions are fulfilled it now seems possible, as shown by the Bragg (1) - Gray (2) theory, to express the ionization within such a cavity in terms of the real absorption coefficients of the medium and its stopping power for electrons. Conversely, if these conditions may be fulfilled satisfactorily, a measurement of the ionization within the cavity may be used to infer the real energy absorption of high voltage radiation within the medium.

The experiments of previous workers, who have made measurements of the ionization produced by high voltage radiation in ionization chambers having walls of various atomic numbers, indicate that although the conditions required by the theory are satisfactorily fulfilled for small ionization chambers of light atom media when very high energy radiation is used (e.g. radium γ rays) the

measurements do not give the results predicted by the theory when the chamber walls are of higher atomic numbers or the radiations used are of longer wavelengths. The dimensions of the chamber also affect the discrepancy between the two.

Mayneord [3] used thin walled chambers of different materials and found that there was a disagreement between the experimental values and those calculated, the former being less than the latter. Clarkson and Mayneord [4] made ionization chambers of carbon (Acheson graphite) electroplated on the inside with a copper layer of thickness 8μ. They found the ionization currents to be appreciably less than the theoretical values. They inferred that the difference was due to the thickness of the copper layer being insufficient to give full equilibrium electronic emission over the short wave region. In order to study the quality of the radiations used in radium γ-ray therapy (5 - 20 X.U.) Wilson [5] prepared chambers of carbon, magnesium with walls 4 mm. thick and of copper with walls one mm. thick. He found a considerable deviation from Mayneord's[3] experimental values. He attributed the discrepancy partly to the fact that the chambers could not be regarded as being sufficiently thin. Clarkson [6], in

his endeavour to use the ionization current produced in a gas contained in a small ionization chamber as an indication of the rate of absorption of energy for X - radiation of wavelength 0.208 Å., used chambers of carbon, magnesium, elektron metal, aluminium, iron, copper, zinc and lead. He came to the conclusion that the experimental values for the ionization currents are less than those obtained from the theoretical considerations of Gray [2], except for substances of low atomic number (less than 12). He suggested that the deviation in the case of media of high atomic number is due to the fact that the binding energy of the electron removed rises relatively to that of the quantum, (see later pp.137-139)

All the previous investigations were made with chambers constructed from materials consisting of simple elements. Recently, conducting, "thermo-setting" resins have been used for the large scale production of ionization chambers for the following reasons.

1) It is possible to press small condenser ionization chambers identical in construction, but different in effective atomic number, which are likely to be used for the simultaneous measurements of "depth quality" and "depth dose". [7]

2) It is also possible to mould very small chambers which are suitable for the study of the quality of the scattered radiation generated in a medium by x - rays [8]. For these reasons Aly and Wilson [7] investigated the behaviour of such pressed ionization chambers and their results showed that: -

1) Chambers moulded from bakelite mixtures are satisfactory electrical conductors and behave consistently in their interaction with the radiation used (0.5 - 0.013 A^{o}.)

2) The ratios of ionization calculated according to Gray's theory agree with the experimental ones up to a wavelength of 0.08 A^{o}. and beyond that the degree of difference increases with increase of wavelength very rapidly. They suggested that such differences between the theoretical and experimental findings are due partly to an incomplete contribution to the ionization by the photoelectrons from the chambers of atomic number greater than air. This contribution being incomplete because of the rather large (approx. 1.5 cm.) dimensions of the chambers relative to the range of the photoelectrons.

Spiers [9] has since suggested that although the mixtures used by Aly and Wilson have approximately the absorption coefficients calculable from their theoretical effective atomic numbers, they will not give rise to the electron emission to be expected on account of the fact that cerium oxide is used for loading the mixtures. Because of the high energy required to remove the K electron from cerium (about 40 ekV.) the photoelectrons will have reduced energies. This will cause a reduced photoelectric contribution to the ionization in the chamber.

Considering these observations it seemed that in order to investigate the subject further it is necessary (a) to study the ionization in chambers with walls composed of simple elements of various atomic numbers in addition to the mixtures previously used by Aly and Wilson and at the same time (b) to use a method which uses very small ionization chambers or better still, has the possibility of eliminating the effect of chamber dimensions altogether.

It seemed that the use of an extrapolation type of chamber (Failla [10], Quimby [11,12]) offered promise of

achieving the elimination of the effect of chamber dimensions and wall absorption. For this reason a chamber of this type was developed in a form which appeared most practicable for the experiments that were considered necessary.

This thesis describes the experiments made with this type of chamber, using electrodes of various elements and of the same pressed mixtures used by Aly and Wilson [7], and attempts to explain the observations and correlate them with previous experimental and theoretical work. It thus differs in an important particular form the work of Failla and Quimby who used only air wall material.

II. THE RATIO OF THE IONIZATION CURRENTS IN CHAMBER PAIRS OF DIFFERENT MATERIALS ACCORDING TO THE THEORY OF BRAGG AND GRAY

a. Introduction

The ionization produced by x-rays in an air filled cavity was first studied by Bragg [1] who found that the total length of the tracks of the β-particles in matter depends on the nature of the substance i.e. upon its atomic number and not its density. In otherwords he defined the range of the β-particles in terms of the amount of matter traversed and not the distance travelled. Therefore, if an air cavity is introduced in the medium it will make no difference to the β-ray density within it unless the atomic number of the medium differs very much from that of air or the pressure of the air is too great so that a large fraction of the β-ray energy is used up in passing through the cavity. To avoid this either the cavity should be small compared to the range of the electron in air or the pressure reduced.

b. The Theory

Gray [2] found that a very simple relation could be derived by theoretical reasoning from certain

experimental facts concerning the loss of energy by swiftly moving electrons. Essentially the same relation had been enunicated in slightly different terms as early as 1912 by Sir William Bragg [1].

It had been shown previously by Gray [2] that the energy equivalent of the ionization per unit volume in the cavity is $\frac{1}{\rho}$ times the γ-ray energy absorbed per unit volume of the solid. The derivation of this relation is somewhat lengthy, because it is necessary to establish that the introduction of a small air cavity into a solid medium does not disturb the distribution as regards direction and velocity, of the β-particles crossing the surface which has become a wall of the cavity (ρ is the ratio of the energy lost by an electron in traversing a certain distance, a small fraction of its range in the two media air and solid)

Attempts [13] have been made to estimate separately the contributions to ionization in an enclosed volume, from the gas, from the corpuscular radiations emerging from the several walls, from the effect of the reflection of these particles from the opposite faces of the volume and so on. In the case of air, the proportion of the

whole energy lost or absorbed which is presented by ionization, has been the subject of nearly a score of separate experimental investigations as well as a very thorough theoretical treatment. From a detailed consideration of the evidence there emerge the following conclusions (Gray).

(1) That the average energy W lost by a β-particle for each ion pair formed, is certainly not far from 5.2×10^{-11} ergs (32.5 e volts)[14]. This value might well be in error by 2 per cent in the light of evidence to be presented later, a slightly higher value is to be preferred.

$$W = 5.3 \times 10^{-11} \text{ ergs.}$$

$$= 33 \text{ e - volt}$$ has been provisionally adopted.

(2) That W is the same for all β-particles having energies between a thousand and a million volts.[15]

The first conclusion enables one to infer the energy in ergs lost by secondary electrons in passing through any volume of air from a measurement of the total ionization produced in air.

The second implies that the conversion factor from ionization to energy is the same over a very wide range of energy of the secondary electrons and hence of all qualities of radiation from the softest x-rays to the hardest γ-rays.

The conclusion is thus arrived at, that, for an infinitely small air volume, the total energy, E, of secondary electrons generated in unit volume of the medium is given by.

$$E = \rho . W . J .$$

or,

$$J = \frac{E}{\rho W} \qquad \ldots\ldots \quad (1)$$

where J is the number of ion - pairs produced per c.c. i.e. the ionization per unit volume.

Since the rate at which the charged particles (electrons) lose energy is due to their encountering the electrons of the medium through which they pass, ρ is proportional to the electron density and is as follows:

$$\rho = \frac{n_1}{n_a} \cdot \frac{S_1}{S} \qquad \ldots\ldots \quad (2)$$

where n_1 and n_a are the electron densities of the medium and the air respectively and S_1 and S are the electronic stopping power in the medium and the air respectively.

Substituting the value of ρ in (1) we find

$$J = \frac{E}{\frac{n_1 S_1}{n_a S} \cdot W} \qquad \ldots\ldots (3)$$

But,

$$E = n_1 (e\sigma a + e\tau 1) I \qquad \ldots\ldots (4)$$

where I is the intensity of radiation falling on the material and is considered constant throughout the volume, $e\sigma a$ and $e\tau_1$ are the absorption scattering and photoelectric absorption coefficients per electron respectively.

from (3) and (4) we have

$$J_1 = \frac{n_1 (e\sigma a + e\tau 1) I}{\frac{n_1 S_1}{n_a S} \cdot W}$$

$$= (e\sigma a + e\tau 1) \frac{S}{S_1} \cdot n_a \cdot \frac{I}{W} \qquad \ldots\ldots (5)$$

Equation (5) represents the ionization per unit volume in a chamber specified by the different coefficients on the right-hand side.

In actual practice this relation cannot be expected to hold exactly because,

(1) The contribution to the ionization from x-ray energy absorbed in the gas is not exactly equivalent to the energy that would be absorbed in the corresponding

volume of solid.

(2) The scattering of the electrons in crossing the air cavity will not be the same as in crossing the solid if these are composed of elements of different atomic number.

Clearly, the disturbing influence of these two factors will be greatest when the gas and solid are composed of elements of widely different atomic number and will be least (approximately zero) when they have the same atomic number.

Equation (5) requires experimentally that:-

(1) The ionization per unit volume should be independent of the size of the chamber.

(2) The ionization in a given chamber should be proportional to gas [16] pressure as the pressure is reduced below the normal value.

(3) The ionization in different chambers should be proportional to the energy absorbed per unit volume of the wall material and inversely as its stopping power.

Similarly for an ionization chamber of another material, the ionization J_2 per unit volume is given by:

$$J_2 = (e^{\sigma a} + e^{\tau 2}) \frac{S}{S_2} \cdot n_a \cdot \frac{I}{W} \qquad \ldots\ldots \quad (6)$$

The ratio "R" of the ionization currents in the two chambers will be,

$$R = \frac{J_2}{J_1}$$

$$= \frac{e^{\sigma a} + e^{\tau 2}}{e^{\sigma a} + e^{\tau 1}} \cdot \frac{S_1}{S_2} \qquad \ldots\ldots \quad (7)$$

This equation will be true only when no reduction of intensity due to absorption in the walls of the chambers takes place.

To allow for the absorption in the walls equation (7) becomes:

$$R' = \frac{e^{\sigma a} + e^{\tau 2}}{e^{\sigma a} + e^{\tau 1}} \cdot \frac{S_1}{S_2} \cdot \frac{e^{-\mu_2' x}}{e^{-\mu_1' x}} \qquad \ldots\ldots \quad (8)$$

If absorption to be allowed for is true absorption only or,

$$R'' = \frac{e^{\sigma a} + e^{\tau 2}}{e^{\sigma a} + e^{\tau 1}} \cdot \frac{S_1}{S_2} \cdot \frac{e^{-\mu_2 x}}{e^{-\mu_1 x}} \qquad \ldots\ldots \quad (9)$$

If absorption to be allowed for is total absorption where x cm. is the thickness of the plane upper electrode (which is perpendicular to the beam direction) of the extrapolation chamber.

$$\mu_2' = (e^{\sigma_a} + e^{\tau_2})\, n_2$$

and,

$$\mu_1' = (e^{\sigma_a} + e^{\tau_1})\, n_1$$

also,

$$\mu_2 = (e^{\sigma_s} + e^{\sigma_a} + e^{\tau_2})\, n_2$$

and,

$$\mu_1 = (e^{\sigma_s} + e^{\sigma_a} + e^{\tau_1})\, n_1$$

Thus,

$$R' = R \cdot r = \frac{J_2}{J_1}$$

where,

$$r = \frac{e^{-\mu_2' x}}{e^{-\mu_1' x}}$$

and,

$$R'' = Rr'$$

where,

$$r' = \frac{e^{-\mu_2 x}}{e^{-\mu_1 x}}$$

Having established these expressions, we proceed to evaluate the theoretical ratio R of the ionization currents. Then evaluating r we determine R' taking into account the absorption in the walls of the plane upper electrode.

It might be desirable to add $\frac{1}{2}\, e^{\sigma_s}$ in the true absorption coefficient instead of e^{σ_s} since this type of scattered radiation would be scattered either at the upper surface of the upper electrode or at its lower surface - Therefore,

$$\mu_2 = (\mu_2' + \tfrac{1}{2} e\sigma_s)$$

and,

$$\mu_1 = (\mu_1' + \tfrac{1}{2} e\sigma_s)$$

For evaluating the ratio R and R" the different coefficients appearing in (7) and (8) were determined as follows.

(c) Theoretical Determination of the effective Atomic Number of the different mixtures used for chambers.

We require to determine the atomic number of the different mixtures used for the construction of the chambers. A statement of "effective atomic number $\bar{Z}$" of pressed materials replaces the atomic number Z which is used for simple elements.

This determination should be based on a consideration of the x-ray absorption coefficient since Z is one of the fundamental factors governing the absorption in a medium. The two components of the absorption coefficient are:

(1) The scattering absorption coefficient "σ"

(2) The photoelectric absorption coefficient "τ"

It is well known that for the range of wavelengths used in this investigation (range from $\lambda_e = 0.5$ A^o to $\lambda_e = 0.08$ A^o) the former is independent of the atomic number.

While the latter depends on it to a large extent. As a result $\bar{Z}$ is usually derived from the relation between τ & $\bar{Z}$

Workers [17, 18] in this field have proposed various formulae for this relation which lead to different values for $\bar{Z}$. The expression we have used for calculating $\bar{Z}$ is based on Walter's formula [18].

viz
$$\tau = 2.64 \; Z^{2.94} \; \lambda^3$$
$$\bar{Z} = \sqrt[2.94]{\sum a_1 \; Z_1^{2.94}}$$

where, a_1 is the fractional content of electrons for an element of atomic number Z, and $\sum$ is made for all the elements pressed in the compound.

d. <u>The electron Density of the Chamber Wall material</u>.

(i) <u>For simple elements</u>

The electron density of the simple elements was determined from the following formula

$$n_Z = NZ \frac{\rho}{m} \quad \text{electron / c.c.}$$

where N is Avogadro's number and equal to 6.06×10^{23}, Z is the atomic number of atomic weight m and ρ is the

density in gm./c.c.

The following table includes the data for calculating the electron density of graphite, aluminium and copper.

Element	Z	m	ρ gm/c.c.	n_z e/c.c. x 10^{23}
Carbon	6	12	2.30	6.969
Aluminium	13	26.97	2.70	7.886
Copper	29	63.57	8.93	24.67

We notice that the electron density varies rapidly with the density of the element.

(ii) For plastic mixtures

The electron density of the chamber wall material was determined from the following formula (19).

$$n_z = N n_M \frac{\rho}{M} \quad e./c.c.$$

where n_M is the number of electrons in the molecules of weight M and density ρ

The following table includes the data for calculating the electron density of the plastic mixtures.

Mixture number.	$\bar{Z}$	M	n_M	ρ gm./c.c. (20)	n_z e./c.c. x 10^{23}
(1)	7.64	46.9	24.87	1.44	4.63
(2)	12.84	46.9	24.84	1.44	4.63
(3)	17.04	47.75	25.13	1.449	4.63
(4)	20.84	49.15	25.74	1.46	4.64

From the previous table we notice that the electron density is independent of the density for the kind of plastic used.

e. Determination of The absorption coefficients for various wall material

If a beam of monochromatic high voltage radiation falls on an absorber it is absorbed according to an exponential law, so that if I_o is the incident intensity of radiation and I is the intensity after passing through a thickness d of material, we may write

$$I = I_o e^{-\mu d} \qquad \ldots\ldots(1)$$

Where μ is a constant for the material and is called the total linear absorption coefficient for the radiation in question. This constant represents the

total absorption that occurs and may be regarded as that fraction of the energy of the beam which is removed per unit volume of the material it traverses.

In the range of wavelengths with which we are concerned μ is actually made up of two separate physical processes known as photo-electric absorption and scattering absorption. There is a linear absorption coefficient which represents each of these processes, a coefficient written as "τ" for photoelectric absorption and "σ" for scattering absorption.

The scattered radiation is of two distinct kinds which are usually referred to as truly scattered radiation and absorption scattered radiation. It is customary to represent the magnitudes of the truly scattered radiation and the absorption scattered radiation by the linear coefficients "σ_s" and "σ_a" respectively i.e.

$$\sigma = \sigma_s + \sigma_a$$

and,

$$\mu = \tau + \sigma_s + \sigma_a$$

(i) The evaluation of $e^{\sigma}s$ and $e^{\sigma}a$

"$e^{\sigma}a$" the scattering absorption coefficient per electron and "$e^{\sigma}s$" the truly scattered coefficient per electron are both independent of the composition of the scatterer but dependent on the range of the wavelengths used in this investigation [21, 22, 23]

The most suitable expressions for calculating "$e^{\sigma}s$" and "$e^{\sigma}a$" are those given by the well-known formulae of Klein and Nishina [24] They are based on the relativistic theory of the electron, namely:

$$e^{\sigma}s = \frac{2\pi e^4}{m^2 c^4} \frac{1+Q}{Q^2} \left\{ \left[\frac{2(1+Q)}{1+2Q} - \frac{1}{Q} \log(1+2Q) \right] + \frac{1}{2Q} \log_e (1+2Q) - \frac{1+3Q}{(1+2Q)^2} \right\}$$

and,

$$e^{\sigma}a = \frac{2\pi e^4}{m^2 c^4} \left\{ \frac{2(1+Q)^2}{Q^2 (1+2Q)} - \frac{1+3Q}{(1+2Q)^2} + \frac{(1+Q)(1+2Q-2Q^2)}{Q^2 (1+2Q)} \right\} - \frac{4Q^2}{3(1+2Q)^2} - \left[\frac{1+Q}{Q^3} - \frac{1}{2Q} + \frac{1}{2Q^3} \right] \log(1+2Q) \Bigg\}$$

where

$Q = \frac{h}{mc^2}$

$m = 9.1066 \times 10^{-28}$ gm.

$c = 2.9977 \times 10^{10}$ cm/sec.

h is Planck's constant $= 6.624 \times 10^{-27}$ ergs. sec.

e is the charge of the electron $= 4.80\ 25 \times 10^{-10}$ e.s.u.

The following values of "$e^{\sigma}s$" and "$e^{\sigma}a$" at different λ's are computed from the previous formulae.

TABLE (1)

The values of $e^{\sigma}s$, $e^{\sigma}a$ and $\bar{e}^{\sigma}$ at different λs in this table are used throughout the present investigation.

λ in. x.u.	$e^{\sigma} \times 10^{25}$	$e^{\sigma}a \times 10^{25}$	$e^{\sigma}s \times 10^{25}$	λ in. x.u.	$\bar{e}^{\sigma} \times 10^{25}$	$e^{\sigma}a \times 10^{25}$	$e^{\sigma}s \times 10^{25}$
10	1.9	0.89	1.01	190	5.37	0.5538	4.832
20	2.64	0.98	1.66	200	5.42	0.520	4.900
30	3.12	0.982	2.138	210	5.46	0.505	4.955
40	3.5	0.955	2.545	220	5.51	0.490	5.02
50	3.78	0.925	2.855	230	5.55	0.475	5.075
60	4.02	0.885	3.135	240	5.59	0.465	5.125
70	4.22	0.85	3.37	250	5.63	0.450	5.18
80	4.4	0.815	3.585	260	5.66	0.440	5.22
90	4.54	0.785	3.755	270	5.68	0.428	5.252
100	4.67	0.75	3.920	300	5.76	0.395	5.365
110	4.78	0.72	4.060	320	5.81	0.380	5.43
120	4.89	0.69	4.20	340	5.86	0.365	5.495
130	4.98	0.66	4.32	360	5.90	0.340	5.56
140	5.07	0.638	4.432	380	5.93	0.330	5.6
150	5.14	0.615	4.525	400	5.96	0.3187	5.641
160	5.2	0.595	4.605	420	5.99	0.306	5.684
170	5.26	0.575	4.685	440	6.00	0.296	5.704
180	5.3	0.555	4.745	500	6.08	0.267	5.813

(ii) Evaluation of the photoelectric absorption coefficient per electron

The photoelectric absorption coefficient is dependent both upon the composition of the absorber and the wavelength of the incident radiation. It is referred to as true absorption since the whole energy of the quantum is absorbed within the atom with the ejection of a photo-electron.

For elements, τ, was obtained from experimental values of the total absorption coefficient μ which = $\tau + \sigma$. Thus by subtracting from these experimental values the theoretical "Klein - Nishina" values of σ, τ are obtained.

For wavelengths exceeding 0.2 A^{o}, the scattering experimentally observed exceeds the Klein - Nishina scattering, owing to the coherent scattering. However, for wavelengths long enough for the difference to be significant, the scattering coefficient is so much less than the photoelectric coefficient that little error is made in the estimation of the latter by the use of the Klein - Nishina formula.

For calculating τ, [25, 26, 27, 28, 18] when measured values of μ are not available several formulae

have been derived based on experimental data but none of them cover a relatively wide range of wavelengths or atomic numbers really well.

The most satisfactory expression seems to be that given recently by Victoreen [29] namely:

$$\frac{\tau}{\rho} = \alpha Z^2 \left(\frac{2Z}{A}\right) \lambda^3 - \beta Z^5 \left(\frac{2Z}{A}\right) \lambda^4$$

This formula holds for all atomic numbers when suitable values for the constants α and β are chosen, provided the wavelength of the radiation used is less than the K absorption line.

$\left(\frac{2Z}{A}\right)$ corrects for the presence of the isotopes and A is the atomic weight.

$$\alpha_k = a\ Z^2 + bZ - c$$

$$\beta_k = d\ Z^2 - eZ + f$$

The values of α and β change at each critical wavelength. The constants, a, b, c, d, e, and f change also at each critical wavelength and on each side of $Z = 5$.

The values of the constants used in calculating the photoelectric absorption coefficient are those corresponding to $Z>5$, since we are interested only in materials of atomic number greater than 5.

$$a = 0.00004$$

$$b = 0.00728$$

$$c = 0.0114$$

$$d = 0.00038$$

$$e = 0.00152$$

$$f = 2.350$$

The values of τ_e are then obtained from the following formula,

$$\tau_e = \frac{\tau}{n_z} = \frac{\tau}{6.06 \times 10^{23}\, n_M \frac{\rho}{M}}$$

$$= \frac{\tau}{\rho} \cdot \frac{M}{6.06 \times 10^{23}\, n_M}$$

For wavelengths greater than the K absorption limit the values of e^{τ_L} are then obtained from the following formula (30)

$$e^{\tau_L} = e^{\tau} \cdot \frac{1}{r_k}$$

where r_K is the absorption jump ratio.

TABLE (2)

The linear absorption coefficient for Carbon

$$\mu' = (e\sigma_a + \tau_e) n_z$$

$$\mu = (e\sigma_a + \tau_e + \tfrac{1}{2} e\sigma_s) n_z$$

$$\rho = 2.30 \text{ gm/c.c.} \quad n_z = 6.969 \times 10^{23} \text{ e./c.c.}$$

λ in A^o	$\frac{\tau_e + e\sigma_a}{\rho}$	$\tau_e + e\sigma_a \times 10^{25}$	μ'	μ
0.01	0.0268	0.6163	0.04295	0.0781
0.02	0.0295	0.6785	0.04729	0.1051
0.03	0.0296	0.6808	0.04744	0.1219
0.04	0.0288	0.6624	0.04617	0.1349
0.05	0.0279	0.6417	0.04473	0.1442
0.06	0.0269	0.6187	0.04312	0.1523
0.08	0.0249	0.5727	0.03991	0.1648
0.10	0.0235	0.5405	0.03767	0.1743
0.12	0.0224	0.5152	0.03591	0.1822
0.15	0.0216	0.4968	0.03462	0.1923
0.20	0.0230	0.5290	0.03687	0.2076
0.25	0.0281	0.6463	0.04504	0.2255
0.30	0.0372	0.8556	0.05964	0.2466
0.35	0.0508	1.1684	0.08139	0.2737
0.40	0.0702	1.6146	0.1126	0.3091
0.45	0.0955	2.1965	0.1531	0.3528
0.50	0.1280	2.944	0.2051	0.4077

TABLE (3)

The linear absorption coefficient for Aluminium

$$\mu' = (e\sigma_a + \tau_e) \cdot n_z$$

$$\mu = (e\sigma_a + \tau_e + \tfrac{1}{2} e\sigma_s + \tfrac{1}{2} K)\, n_z$$

$$\rho = 2.7 \text{ gm./c.c. } n_z = 7.886 \times 10^{23} \text{ e./c.c.}$$

λ in A°	$\frac{\tau_e + e\sigma_a}{\rho}$	$(\tau_e + e\sigma_a) \times 10^{25}$	μ'	μ
0.01	0.0260	0.702	0.05535	0.1037
0.02	0.0287	0.774	0.06102	0.1345
0.03	0.0288	0.779	0.06142	0.1547
0.04	0.0284	0.768	0.06056	0.1693
0.05	0.0278	0.752	0.05929	0.1817
0.06	0.0275	0.743	0.05859	0.1928
0.08	0.0278	0.750	0.05914	0.2145
0.10	0.0303	0.820	0.06466	0.2363
0.12	0.0359	0.970	0.07649	0.2642
0.15	0.0497	1.340	0.1056	0.3208
0.20	0.0967	2.610	0.2058	0.4594
0.25	0.180	4.860	0.3832	0.6916
0.30	0.307	8.30	0.6545	1.0522
0.35	0.504	13.6	1.073	1.5665
0.40	0.760	20.5	1.616	2.233
0.45	1.115	30.1	2.373	3.1315
0.50	1.55	41.9	3.304	4.237

K is the coherent coefficient

TABLE (4)

The linear absorption coefficient for copper.

$\mu' = ({}_e\sigma_a + \tau_e)\, n_z$

$\mu = ({}_e\sigma_a + \tau_e + \frac{1}{2}\, e\sigma_s) n_z$

$\rho = 8.93$ gm./c.c. $\quad n_z = 24.67 \times 10^{23}$ e./c.c.

λ in A^o.	$({}_e\sigma_a + \tau_e) \times 10^{25}$	μ'	μ
0.01	0.9361	0.2309	0.3555
0.02	1.137	0.2805	0.4853
0.03	1.268	0.3127	0.5764
0.04	1.509	0.3723	0.6862
0.05	1.888	0.4658	0.8179
0.06	2.46	0.6068	0.9934
0.08	4.281	1.0557	1.4979
0.10	7.19	1.773	2.2565
0.12	11.61	2.864	3.382
0.15	21.83	5.384	5.942
0.20	47.4	11.691	12.2955
0.25	88.06	21.723	22.3615
0.30	151.9	37.477	38.1385
0.35	245	60.439	61.12
0.40	357.2	88.108	88.804
0.45	492.9	121.586	122.298
0.50	663.3	163.566	164.283

TABLE (5)

The linear absorption coefficient for the chamber of effective atomic number 7.64

$\mu' = ({}_e\sigma_a + \tau_e)n_z$

$\mu = ({}_e\sigma_a + \tau_e + \frac{1}{2}\, {}_e\sigma_s)n_z$

$\rho = 1.44$ gm./c.c. $n_z = 4.65 \times 10^{23}$ e./c.c.

λ in A^o_u	$\tau_e \times 10^{26}$ vict	$(e^{\tau} + e^{\sigma}a) \times 10^{26}$	μ'	μ
0.04	0.055	9.6250	0.0447	0.1039
0.06	0.185	9.0450	0.0421	0.1150
0.08	0.4365	8.5885	0.0399	0.1233
0.10	0.855	8.343	0.0388	0.1300
0.12	1.47	8.376	0.0389	0.13655
0.15	2.84	8.978	0.0418	0.147
0.20	6.69	11.915	0.0554	0.1694
0.25	11.95	17.45	0.081	0.2014
0.30	22.20	26.15	0.122	0.2468
0.35	34.80	38.292	0.178	0.3063
0.40	51.50	54.687	0.254	0.385
0.45	72.9	75.803	0.353	0.486
0.50	99.0	101.668	0.473	0.608

TABLE (6)

The linear absorption coefficient for chamber of effective atomic number 12.84

$\mu' = (e\sigma_a + \tau_e)\, n_z$

$\mu = (e\sigma_a + \tau_e + \frac{1}{2} e\sigma_s)\, n_z$

$\rho = 1.44$ gm./c.c. $n_z = 4.63 \times 10^{23}$ e./c.c.

λ in A°.	$e^{\tau} \times 10^{26}$ viet	$(e^{\tau} + e^{\sigma_a}) \times 10^{26}$	μ'	μ
0.04	0.272	9.8420	0.04557	0.1045
0.06	0.9175	9.7775	0.04528	0.1179
0.08	2.18	10.3320	0.04783	0.1308
0.10	4.25	11.738	0.05437	0.1451
0.12	7.30	14.206	0.06580	0.1630
0.15	14.31	20.448	0.09469	0.1994
0.20	33.80	39.103	0.1806	0.294
0.25	65.88	71.380	0.3306	0.4505
0.30	113.3	117.25	0.5431	0.6673
0.35	179.5	182.995	0.8474	0.9752
0.40	43.25	46.44	0.215	0.3456
0.45	61.52	64.42	0.2983	0.4311
0.50	83.99	86.66	0.4013	0.5357

TABLE (7)

The linear absorption coefficients for chamber of effective atomic number 17.04.

$\mu' = (\tau_e + e\sigma_a)\, n_z$

$\mu = (\tau_e + e\sigma_a + \frac{1}{2} e\sigma_s)\, n_z$

$\rho = 1.449$ gm/c.c. $\quad n_z = 4.63 \times 10^{23}$ e./c.c.

λ in A.	$\tau_e \times 10^{26}$ vict.	$(\tau_e + e\sigma_a) \times 10^{26}$	μ'	μ
0.04	0.743	10.313	0.04774	0.1067
0.06	2.50	11.360	0.05260	0.1252
0.08	5.90	14.052	0.06504	0.148
0.10	11.48	18.968	0.08784	0.1786
0.12	19.78	26.686	0.1233	0.2206
0.15	38.43	24.568	0.2064	0.3112
0.20	90.40	95.625	0.4428	0.5563
0.25	175.0	180.5	0.8358	0.9557
0.30	299.2	303.15	1.404	1.5282
0.35	471.5	474.992	2.20	2.3278
0.40	113.0	116.19	0.538	0.6686
0.45	159.3	162.20	0.7511	0.8839
0.50	217.2	219.87	1.018	1.153

TABLE (8)

The linear absorption coefficient for chambers of effective atomic number 20.84.

$\mu' = ({}_e\sigma_a + {}_e\tau)\, n_z$

$\mu = ({}_e\sigma_a + {}_e\tau + \frac{1}{2}\, {}_e\sigma_s) n_z$

$\rho = 1.46$ gm./c.c. $\quad n_z = 4.64 \times 10^{23}$ e./c.c.

λ in A.	$\tau_e \times 10^{26}$ vict.	$({}_e\tau + {}_e\sigma_a) \times 10^{26}$	μ'	μ
0.04	1.415	10.985	0.05099	0.11
0.06	4.76	13.620	0.0632	0.1359
0.08	11.32	19.472	0.09035	1.735
0.10	22.15	29.638	0.1375	0.2285
0.12	37.55	44.456	0.2063	0.3037
0.15	73.05	79.188	0.3675	0.4725
0.20	172.2	177.425	0.8231	0.9368
0.25	334.0	339.5	1.575	1.695
0.30	572.0	575.95	2.673	2.798
0.35	900	903.49	4.192	4.320
0.40	216.5	219.69	1.020	1.150
0.45	304.7	307.60	1.428	1.561
0.50	416.0	418.67	1.943	2.077

(f) The stopping power per electron "S"

The stopping power per electron "S" has been investigated by many investigators either theoretically or experimentally and seems to present practical difficulties.

Madgwick [31] measured the stopping power "S" relative to air and came to the conclusion that "S" is independent of the atomic number "Z" from "Z" = 13 to "Z" = 79 (S showed little tendency to decrease as Z increased).

Later Gray [32] concluded that:-

(1) The relative stopping powers of any two media are independent of the speed of the particles.

(2) It is independent of the wavelength of the radiation whatever the nature of the wall material may be to an accuracy of 1 or 2%

(3) There is a change of about 9% from Z = 6 to Z = 13 and another 8% between Z = 13 and Z = 29.

(4) The experimental results are in good agreement with Bethe's theoretical values [33]

The following values of the ratio of the stopping powers for various atomic numbers are calculated from Gray's values of "S".

$$\frac{S(6)}{S(13)} = 1.09 \qquad \frac{S(6)}{S(29)} = 1.19$$

$$\frac{S(6)}{S(7.64)} = 1.026 \qquad \frac{S(6)}{S(12.84)} = 1.08$$

$$\frac{S(6)}{S(17.04)} = 1.112 \qquad \frac{S(6)}{S(20.84)} = 1.128$$

(g) Calculation of the ratio of the ionization current "R"

The theoretical ratio of the ionization currents "R" (see p. 13) were calculated by substituting the values of the ratio of stopping powers together with the values of the quantities "$e\sigma_a$" and "τ_e" (collected in the previous tables (1, 2, 3, 4, 5, 6, 7, 8)) in equation (7) p. (13). These ratios should agree fairly well with experimental values if the theory is a full explanation of the whole facts, provided of course that the experimental conditions are such that they fulfil the essential requirements of the theory.

The following tables, (9, 10, 11, 12, 13, 14) represent the calculated ratio of the ionization currents for the different simple elements and bakelite mixtures used in our investigation.

TABLE (9)

Theoretical ratio of ionization in chamber pair of atomic numbers 13 and 6, (e^{τ} + $e^{\sigma}a$) for Z = 6 and Z = 13 are taken from previous tables

$$R = \frac{e^{\sigma}a + e^{\tau}2}{e^{\sigma}a + e^{\tau}1} \frac{S1}{S_2}$$

λ in A°	R	λ in A°	R
0.01	1.242	0.12	2.052
0.02	1.244	0.15	2.940
0.03	1.248	0.20	5.376
0.04	1.264	0.25	8.196
0.05	1.277	0.30	10.57
0.06	1.309	0.35	12.69
0.08	1.428	0.40	13.84
0.1	1.654	0.45	14.94
		0.50	15.51

TABLE (10)

Theoretical ratio of ionization in chamber pair of atomic numbers 29 and 6, ($^{\tau}e$ + $e^{\sigma}a$) for Z = 6 and Z= 29 are taken from previous tables

$$R = \frac{e^{\sigma}a + e^{\tau}2}{e^{\sigma}a + e^{\tau}1} \frac{S1}{S_2}$$

λ in A°	R	λ in A°	R
0.01	1.809	0.15	52.36
0.02	1.995	0.2	106.6
0.03	2.216	0.25	162.1
0.04	2.710	0.3	211.3
0.05	3.501	0.35	249.7
0.06	4.731	0.40	263.1
0.08	8.894	0.45	266.9
0.1	15.82	0.5	268.1
0.12	26.81		

TABLE (11)

Theoretical ratio of ionization in chamber pair of atomic numbers

7.64 and 6. $(e^{\tau} + e^{\sigma}a)$ for Z= 6

and $\bar{Z} = 7.64$ are taken from previous tables.

$$R = \frac{e^{\sigma}a + e^{\tau}2}{e^{\sigma}a + e^{\tau}1} \frac{S_1}{S_2}$$

λ in A^{o}	R	λ in A^{o}	R
0.04	1.49	0.25	2.77
0.06	1.5	0.30	3.135
0.08	1.539	0.35	3.364
0.10	1.584	0.4	3.474
0.12	1.672	0.45	3.541
0.15	1.855	0.5	3.545
0.20	2.312		

TABLE (12)

Theoretical ratio of ionization in chamber pair of atomic numbers

12.84 and 6. $(e^{\tau} + e^{\sigma}a)$ for Z= 6

and $\bar{Z} = 12.84$ are taken from previous tables.

$$R = \frac{e^{\sigma}a + e^{\tau}2}{e^{\sigma}a + e^{\tau}1} \frac{S_1}{S_2}$$

λ in A^{o}	R	λ in A^{o}	R
0.04	1.604	0.25	11.93
0.06	1.707	0.30	14.78
0.08	1.948	0.35	16.92
0.10	2.346	0.40	3.179
0.12	2.979	0.45	3.166
0.15	4.436	0.50	3.100
0.20	7.982		

TABLE (13)

Theoretical ratio of ionization in chamber pair of atomic numbers

17.04 and 6. ($e^{\tau} + e^{\sigma}a$) for Z = 6

and $\bar{Z}$ = 17.04 are taken from previous tables

$$R = \frac{e^{\sigma}a + e^{\tau}2}{e^{\sigma}a + e^{\tau}1} \frac{S_1}{S_2}$$

λ in A^{o}	R	λ in A^{o}	R
0.04	1.731	0.25	31.06
0.06	2.042	0.30	39.41
0.03	2.728	0.35	45.2
0.10	3.903	0.40	8.00
0.12	5.761	0.45	8.212
0.15	9.977	0.50	8.307
0.20	20.1		

TABLE (14)

Theoretical ratio of ionization in chamber pair of atomic numbers

20.84 and 6. ($e^{\tau} + e^{\sigma}a$) for Z = 6

and $\bar{Z}$ = 20.84 are taken from previous tables.

$$R = \frac{e^{\sigma}a + e^{\tau}2}{e^{\sigma}a + e^{\tau}1} \frac{S_1}{S_2}$$

λ in A^{o}	R	λ in A^{o}	R
0.04	1.871	0.25	59.24
0.06	2.482	0.30	75.91
0.08	3.834	0.35	87.24
0.10	6.184	0.40	15.34
0.12	9.731	0.45	15.81
0.15	17.98	0.50	16.04
0.20	37.82		

III. EXPERIMENTAL DETERMINATION OF THE RATIO "R"

(a) The processing of the pressed electrode

The details of this have already been described by Aly and Wilson [20]. The bakelite synthetic resin was obtained from Messrs "Bakelite Ltd"., the vanadium oxide (V_2O_5) and the cerium oxide (CeO_2) from Messrs Griffin and Tatlock, and the graphite from Messrs Cromile and Piercy. The latter was guaranteed very pure.

Electrodes were made from the mixtures given in the following table which are identical mixtures to those already used by Aly[7]

No.	Composition	$\bar{Z}$ calculated on basis of $\bar{Z} = \sqrt[2.94]{a_1 Z_1^{2.94}}$ (18)
1	100 gm. of bakelite 20 " " graphite 2 " " V_2O_5	7.64
2	100 gm. of bakelite 20 " " graphite 2 " " CeO_2	12.84
3	100 gm. of bakelite 20 " " graphite 5 " " CeO_2	17.04
4	100 gm. of bakelite 20 " " graphite 10 " " CeO_2	20.84

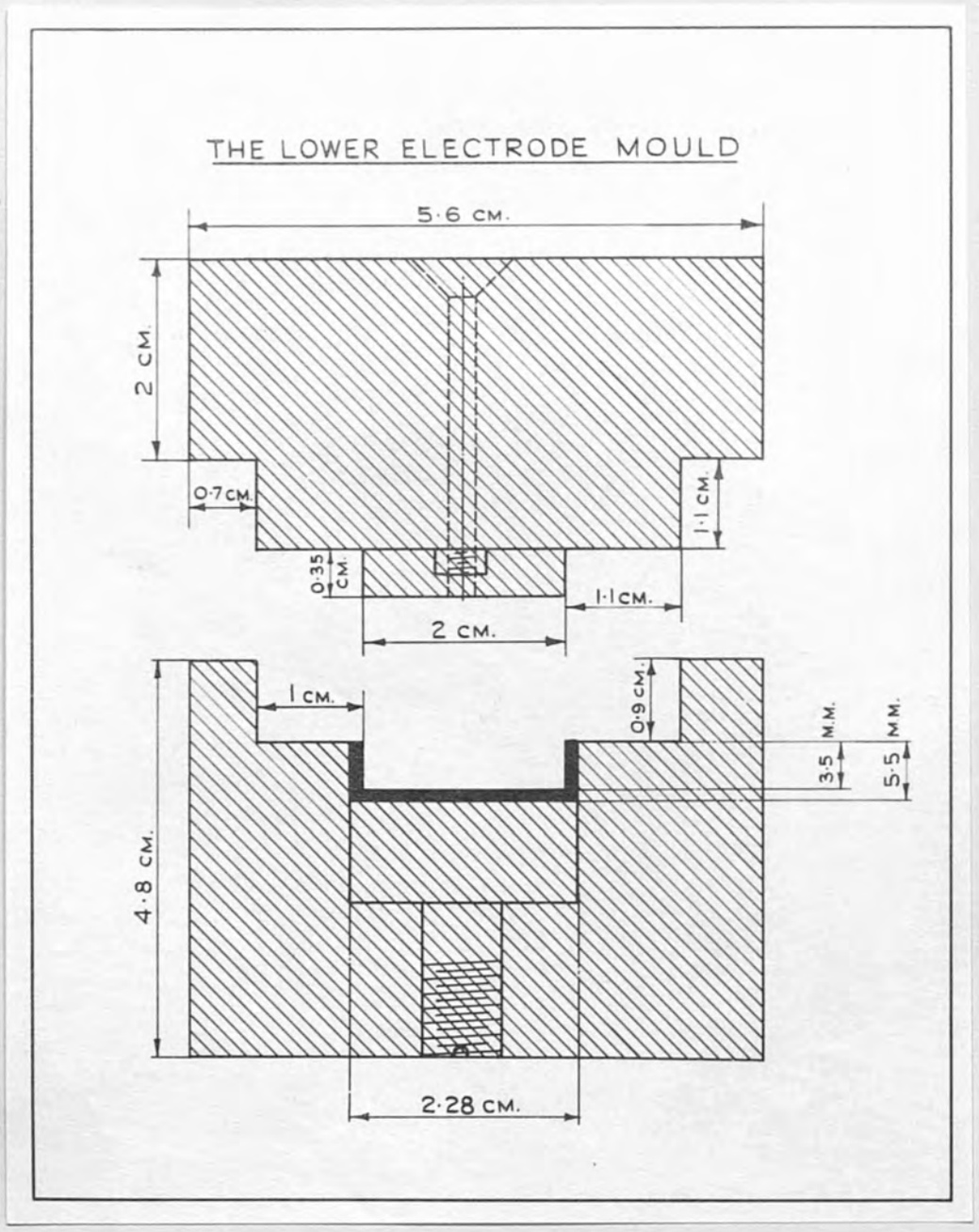
THE LOWER ELECTRODE MOULD
5·6 CM.
2 CM.
0·7 CM.
1·1 CM.
0·35 CM.
1·1 CM.
2 CM.
1 CM.
0·9 CM.
3·5 M.M.
5·5 M.M.
4·8 CM.
2·28 CM.

Figure (1).

THE UPPER ELECTRODE MOULD

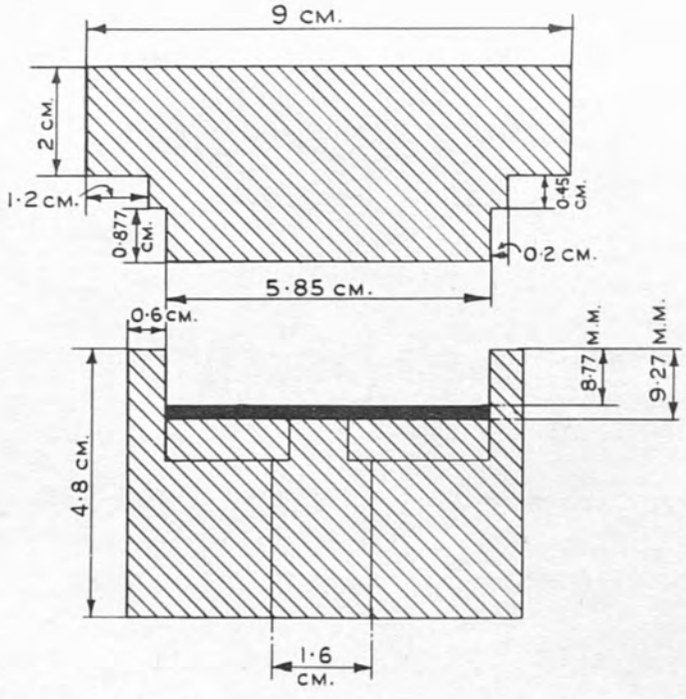

Figure (2).

The bakelite resin was first ground in a ball mill, for about twelve hours. It was then sieved through a mesh 60 to the inch. The fine bakelite powder so obtained was mixed with the graphite and the necessary amount of $V_2 O_5$ and $Ce O_2$. The complete mixture was placed in the ball mill and ground for another twelve hours to ensure good mixing.

The moulds in which the lower (collecting) and upper electrodes were moulded are shown in figs (1 & 2). These were made of high tensile steel. The mould was first warmed on a bunsen flame and lubricated with paraffin wax after which it was filled with a weighed amount of powder. It was then put in a suitable hydraulic press and heated by a gas ring up to about 200°C. Simultaneously the pressure was raised gradually up to about 2500 pounds to the square inch. Under these conditions the synthetic resin polymerises, passes into a state of flux and takes the shape of the mould. After this it was kept in the mould until it became a hard solid material. The time required for the polymerization was about 8 minutes, 3 under heat and pressure, and 5 under pressure alone.

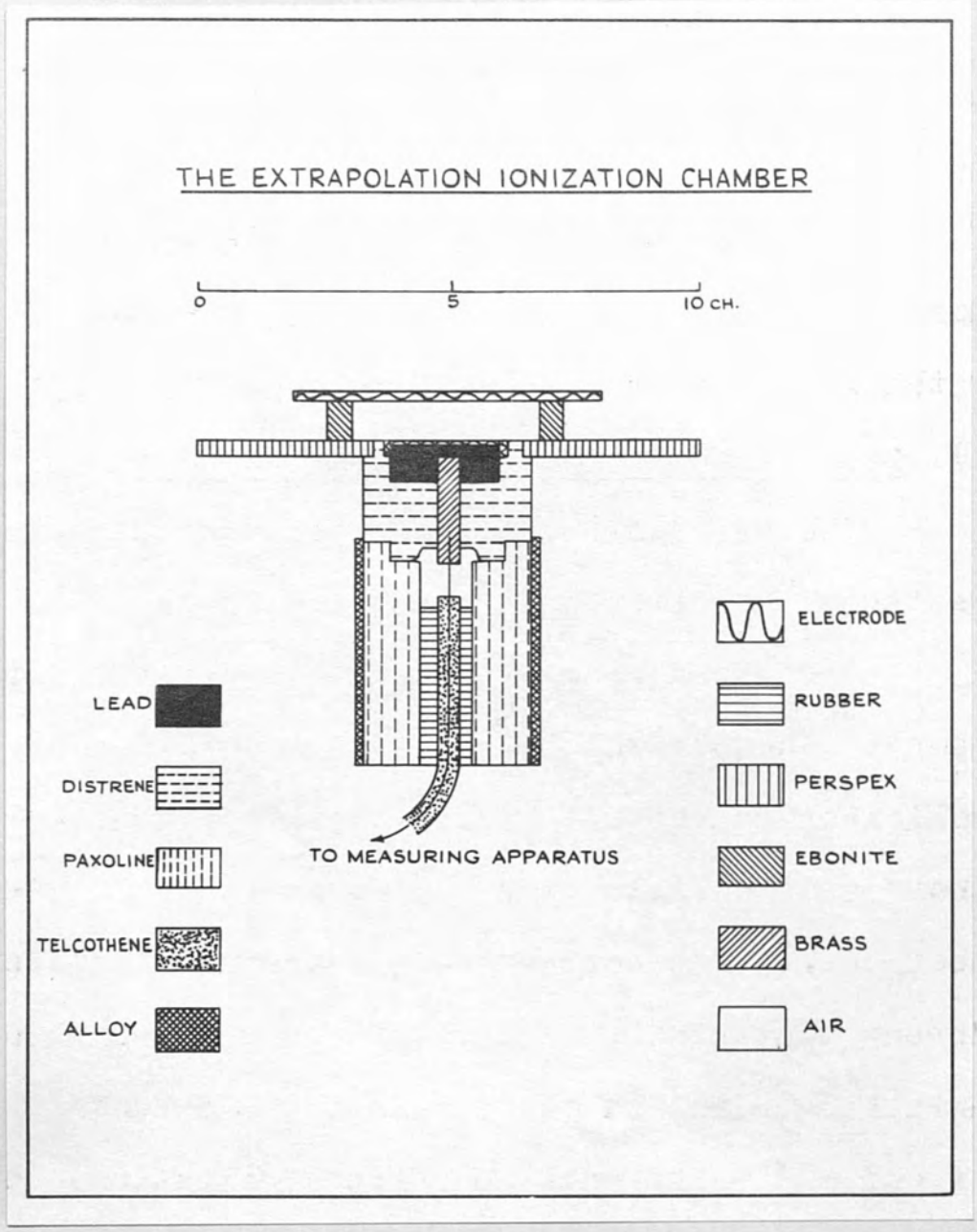
THE EXTRAPOLATION IONIZATION CHAMBER
0
5
10 CH.
TO MEASURING APPARATUS
LEAD
DISTRENE
PAXOLINE
TELCOTHENE
ALLOY
ELECTRODE
RUBBER
PERSPEX
EBONITE
BRASS
AIR

Figure (3).

After processing the electrodes may be removed from the mould. The method of construction enables the electrodes to be made exactly to one pattern.

The thickness of the upper electrode can be increased by increasing the charge of powder and design of the upper portion of the mould. (fig. 2.)

(b) The Extrapolation Ionization Chamber

The extrapolation ionization chamber used for these experiments is shown in figure (3).

The guard ring was a disc of perspex (10 cm. in diameter and thickness 3 mm.) coated with dag, (colloidal graphite). This helps provide a uniform electrostatic field over the entire area of the collecting electrode. The collecting electrode is connected to the current measuring instrument through a very fine telcothene cable itself insulated by paxoline and rubber. The wire does not extend to the surface of the collecting electrode but good electrical contact is effected by soldering it to a screw screwed to a block of lead on which the lower electrode cap is inserted. The space below the lower electrode and between it and the guard ring was filled with a block of distrene to provide good insulation.

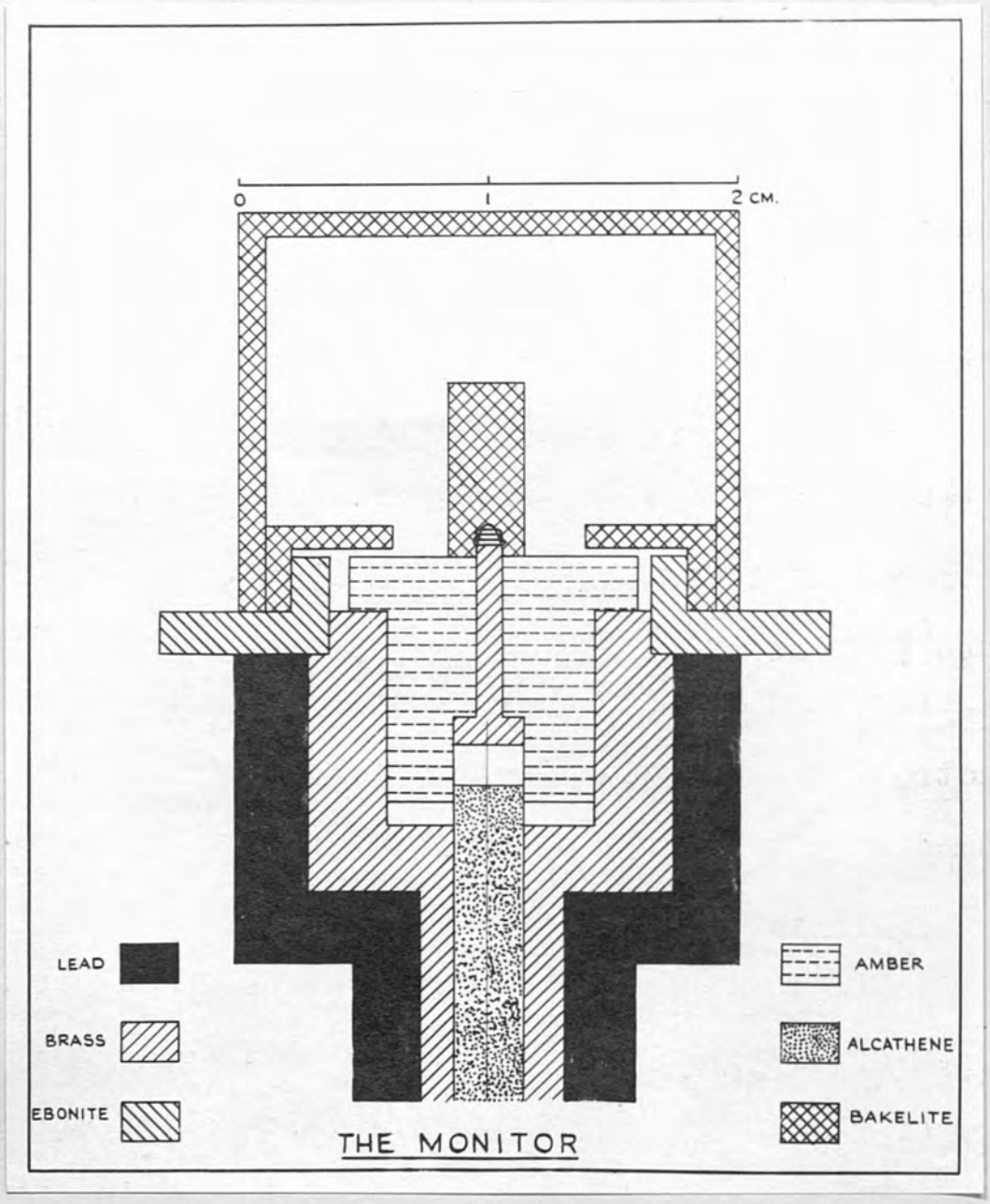
0
1
2 CM.
LEAD
BRASS
EBONITE
AMBER
ALCATHENE
BAKELITE
THE MONITOR

Figure (4).

It was necessary to leave a small air space at the junction of the wire and the screw in order to provide suitable insulating surfaces. In order to reduce ionization losses in this space to negligible proportions a disc of lead 9 mm. thick was mounted directly beneath the lower electrode to prevent radiation reaching the air space.

In order to provide simple and precise adjustment of the spacing between the electrodes, ebonite rings* of different thickness ranging from 0.5 mm. to 10 mm. were used (see fig 3). The inner diameter of each ring is slightly larger than the collecting electrode. The upper electrode was held in place by a lead ring of large diameter to which the polarising voltage was also applied.

The other ionization chamber

The ionization chamber, used as a monitor in the investigation, was moulded from a mixture of bakelite resin, pure graphite and vanadium oxide (Air-walled material).

The essential parts are illustrated in figure (4). The guard ring was provided so that the electrons coming from the amber insulator are prevented from contributing very much to the ionization.

(c) The Leads

The leads are telcothene cables about four metres in length connected at one end to the collecting electrode

* These are not irradiated.

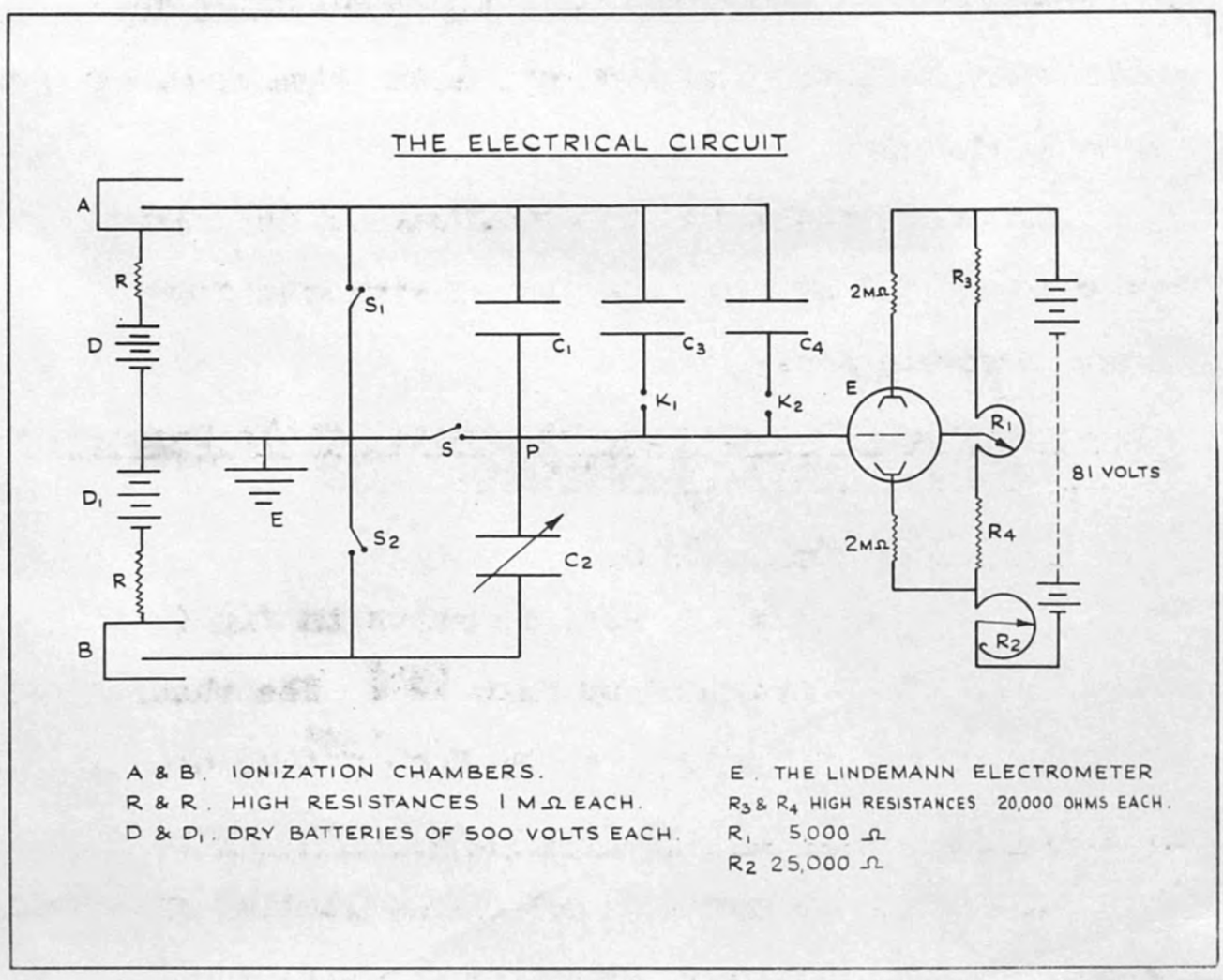
THE ELECTRICAL CIRCUIT
A
R
D
D1
R
B
S1
S2
S
P
E
C1
C3
C4
K1
K2
C2
2MΩ
2MΩ
R3
R4
R1
R2
E
81 VOLTS
A & B. IONIZATION CHAMBERS.
R & R. HIGH RESISTANCES 1 MΩ EACH.
D & D1. DRY BATTERIES OF 500 VOLTS EACH.
E. THE LINDEMANN ELECTROMETER
R3 & R4 HIGH RESISTANCES 20,000 OHMS EACH.
R1 5,000 Ω
R2 25,000 Ω

Figure (5).

The electrodes of copper had wall-thickness 0.00125, 0.0025, 0.00375, 0.005, 0.0075, & 0.01 cm. respectively. In order to ensure the flatness of these surfaces and simplicity of use, they were fixed to graphite discs with glue and kept under blocks of lead for a couple of days.

In our experiments the surfaces of the electrodes were cleaned and not greasy, but no vigorous chemical preparation was done.

(e) Apparatus for measuring the ratio of the ionization currents in pairs of chambers

(i) The electrical circuit

The basic circuit used, is shown in fig (5). It is essentially that described by Kemp (34). The theoretical details, which have been given by Kemp (35) are as follows.

(ii) The theoretical considerations of the apparatus

The two condensers C_1 & C_2 constituting a capacity potential divider (one of whose components, say C_2, is made variable) are connected to the collecting electrodes of the two ionization chambers A & B. The voltages applied to the chambers are such that the collecting electrode in one of them say (A) accumulates a positive

charge whilst the other one (B) accumulates a negative charge. The junction P between the two condensers C_1 & C_2 and the two collecting electrodes may be earthed by the switches S, S_1 and S_2 which may be operated simultaneously.

If V_1 is the potential of the collecting system of A due to the positive charge + Q_1 and V_2 is the potential of the collecting system of B due to the negative charge - Q_2 then,

$$V_1 = \frac{+ Q_I}{C_1 + C'} \qquad \ldots\ (1)$$

and,

$$V_2 = \frac{- Q_2}{C_2 + C''} \qquad \ldots\ (2)$$

where C' and C'' are the capacities to earth of the collecting systems of A and B respectively.

Thus,

$$\left|\frac{V_2}{V_1}\right| = \frac{Q_2}{Q_1} \cdot \frac{C_1 + C'}{C_2 + C''} \qquad \ldots\ (3)$$

Now, if the point P between C_1 & C_2 is earthed V_1 and V_2 are the potential differences across C_1 and C_2. Hence,

$$\frac{V_2}{V_1} = \frac{C_1}{C_2} \qquad \ldots\ (4)$$

Thus, from (3) and (4) we have:

$$\frac{Q_2}{Q_1} = \frac{C_1}{C_2} \quad \frac{C_2 + C''}{C_1 + C'} \qquad \ldots\ (5)$$

C' and C'' are almost entirely composed of the capacities of the cables connecting the collecting electrodes of each chamber to the instrument. They can be made practically equal and much greater than C_1 or C_2 for all possible values of C_1 and C_2. If, however any slight difference between the values of C' and C'' exists it can be included in the calibration of the instrument and therefore will not affect the observations.

Hence,

$$R = \frac{Q_2}{Q_1} \simeq \frac{C_1}{C_2} \qquad \ldots\ (6)$$

where, "R" is the ratio of the ionization currents in the two chambers.

Therefore, the setting of the capacity potential divider which keeps P at zero potential after opening the switches S, S_1 and S_2, is a measure of the ratio of the ionization currents in the two chambers.

(iii) Practical construction of the apparatus

The form of instrument which we have used is somewhat different from that originally described by Kemp (34, 35). It is considered that the modifications we have made have certain desirable advantages.

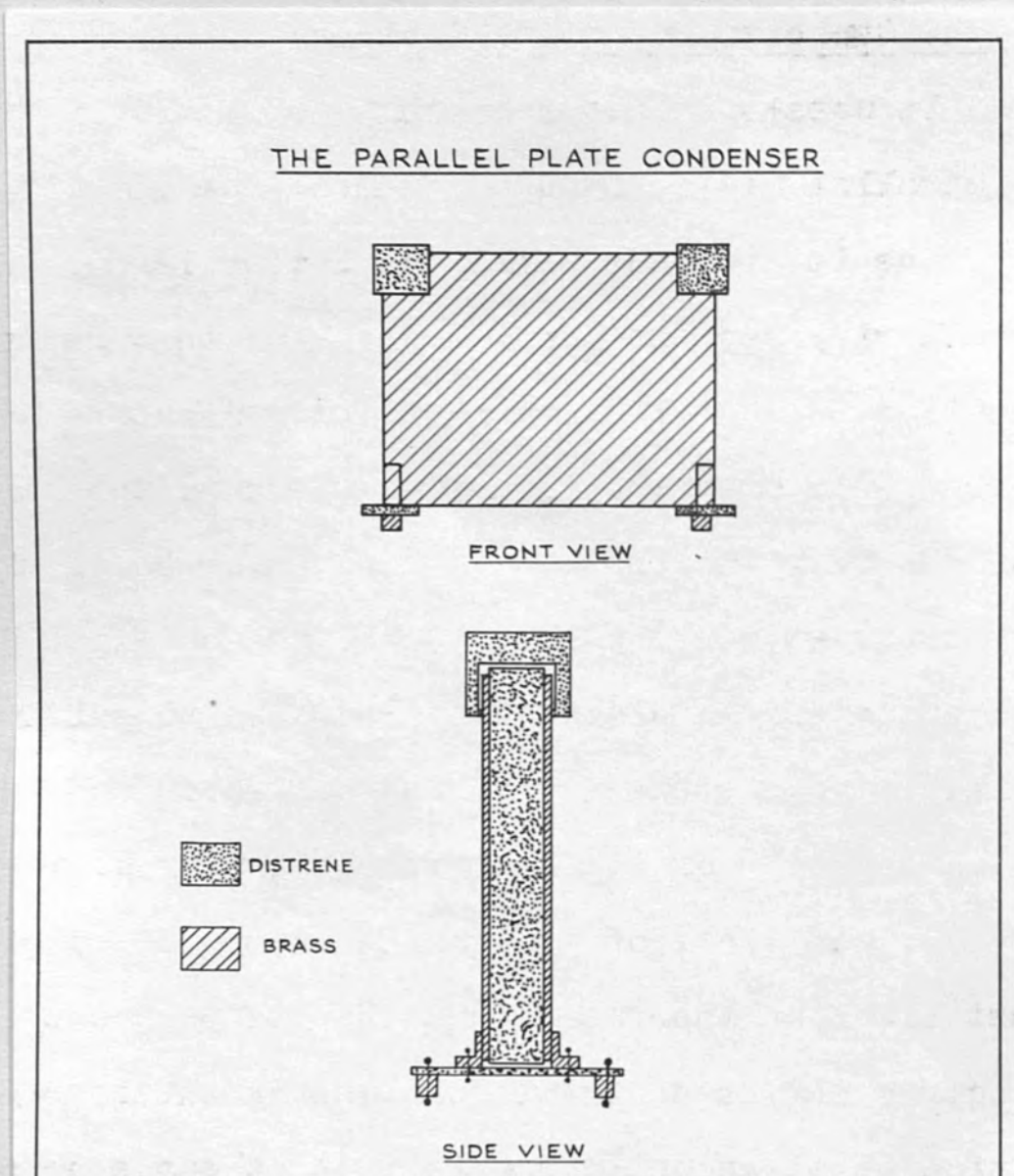
THE PARALLEL PLATE CONDENSER
FRONT VIEW
DISTRENE
BRASS
SIDE VIEW

Figure (6).

(1) The Capacity Potential divider:

It consists of two condensers C_1 & C_2. The former is a parallel Plate fixed condenser, the insulator between its plates is distrene while the latter is an ordinary variable wireless air condenser joined through distrene insulation to a dial control. Both condensers are provided with distrene insulated leads to the rest of the apparatus i.e. the insulation throughout is of distrene.

The use of a dielectric filled, parallel plate fixed condenser in place of an ordinary air-dielectric wireless type condenser leads to a simpler and better solution of some of the high insulation problems see fig (6). One plate of the condenser may be mounted on robust distrene insulators and the distrene sheet dielectric serves as the insulator for the condenser junction point which in use is kept at earth potential. The second variable condenser may be mounted directly and securely on the insulated plate. The distrene dielectric of the fixed condenser prevents dust, moisture etc. from getting between the plates and causing electrical leakage.

(2) The Balance Potential Indicator

Kemp used an electrometer valve type ET 1. as the indicator of potential balance. In our circuit we have replaced this by a Lindemann (36) Electrometer. The advantages of the latter are:-

1) The insulation of the electrometer may be made good and kept so much more easily than is the case with an electrometer valve.

2) It is possible to keep the de-earthing switches open for a considerable period of time and so obtain theoretically unlimited sensitivity; although the grid current of an electrometer valve is very small it does nevertheless, limit the time for which it is possible to keep the switches open for an observation of balance.

3) The sensitivity of the Lindemann electrometer may be varied quite simply (see later) and may be made very great.

4) It is possible, also, to use the Lindemann electrometer to test directly the insulation of all the various parts of the circuit. This is a very great advantage.

A SENSITIVITY CONTROL FOR THE LINDEMANN

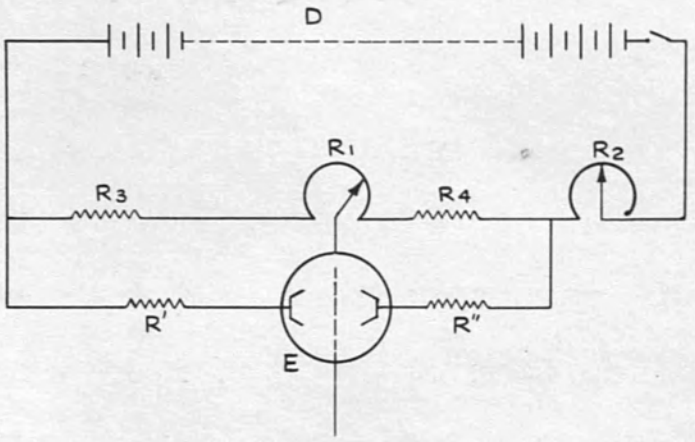

D	81 VOLT
R' & R"	HIGH RESISTANCES, 1 M Ω EACH.
R_3 & R_4	20,000 Ω EACH.
R_1	5,000 Ω
R_2	25,000 Ω

Figure (7).

The needle of the instrument was observed by a suitable microscope system and artificial light from a small 2.5 volts lamp. Adjustment of zero and sensitivity was accomplished as follows.

(3) Sensitivity Control for the Electrometer

For varying the sensitivity of the Lindemann electrometer by means of one adjustment only the following circuit fig (7) was used (37)

R_1 and R_2 are two variable resistances of the order of 25000 ohms connected to two fixed resistances R_3 amd R_4 of the same order in series with a dry battery of from 70 to 90 volts. The quadrants A and B of the electrometer are connected through safety resistances of 2Mn each to the ends of the fixed resistances, and the earthed case of the electrometer is connected to the moving arm of the variable resistance R_1. The latter is adjusted once for all, in order that the electrical zero may coincide with the mechanical zero. The potentials applied to the quadrants may then be simultaneously varied by altering the value of the series resistance R_2 whilst the ratio of the potentials remains constant so that the sensitivity can be varied whilst the zero remains almost undisturbed.

(iv) Other Parts of the circuit

With the parallel-plate, dielectric filled condenser alone, the instrument was suited for the measurement of ionization currents of ratio 1: 3*.

In order to increase the range of the capacity potential divider for the measuring of ionization currents of ratio 1: 10 the following arrangements were made.

A fixed condenser C_3 made of brass plates and distrene as insulator was connected in parallel with the fixed condenser C_1 via a switch K_1. The capacity of this condenser is 110 cm. and this increased the range to 1: 7.

The switch K_1 consists of two brass strips each provided with a platinum . contact at its free end and mounted at one end on a disc of distrene. These contacts are held against similar platinum contacts mounted in the same disc. The brass strips are provided with leads which connected them with the external condenser C_3 while the other contacts are connected to the rest of the

---

* This was because the apparatus had originally been designed for another purpose than the present experiments.

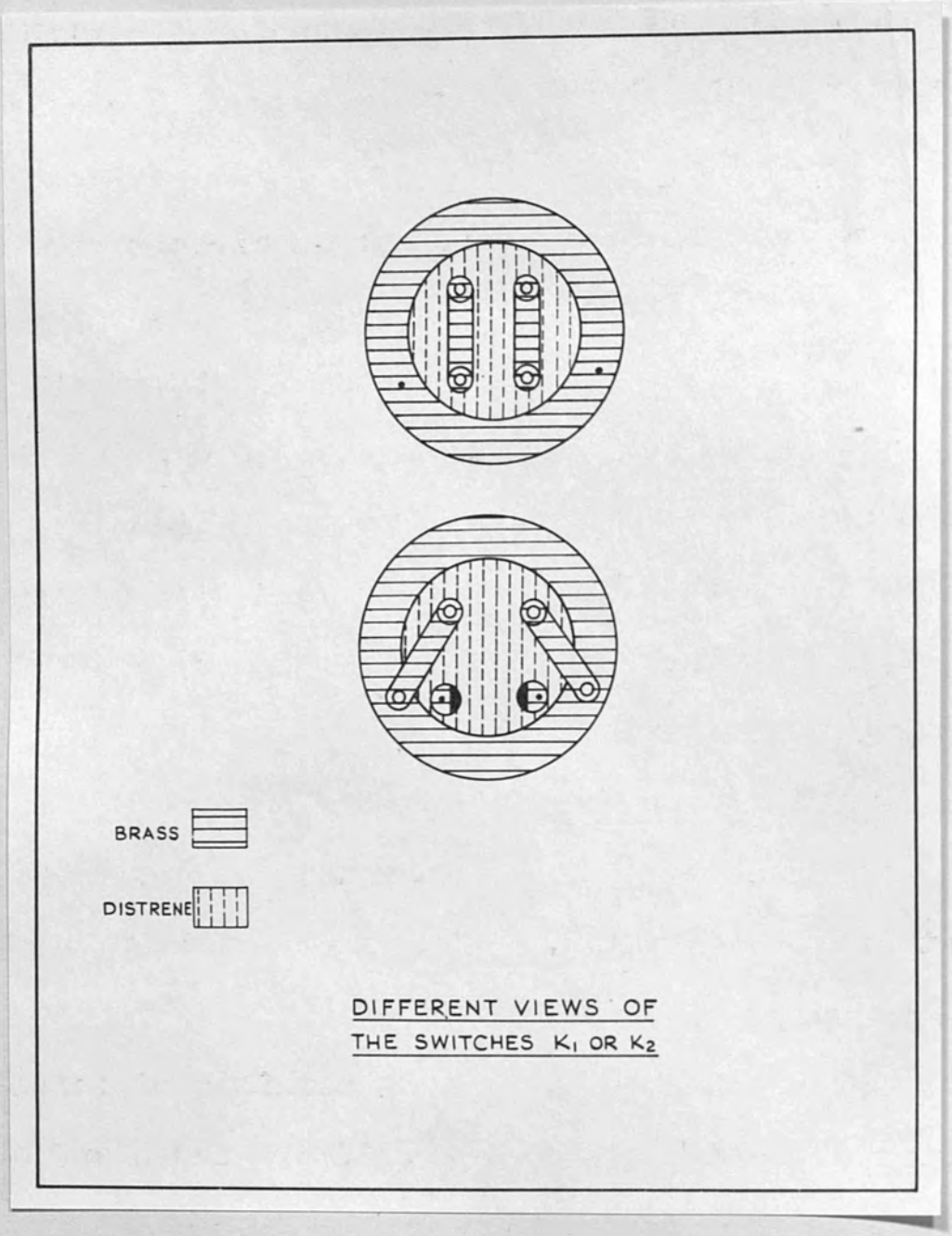

Figure (8).

circuit. This distrene disc is surrounded with a circular earthed brass ring provided with platinum contacts so that when the brass strips are connected to them the condenser C_3 is out of circuit and earthed.

Another fixed condenser C_4 was connected in parallel with the fixed condenser C_1 via a switch K_2. The capacity of this condenser is 230 cm. and this helps provide the required range of ratio 1: 10.

The switch K_2 is similar to K_1 and is connected to a second fixed condenser C_4. Fig (8) shows different views of these switches.

(v) The Earthing Keys

The earthing keys constitute a very important part of the apparatus. They need skill in construction and adjustment.

The switches S, S_1 & S_2 consists of three light strips of spring (7 cm. long, 0.75 breadth and 0.05 thickness) each carrying a platinum contact at its free end and mounted at one end on a block of brass. These contacts are held against similar platinum contacts mounted in distrene insulators set in a brass block. They are separated to break the circuit by three cams

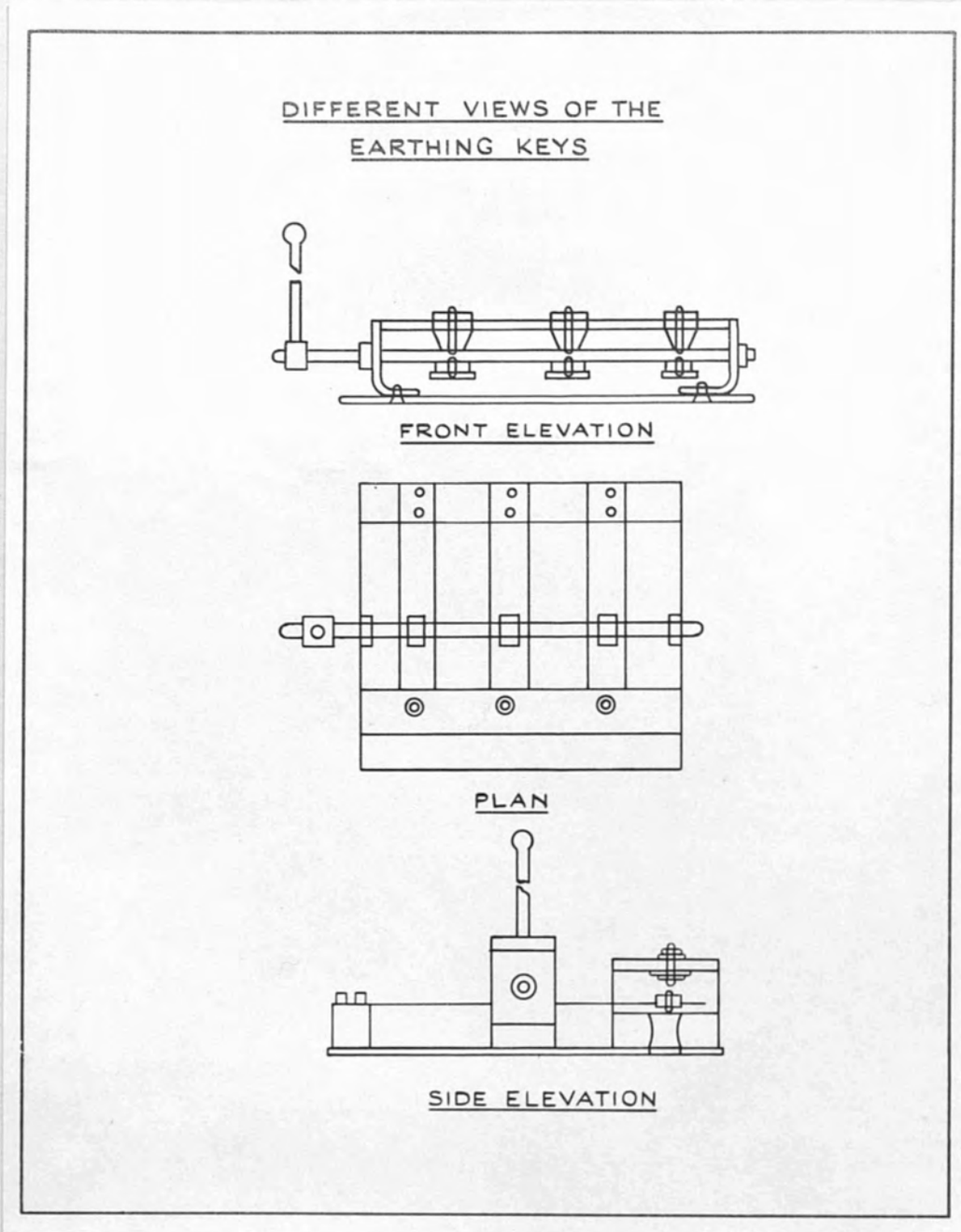
DIFFERENT VIEWS OF THE
EARTHING KEYS
FRONT ELEVATION
PLAN
SIDE ELEVATION

Figure (9).

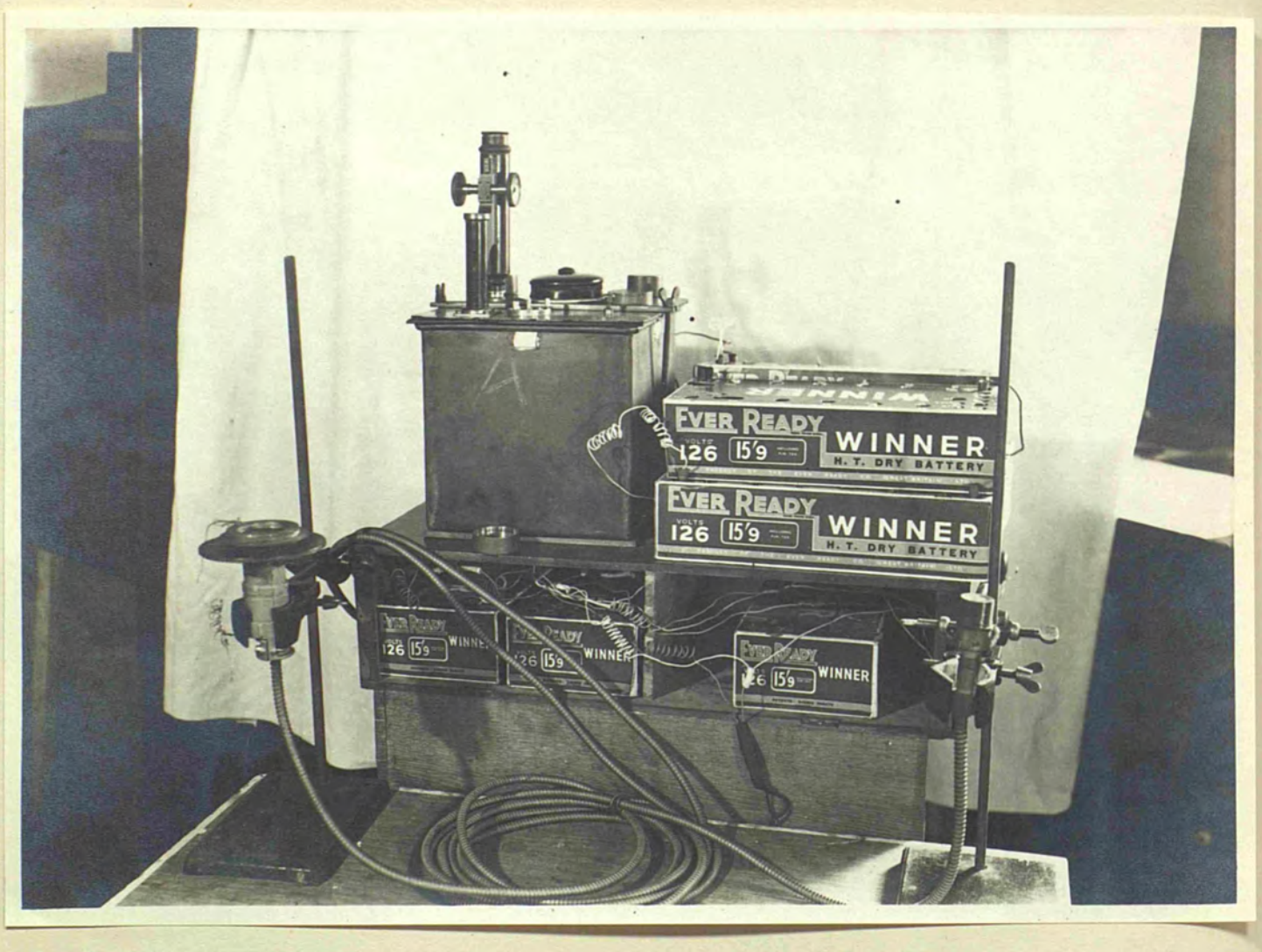

Figure (10).

The apparatus, chambers, sensitivity control, high tension and leads.

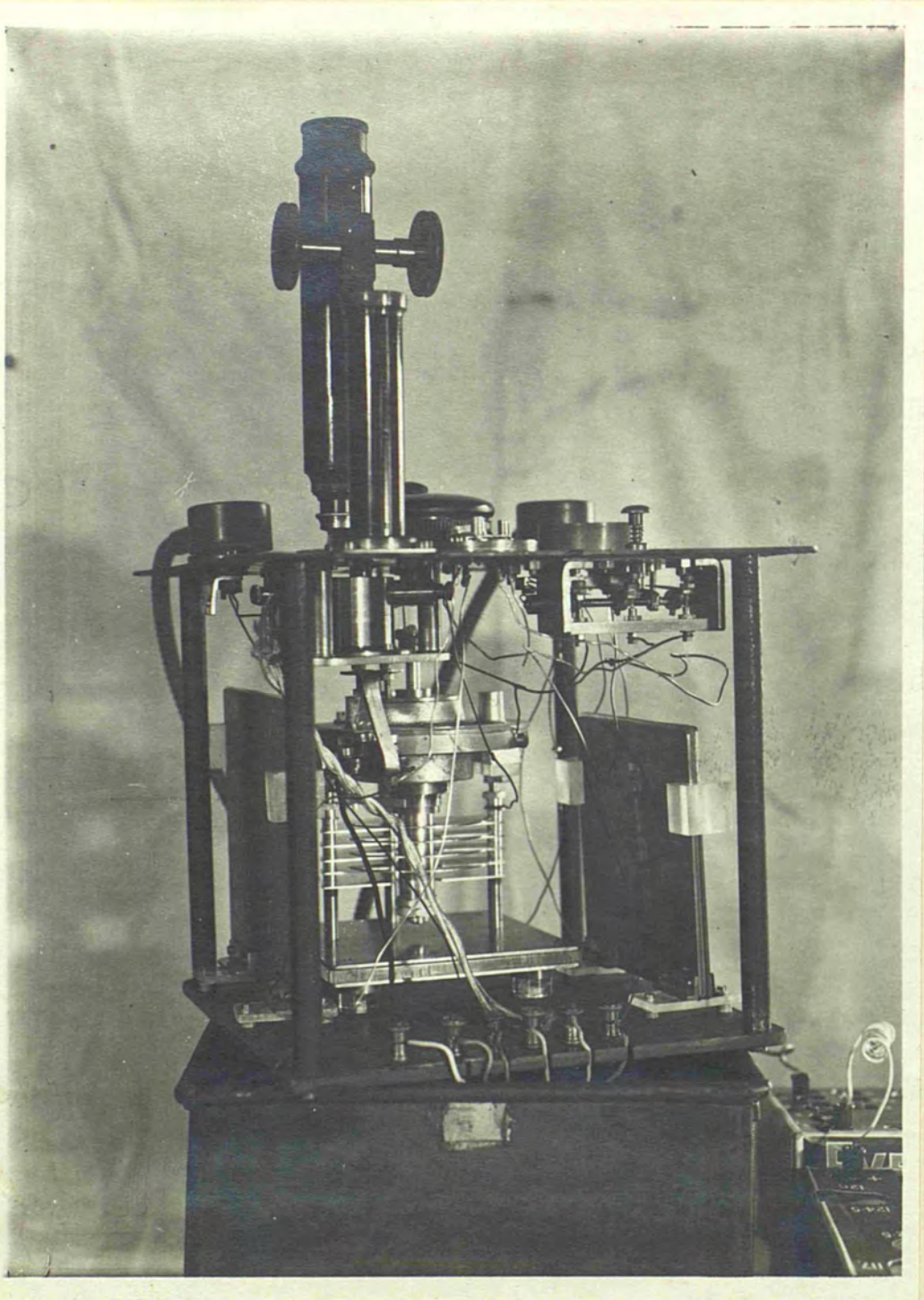

Figure (11).

Interior of the apparatus showing Lindemann electrometer, capacity potential divider, switches, etc.

which are mounted on a shaft and press on to the steel spring so as to deflect them when rotated. The cams are operated together by a lever which is attached to the cam shaft. The three distrene insulated contacts are provided with leads which connect them with the rest of the circuit while the contacts on the steel springs are connected through the frame to earth. The brass block carrying the earth and the insulated contacts are both mounted on a brass plate. Two brackets also mounted on the brass plate to hold the cam shaft in position. The time of opening each contact with respect to the others is arranged by the settling of its cam on the cam shaft. Fig (9) shows different views of the earthing keys. Figs (10, 11) show photographs of the apparatus and chambers.

(vi) Adjustment of the order of opening the switches.

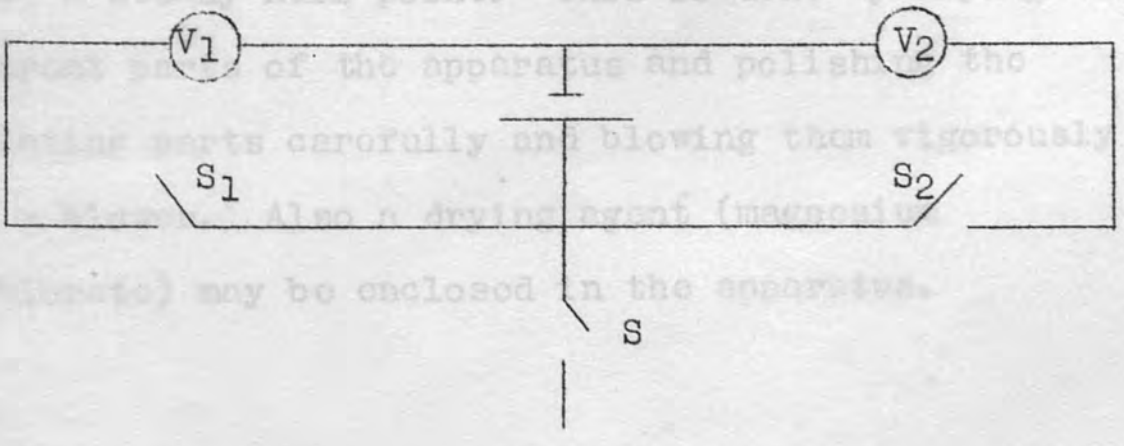

fig (12)

For adjusting the order of opening of the earthing keys S_1, S_2 & S a circuit such as that shown in figure (12) may be used. According to the theoretical considerations of the apparatus the switch S which is connected to the needle of the electrometer should open first in all cases while the switches S_1, and S_2 should open simultaneously.

S_1 and S_2 are adjusted by their screws so that they open simultaneously after S. This can be indicated by the movement of the needles of the voltmeters connected in the circuit above.

(vii). Precautions and Procedure

All parts of the apparatus and the insulating parts in it must be absolutely dry and clean, for any slight dirt or moisture may give rise to a drift in the Lindemann electrometer needle and make it difficult to get a steady null point. This is done by drying the different parts of the apparatus and polishing the insulating parts carefully and blowing them vigorously with a blower. Also a drying agent (magnesium perchlorate) may be enclosed in the apparatus.

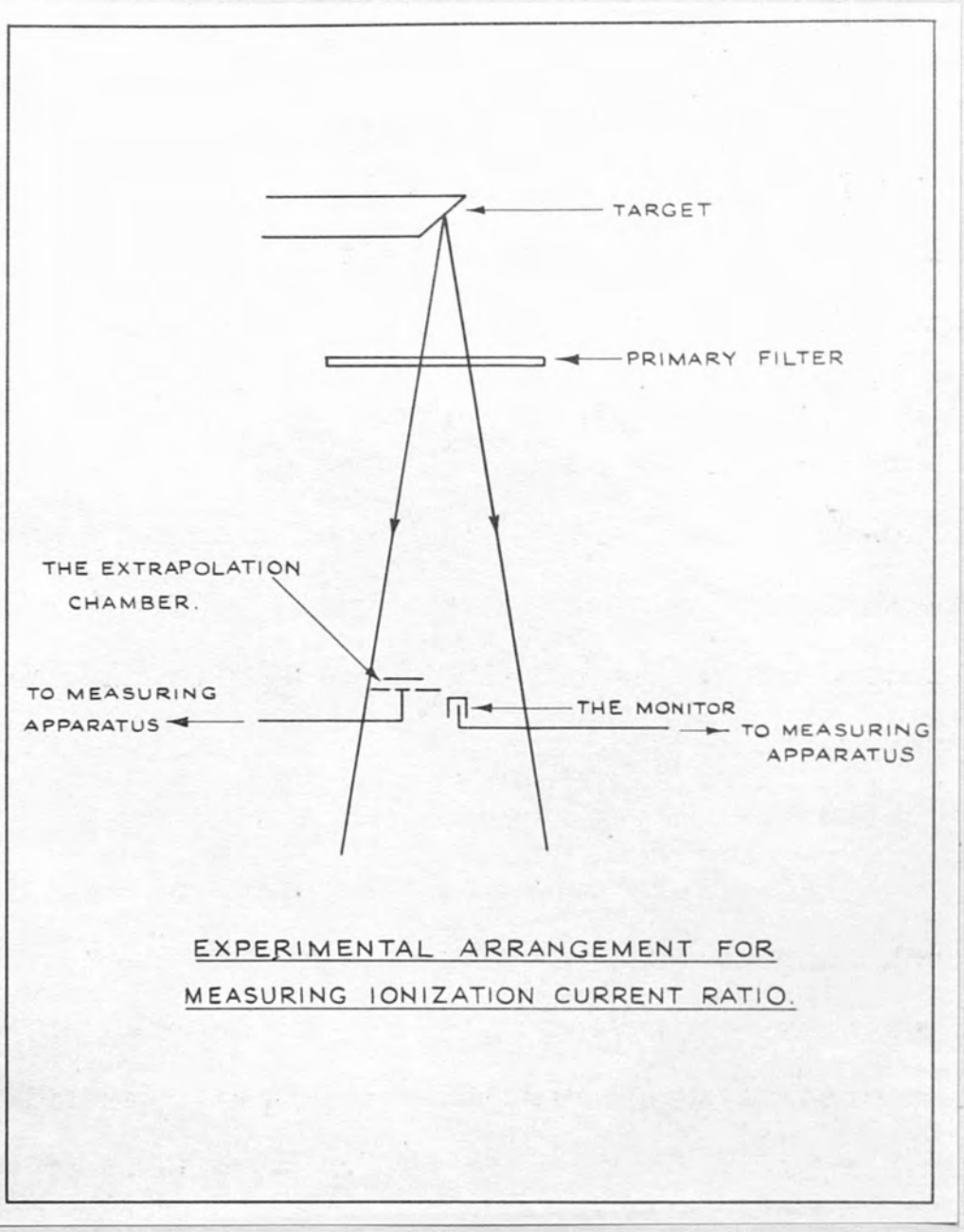

EXPERIMENTAL ARRANGEMENT FOR MEASURING IONIZATION CURRENT RATIO.

Figure (13).

The circuit is connected and the zero control is adjusted and so also the required sensitivity. The whole apparatus after connecting the leads to the chambers (one of them the extrapolation chamber while the other the monitor) and connecting the latter with the high tension is tested for leakage. To ensure that there is no leakage in any part of the apparatus, leads or chamber insulation, this can be done by opening the switches and observing the needle of the Lindemann electrometer. If no drift is observed the insulation everywhere is good and the apparatus is ready for practical observations.

In order to ensure saturation potential on each chamber, the air wall (monitor) chamber and the copper extropolation chamber were mounted on the measuring instrument. They were put symmetrically with respect to the axis of an x-ray beam of known quality as shown in fig (13). The voltage applied to the air wall chamber was kept constant while the voltages applied to the extrapolation chamber were varied till saturation occurred.

Since the greatest ionization current was anticipated in the copper extrapolation chamber of atomic number 29 it was quite safe to use this saturation voltage for the other chambers of lower atomic number in which the ionization current was expected to be less.

To obtain saturation potential to the monitor the same previous steps were repeated with constant voltage was applied to the extrapolation chamber while the voltage of the monitor was increased.

In our experiments there is no need to consider the temp. and pressure corrections for the two factors affect the two chambers simultaneously and therefore have no effect at all on the measured ratio.

In use the chambers were adjusted in the beam of radiation at a considerable distance from the applicator which defined the beam of X-rays from the X-ray tube. The setting of the variable condenser C_2 is found in each case for zero deflection whether the switches S, S_1 & S_2 were opened or closed. This indicates the correct ratio $\frac{C_2}{C_1}$ which maintains the point P at earth potential after opening the switches which is the required condition by the given theory.

The reading of the scale of the variable condenser C_2 is noted and from the calibration curves the corresponding ratio of the charges in the two chambers is obtained.

The X-radiationsavailable, enabled us to take measurements over a wide range of qualities from 0.08 A°. to 0.5 A°. The following sources were used.

1) A Siemen's tube for measurement in the medium kilovoltage region (60 - 110 KV_P) was used for obtaining qualities in the range 0.3 to 0.6 A°.
2) A Westinghouse tube with Villard circuit was used for measurements in the region of 0.1 - 0.3 A° .
3) A Victor Maximar tube having electrodes designed such that it operates almost as a constant potential x-ray generator, the exciting voltage being nearly the peak kilovoltage. With 220 KV_P. and suitable filters, x-rays of effective wave-lengthsfrom about 0.1 A°. to 0.08 A°. were obtained.

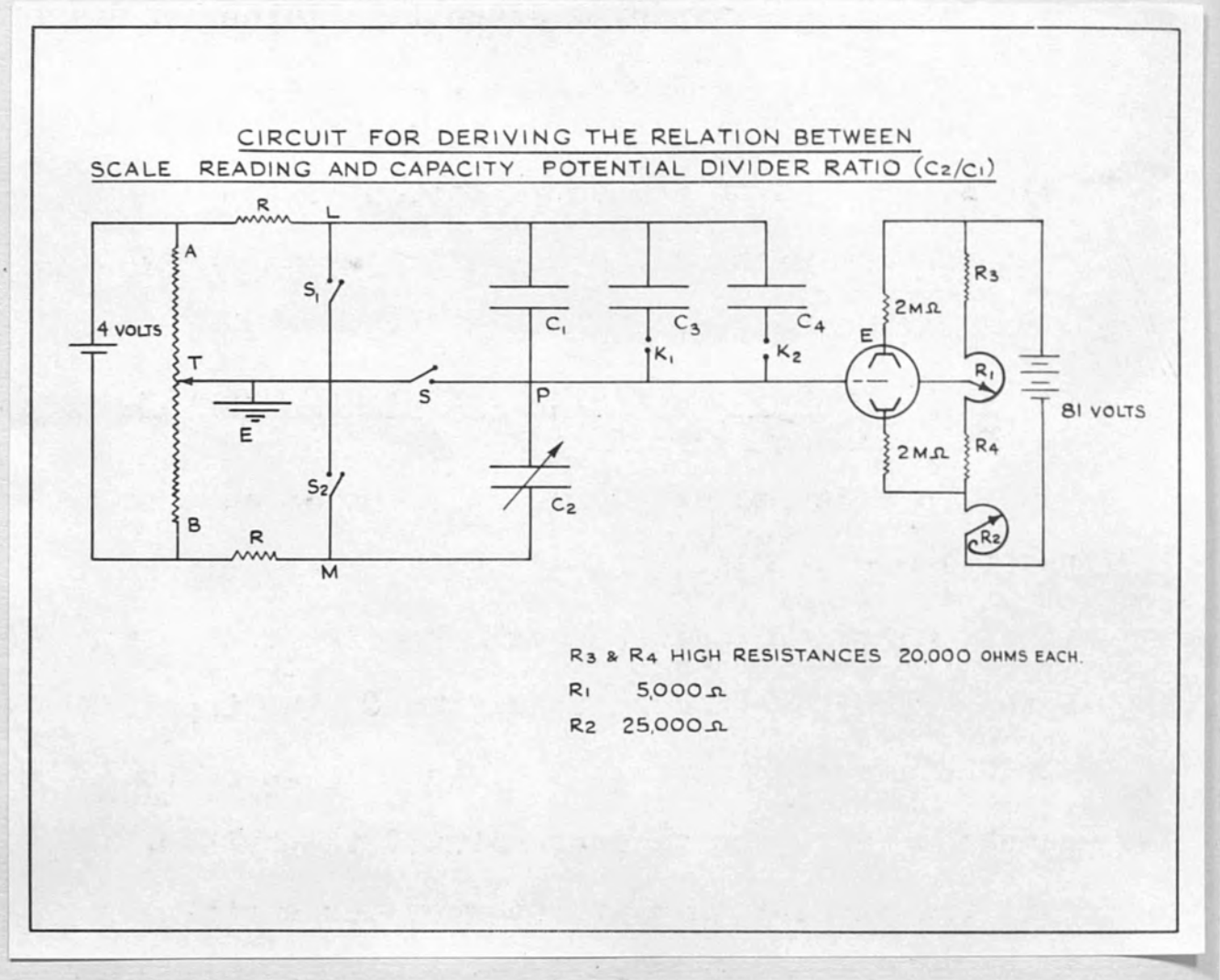
CIRCUIT FOR DERIVING THE RELATION BETWEEN
SCALE READING AND CAPACITY POTENTIAL DIVIDER RATIO (C2/C1)
R
L
A
S1
4 VOLTS
T
E
S
C1
C3
C4
K1
K2
P
2MΩ
R3
E
R1
81 VOLTS
2MΩ
R4
S2
C2
B
R
M
R2
R3 & R4 HIGH RESISTANCES 20,000 OHMS EACH.
R1 5,000Ω
R2 25,000Ω

Figure (14).

(viii) CALIBRATION OF THE APPARATUS

The apparatus was calibrated in two steps.

1) An investigation of the relation between scale reading and capacity potential divider ratio $\left(\frac{C_2}{C_1}\right)$, $\left(\frac{C_2}{C_1 + C_3}\right)$ and $\left(\frac{C_2}{C_1 + C_3 + C_4}\right)$

2) Determination of the variation of the scale reading with charge ratio corresponding to the previous cases.

(1) Relation between Scale Reading and Capacity Potential Divider Ratio

In order to determine this the circuit shown in fig (14) may be used. It consists of a calibrated potentiometer ATB across a cell V. The ends A and B of the potentiometer are connected to the inputs L and M of the capacity potential divider C_1 C_2 of the apparatus while the topping point T is earthed. To limit the current which flows when the earthing keys in the instrument are closed resistances RR of high value are included in the connecting leads.

In this way, potentials, one positive and the other negative with respect to earth, are applied at the input points, the ratio of which may be varied in a

known manner by altering the position of the tapping point T on the potentiometer network. For each input potential ratio, the capacity potential divider setting was found which gave a balance on opening the earthing keys.

Table (15) shows the relation between $\frac{V_1}{V_2}$ (and hence $\frac{C_2}{C_1}$, $\frac{C_2}{C_1 + C_3}$ & $\frac{C_2}{C_1 + C_3 + C_4}$), and the scale reading of the apparatus. This table constitutes the calibration for use in the measurement of potential electrostatically. It is also required when the instrument is used to measure quantities of charge or x-ray exposures.

(2) Relation Between Scale Reading and Charge ratio

In his original work Kemp determined the relation between the scale reading and charge ratio by means of known x-ray intensities applied to his ionization chambers. A defect of such a method is that its accuracy depends upon the accuracy with which the x-ray intensities may be known.

Greening (38), working in the laboratory in which the present work was done, has shown that with this apparatus it is possible to determine the required

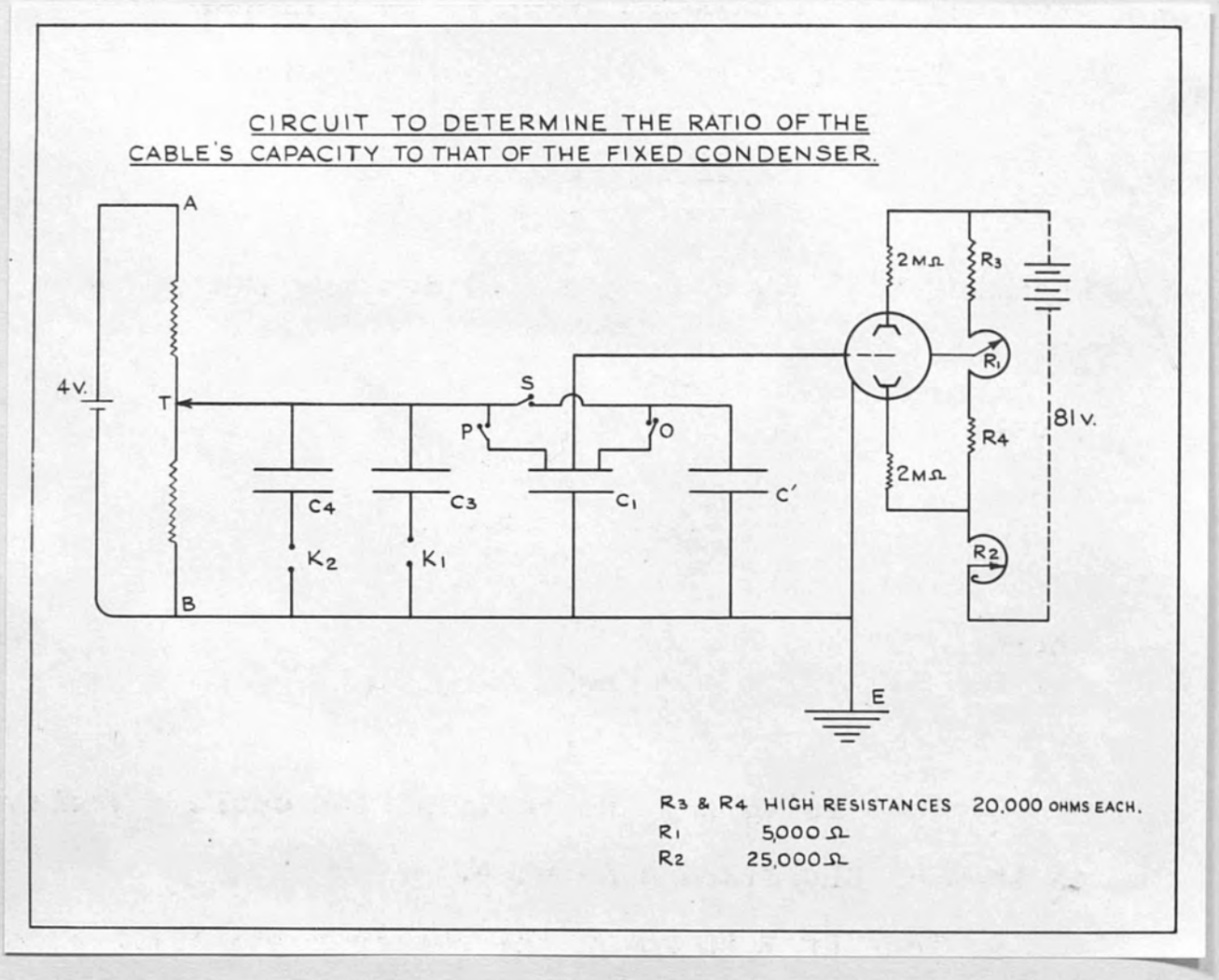
CIRCUIT TO DETERMINE THE RATIO OF THE
CABLE'S CAPACITY TO THAT OF THE FIXED CONDENSER.
A
4V.
T
B
S
P
O
C4
C3
C1
C'
K2
K1
2MΩ
R3
R1
R4
2MΩ
R2
81V.
E
R3 & R4 HIGH RESISTANCES 20,000 OHMS EACH.
R1 5,000 Ω
R2 25,000 Ω

Figure (15).

relation via measurements only of potentials after various operations of sharing of electric charge; furthermore the method is of great accuracy. We have used the same procedure which is as follows:

The theory of the instrument indicates that,

$$\frac{Q_1}{Q_2} = \frac{C_1 + C'}{C_2 + C''} \frac{C_2}{C_1}$$

Assuming that the cables capacities are equal, therefore,

$$C' = C''$$

Thus,

$$\frac{Q_1}{Q_2} = \frac{1 + x}{\frac{C_2}{C_1} + x} \frac{C_2}{C_1}$$

where,

$$x = \frac{C'}{C_1}$$

That is to say the ratio of the cable capacity to that of the fixed condenser.

Thus if x is known the charge ratio calibration curves are easily and accurately obtainable.

Determination of The Value of x

To find this the circuit shown in fig (15) may be employed. ATB constitutes a potentiometer network across a cell V. The end B is earthed while the point

T is connected via a switch p to a fixed condenser C_1.

The fixed condenser C_1 is charged by closing the switch p and opening the switch o while the value of R is noted. This charge is shared with the cable capacity by opening p and closing o and the deflection θ of the electrometer needle is observed.

Then, the switch P is closed while S & o are opened. The value of R is adjusted until the same deflection θ of the electrometer needle is obtained. Let this value be R_1 (The value of the total resistance in the potentiometer circuit is constant).

Therefore, the charge q which passed from C_1 to the electrometer being,

$$q = C_1 v = (C_1 + C') V'$$
$$= C_1 R = (C_1 + C') R_1$$

and,

$$x = \frac{R}{R_1} - 1$$

If C_1 and C' in circuit interchanged i.e. charge the cable and share it with apparatus.

$$\therefore \quad q = (C_1 + C') V' = C' V$$

i.e. $$(C_1 + C') R_1 = C'R$$

and

$$\frac{1}{x} = \frac{R}{R_1} - 1$$

Repeat the previous experiments by connecting in parallel with the fixed condenser the other two fixed condensers C_3 and C_4 respectively. During the sharing preocesses referred to above the electrometer was used as the voltage indicator (no linearity of the scale assumed).

The mean value of x obtained from values obtained from sharing processes over a period of days gave an average value of $x = 4.2$, with the additional condenser (C_3) in parallel with (C_1) the average value of $x = 1.312$ and with the additional condenser (C_4) in parallel with (C_1) the average value of $x = 0.538$.

x does not need to be known with great accuracy in order to obtain an accurate charge ratio calibration. As the instrument is capable of such precise measurements it is undesirable to calibrate it by using other ionization instruments, or by assuming the inverse square law and the absence of scattered radiation.

The following tables give the relation between scale reading and charge ratio together with the experimental results already taken.

TABLE (15)

V = 4 volts

R = 1 MΩ

Scale Reading	$\frac{C_2}{C_1}$	$\frac{C_2}{C_1 + C_3}$	$\frac{C_2}{C_1 + C_3 + C_4}$	Scale Reading	$\frac{C_2}{C_1}$	$\frac{C_2}{C_1 + C_3}$	$\frac{C_2}{C_1 + C_3 + C_4}$
0	0.32	0.102	0.040	50	0.745	0.233	0.96
2.5	0.33	-	-	55	0.793	0.247	0.103
5	0.355	0.113	0.046	60	0.835	0.260	0.108
7.5	0.370	-	-	65	0.879	0.275	0.113
10	0.396	0.125	0.052	70	0.930	0.290	0.118
15	0.437	0.138	0.057	75	0.971	0.303	0.124
20	0.484	0.150	0.063	80	1.021	0.316	0.129
25	0.524	0.165	0.070	85	1.062	0.329	0.134
30	0.573	0.178	0.075	90	1.112	0.343	0.139
35	0.616	0.190	0.080	95	1.154	0.354	0.144
40	0.666	0.204	0.085	100	1.173	0.360	0.147
45	0.706	0.218	0.091				

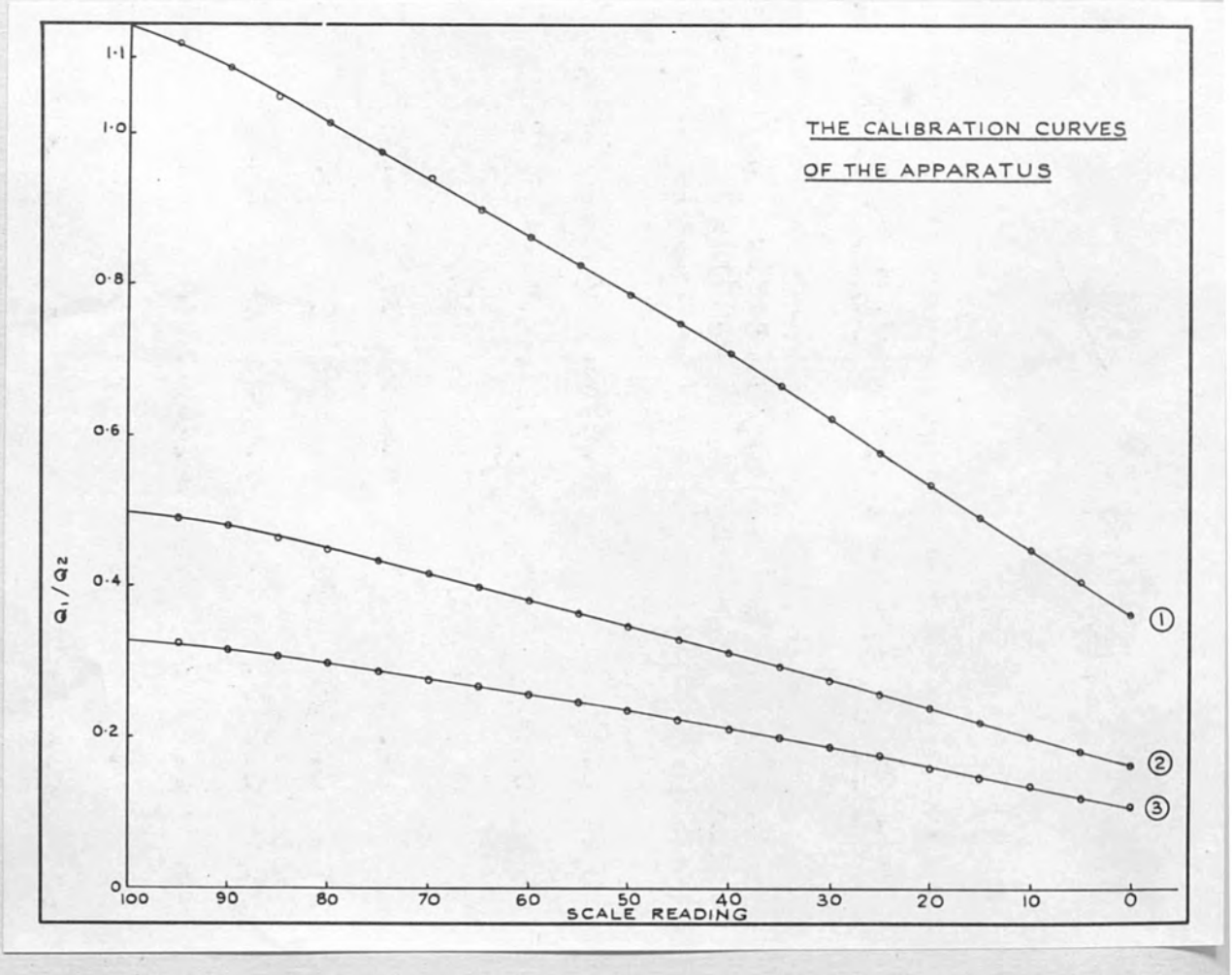

Figure (16).

(1) When both C_3 & C_4 were out of circuit.

(2) When C_3 was in circuit only.

(3) When both C_3 & C_4 were in circuit.

TABLE (16)

C_1 = 50 cm. x = 4.2				$\frac{C_1 + C_3}{C_1}$ = 3.2 x' = 1.312				$\frac{C_1 + C_3 + C_4}{C_1}$ = 7.8 x'' = 0.538			
Scale Reading	Q_1/Q_2	Scale Reading	Q_1/Q_2	Scale Reading	Q_1/Q_2	Scale Reading	Q_1/Q_2	Scale Reading	Q_1/Q_2	Scale Reading	Q_1/Q_2
0	0.368	55	0.8256	0	0.1668	55	0.3664	0	0.1064	55	0.2471
5	0.407	60	0.8626	5	0.1833	60	0.3823	5	0.1212	60	0.2571
10	0.448	65	0.8993	10	0.2011	65	0.4005	10	0.137	65	0.2670
15	0.490	70	0.9430	15	0.2201	70	0.4185	15	0.147	70	0.2767
20	0.5371	75	0.9768	20	0.2372	75	0.4337	20	0.159	75	0.288
25	0.5769	80	1.016	25	0.2583	80	0.4487	25	0.177	80	0.2975
30	0.6240	85	1.049	30	0.2762	85	0.4635	30	0.186	85	0.3067
35	0.6653	90	1.088	35	0.2925	90	0.4792	35	0.1991	90	0.3158
40	0.7119	95	1.119	40	0.3111	95	0.4912	40	0.2098	95	0.3248
45	0.7484	100	1.137	45	0.3295	100	0.4978	45	0.2225	100	0.3301
50	0.7838	-	-	50	0.3487	-	-	50	0.2329	-	

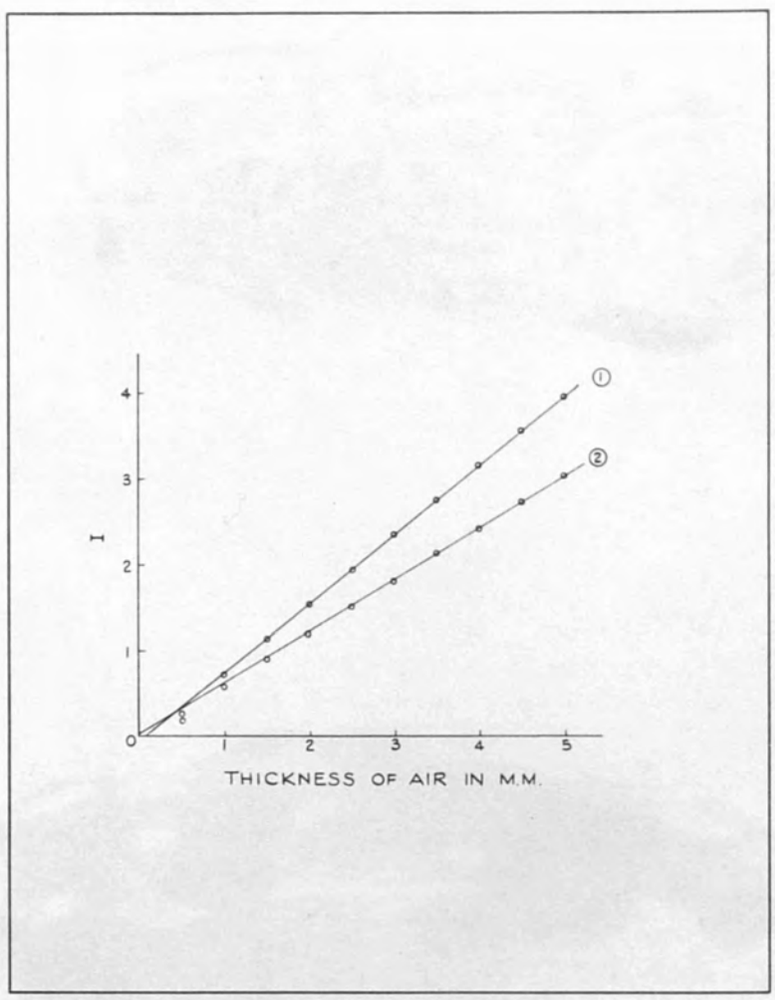

Figure (17).

Ionization - Electrode Spacing Curves.
Electrodes:- Perspex coated with dag.

(1) Effective wavelength = 0.5 A°.
(2) " " = 0.425 A°.

TABLE (17)

Upper electrode perspex coated with dag.

60 KV_P. 4 m.a.
1 mm. Aluminium (Primary filter)
$\lambda e = 0.5$ A°.

Air thickness in M.M.	Scale Reading	$\frac{I}{R'}$	R′
0.5	26.0	-	0.263
1.0	42.5	-	0.732
1.5	62.1	0.8733	1.145
2.0	33.6	0.6452	1.55
2.5	17.5	0.5132	1.95
3.0	72.5	0.4252	2.35
3.5	54.6	0.3635	2.75
4.0	41.8	0.3178	3.15
4.5	31.4	0.2817	3.55
5.0	23.9	0.2533	3.95

The slope of the curves = 0.8
See figure (17) curve (1)

80 KV_P. 3 m.a.
2 mm. Aluminium (Primary filter)
$\lambda e = 0.425$ A°.

Air thickness in M.M.	Scale Reading	$\frac{I}{R'}$	R′
0.5	12.8	-	0.211
1.0	24.5	-	0.5733
1.5	92.5	1.1	0.909
2.0	55.1	0.8256	1.212
2.5	34.5	0.66	1.515
3.0	21.9	0.55	1.818
3.5	81.5	0.472	2.118
4.0	68.5	0.4133	2.419
4.5	55.7	0.3676	2.72
5.0	45.3	0.331	3.021

The slope of the curve = 0.6
See figure (17) curve (2)

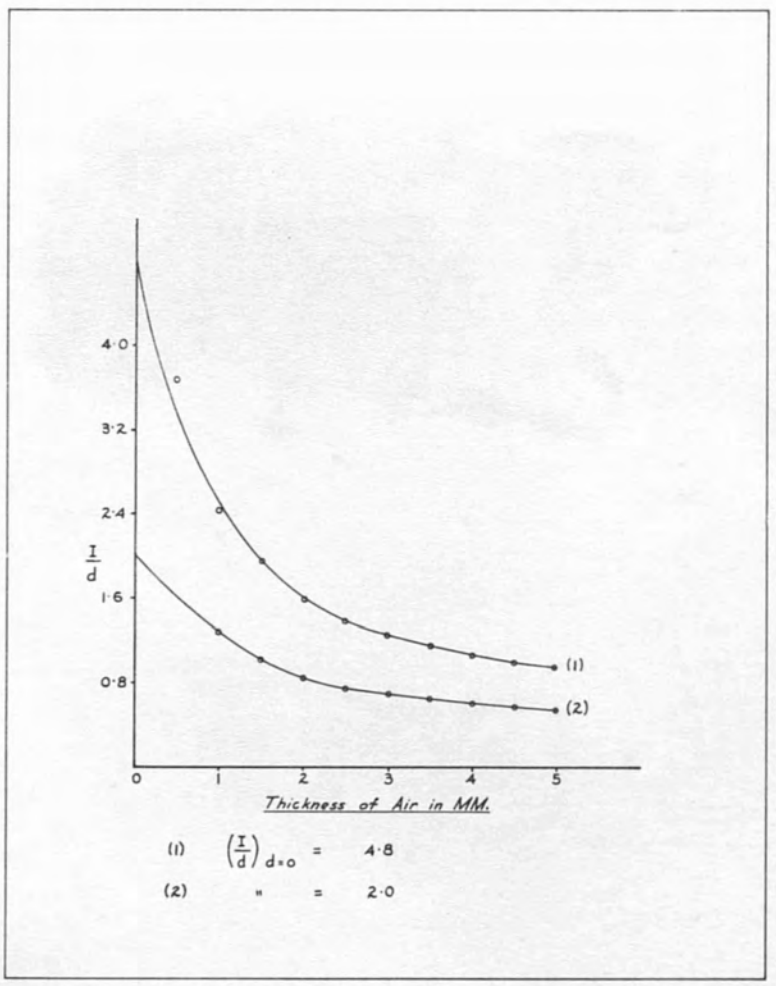

Figure (18).

Ionization per unit spacing - Electrode Spacing Curves.
Electrodes:- Aluminium.

(1) Effective wavelength = 0.5 A°.
(2) " " = 0.425 A°.

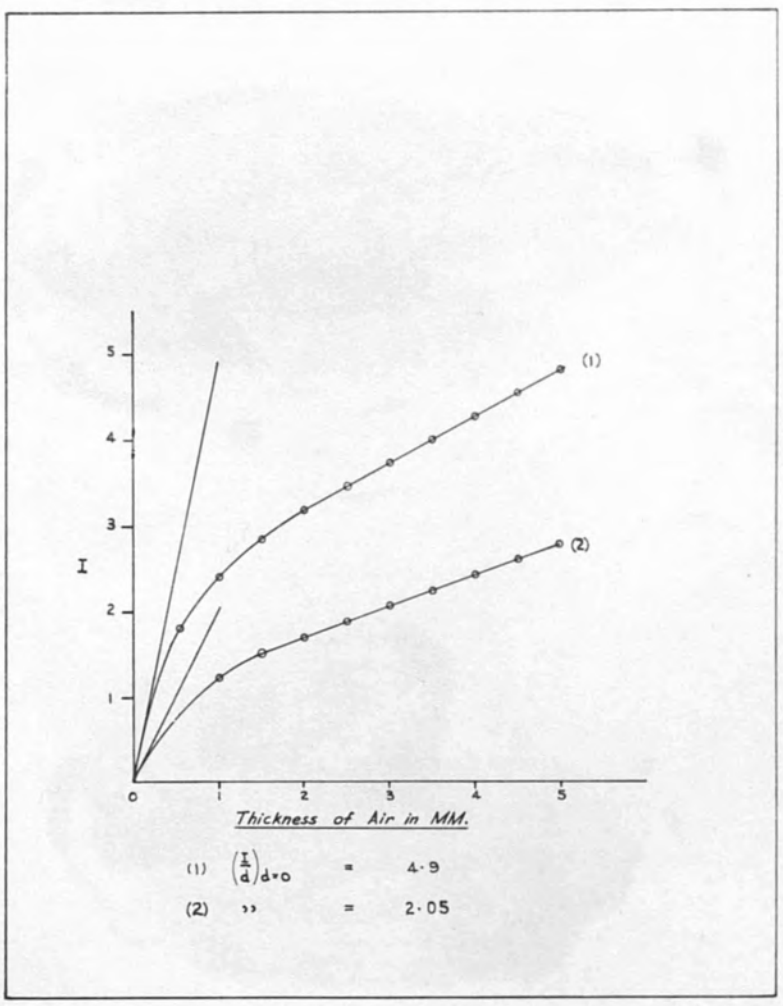

Figure (19).

Ionization - Electrode Spacing Curves.
Electrodes:- Aluminium.

(1) Effective wavelength = 0.5 A°.
(2) " " = 0.425 A°.

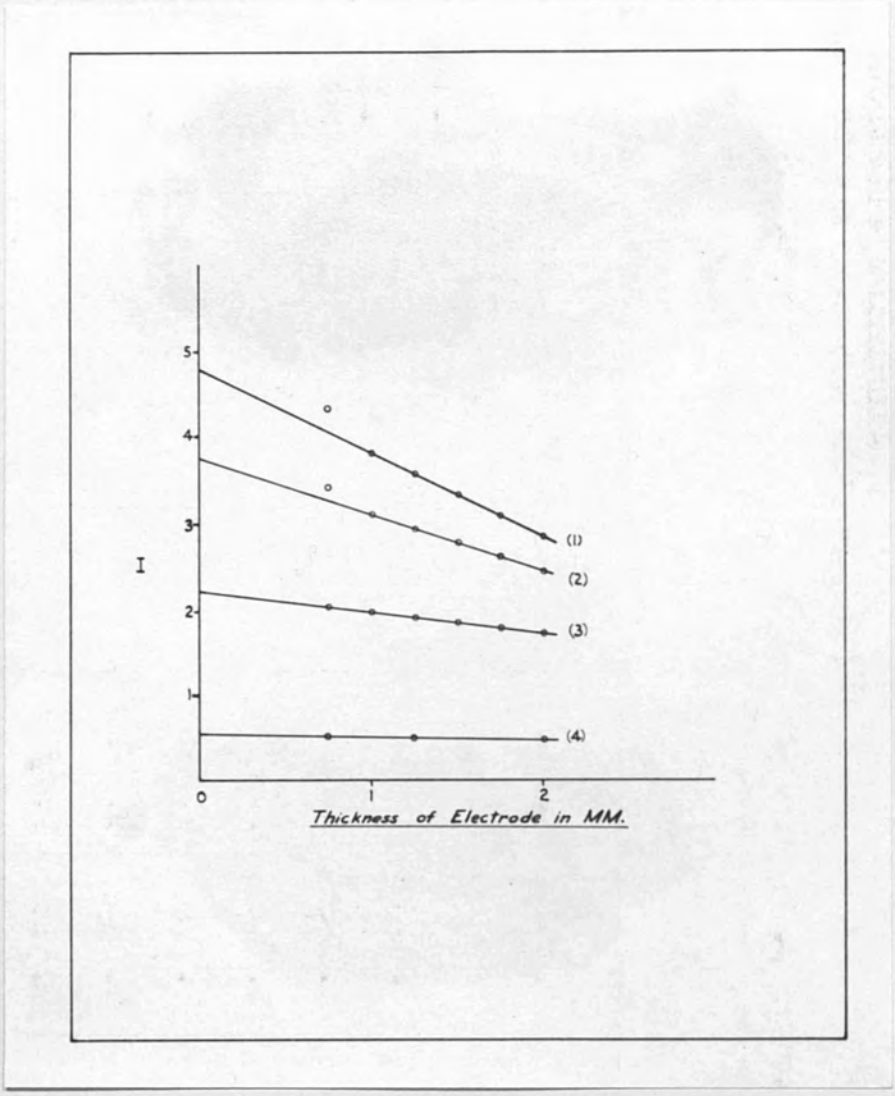

Figure (20).

Extrapolation of I to zero electrode thickness.
Electrodes:- Aluminium.

(1) Effective wavelength = 0.5 A°.
(2) " " = 0.425 A°.
(3) " " = 0.328 A°.
(4) " " = 0.256 A°.

TABLE (18)

60 KV_p. 4 m.a.
1 mm. Aluminium (Primary filter)

$\lambda_e = 0.5\ A^o$

Thickness of the upper electrode 0.75 M.M. Al.

Air thickness in M.M.	Scale Reading	$\frac{1}{I}$	I	$\frac{I}{d}$
0.5	20.9	0.5433	1.841	3.682
1.0	67.5	0.41	2.44	2.44
1.5	48.5	0.3433	2.913	1.942
2.0	43.2	0.3233	3.093	1.546
2.5	33.9	0.29	3.448	1.3792
3.0	26.5	0.265	3.774	1.258
3.5	21.9	0.2467	4.054	1.158
4.0	18.1	0.2317	4.316	1.079
4.5	15.0	0.2201	4.543	1.009
5.0	12.5	0.21	4.762	0.9524

See figures (18 & 19) curves (1 & 1)

TABLE (19)

Extrapolation of I to Zero Electrode Spacing

Aluminium Electrode
(Separation between electrodes 4 M.M.)

$\lambda_e = 0.5\ A^o$

Thickness of Electrode in cm.	I
0.075	4.316
0.10	3.822
0.125	3.572
0.15	3.333
0.175	3.035
0.20	2.817

Monitor factor = $\frac{1}{0.4112}$

See figure (20) curve (1)

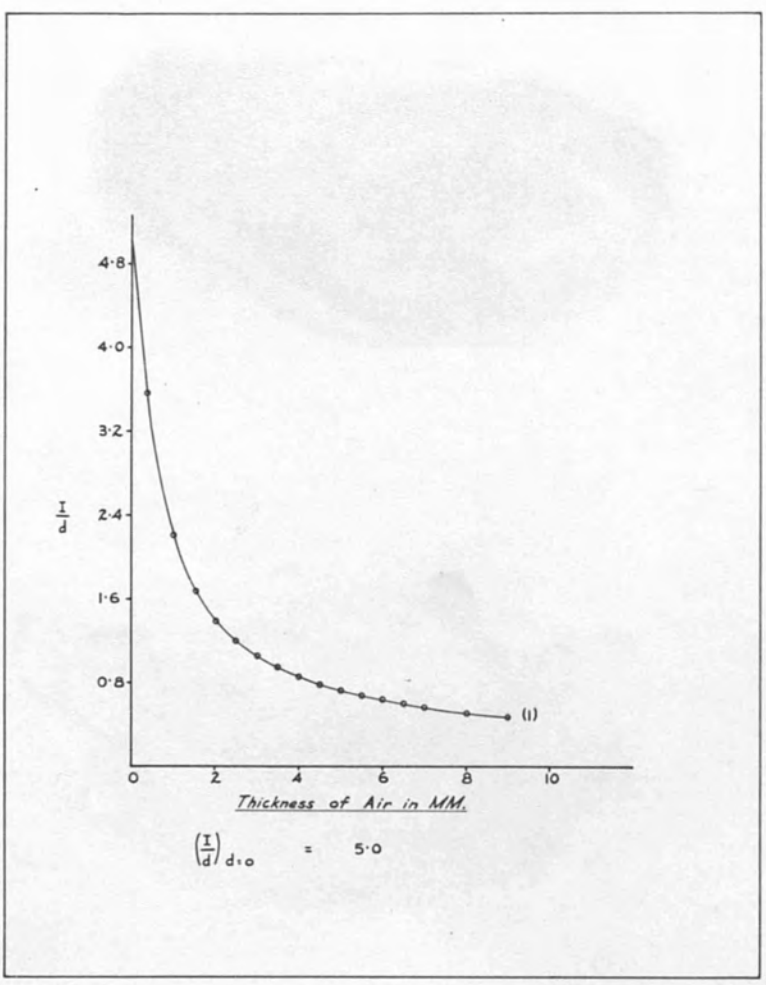

Figure (21).

Ionization per unit spacing - Electrode Spacing Curves.
Electrodes:- Copper.

Effective wavelength = 0.5 A^{o}.

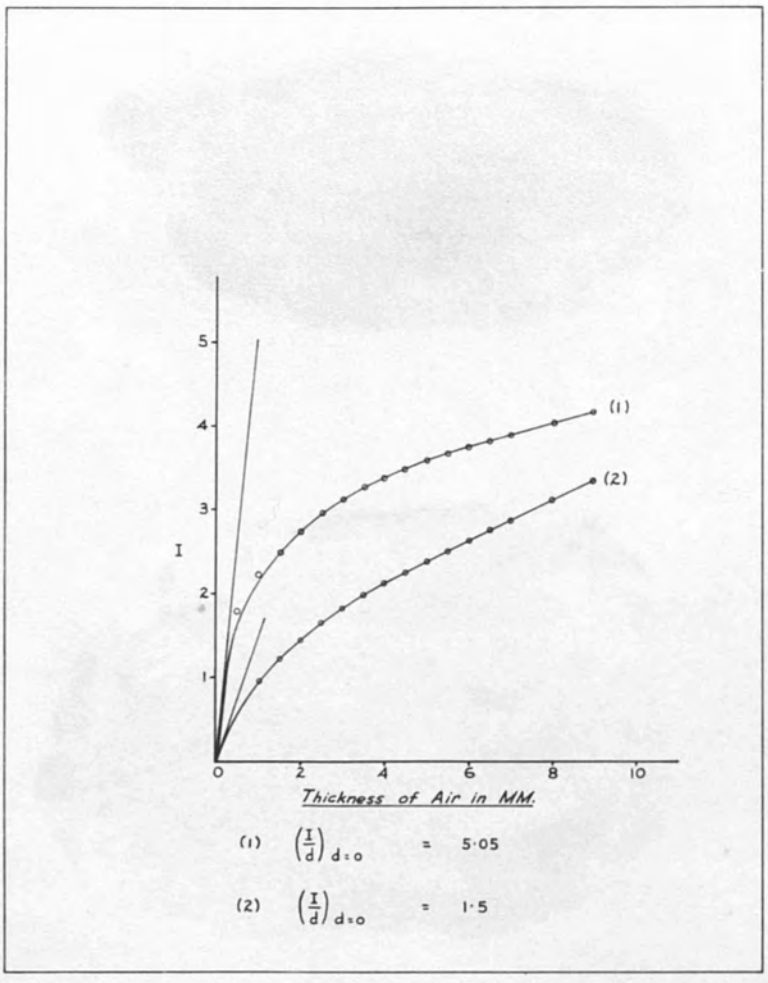

Figure (22).

Ionization - Electrode Spacing Curves.
Electrodes:- Copper.

(1) Effective wavelength = 0.5 A°.
(2) " " = 0.172 A°.

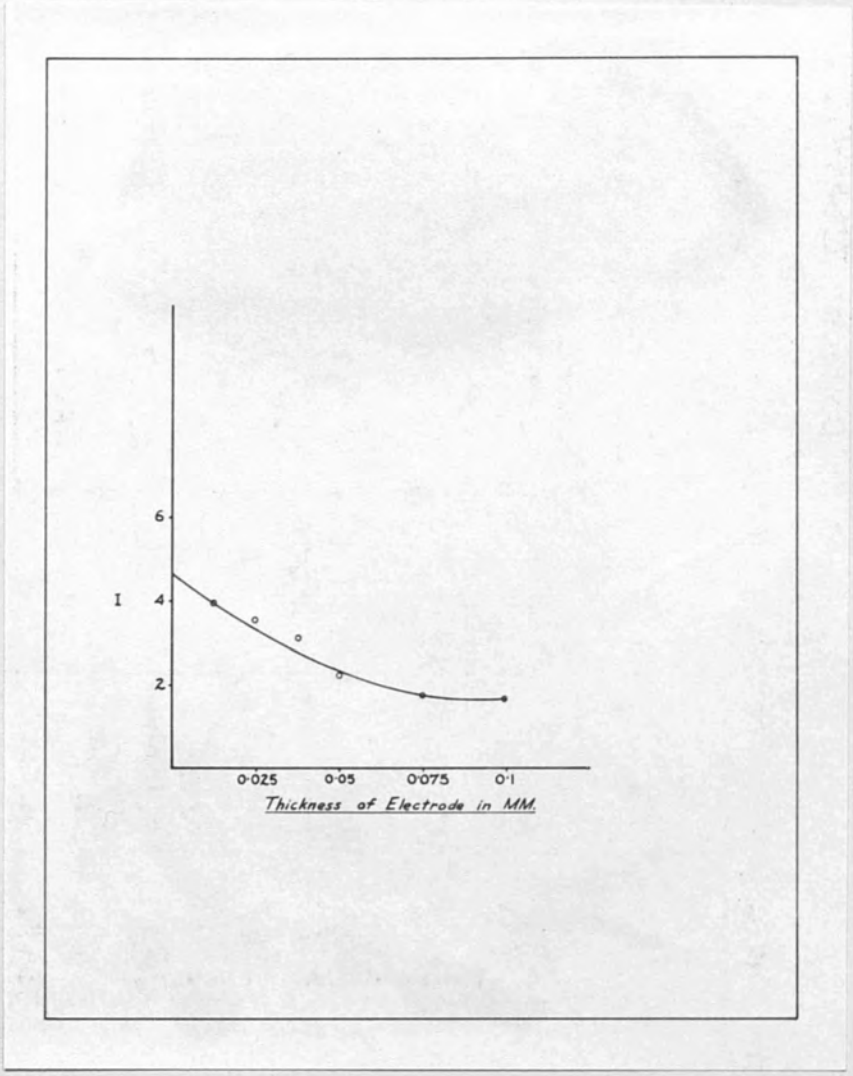

Figure (23).

Extrapolation of I to zero electrode thickness.
Electrodes:- Copper.

Effective wavelength = 0.5 A°.

TABLE (20)

60 KV_p. 4 m.a.
1 mm. Aluminium (Primary filter)

$\lambda_e = 0.5\ A^o$

Thickness of the upper electrode 0.0125 M.M. copper.

Air thickness in M.M.	Scale Reading	$\frac{1}{I}$	I	$\frac{I}{d}$
0.5	22.5	0.5567	1.797	3.594
1.0	80.3	0.4500	2.222	2.222
1.5	65.5	0.4033	2.479	1.653
2.0	55.0	0.3664	2.729	1.364
2.5	46.9	0.3367	2.97	1.188
3.0	41.5	0.3167	3.157	1.052
3.5	38.0	0.304	3.290	0.94
4.0	35.5	0.295	3.39	0.8475
4.5	33.3	0.2873	3.481	0.7735
5.0	31.1	0.280	3.571	0.7142
5.5	29.4	0.2733	3.659	0.665
6.0	27.5	0.2667	3.741	0.623
6.5	25.7	0.2617	3.822	0.588
7.0	24.4	0.2567	3.895	0.556
8.0	22.5	0.2483	4.027	0.503
9.0	21.0	0.2417	4.138	0.460

See figures (21 & 22) curves (1 & 1)

TABLE (21)

Extrapolation of I to Zero Electrode Spacing

Copper Electrode
(Separation between electrodes 7 M.M.)

$\lambda_e = 0.5\ A^o$

Thickness of Electrode in cm.	I
0.00125	3.895
0.00250	3.536
0.00375	3.087
0.005	2.2
0.0075	1.766
0.01	1.602

Monitor factor = $\frac{1}{0.05996}$

See figure (23)

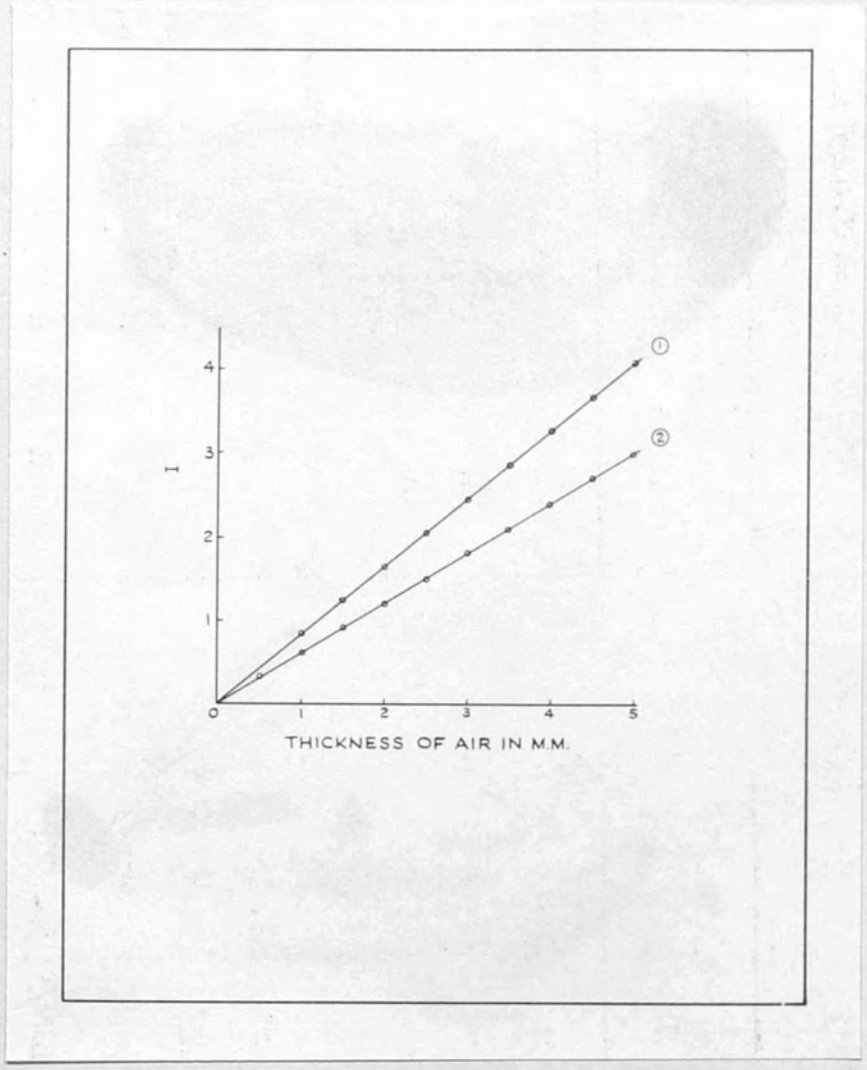

Figure (24).

Ionization - Electrode Spacing Curves.
Electrodes:- Pressed mixture of $\bar{Z} = 7.64$.

(1) Effective wavelength = 0.5 A°.
(2) " " = 0.425 A°.

TABLE (22)

Electrodes of effective atomic number (7.64)

60 KVp. 4 m.a.
1 mm. Aluminium (Primary filter)
$\lambda_e = 0.5$ A°

Air thickness in M.M.	Scale reading	$\frac{I}{R'}$	R´
0.5	41.8	-	0.3178
1.0	56.9	-	0.84
1.5	51.5	0.7967	1.255
2.0	28.0	0.6046	1.654
2.5	92.0	0.4867	2.055
3.0	66.9	0.4075	2.454
3.5	51.0	0.3502	2.855
4.0	38.5	0.3067	3.255
4.5	39.2	0.2736	3.655
5.0	21.9	0.2467	4.054

The slope of the curve = 0.8

See figure (24) curve (1)

80 KVp. 3 m.a.
2 mm. Aluminium (Primary filter)
$\lambda_e = 0.425$ A°.

Air thickness in M.M.	Scale reading	$\frac{I}{R'}$	R´
0.5	36.9	-	0.30
1.0	27.5	-	0.60
1.5	60.5	-	0.90
2.0	56.3	0.8333	1.2
2.5	35.5	0.6667	1.5
3.0	22.3	0.5555	1.8
3.5	88.5	0.4763	2.099
4.0	69.5	0.4167	2.4
4.5	56.9	0.370	2.7
5.0	46.0	0.333	3.00

The slope of the curve = 0.6

See figure (24) curve (2)

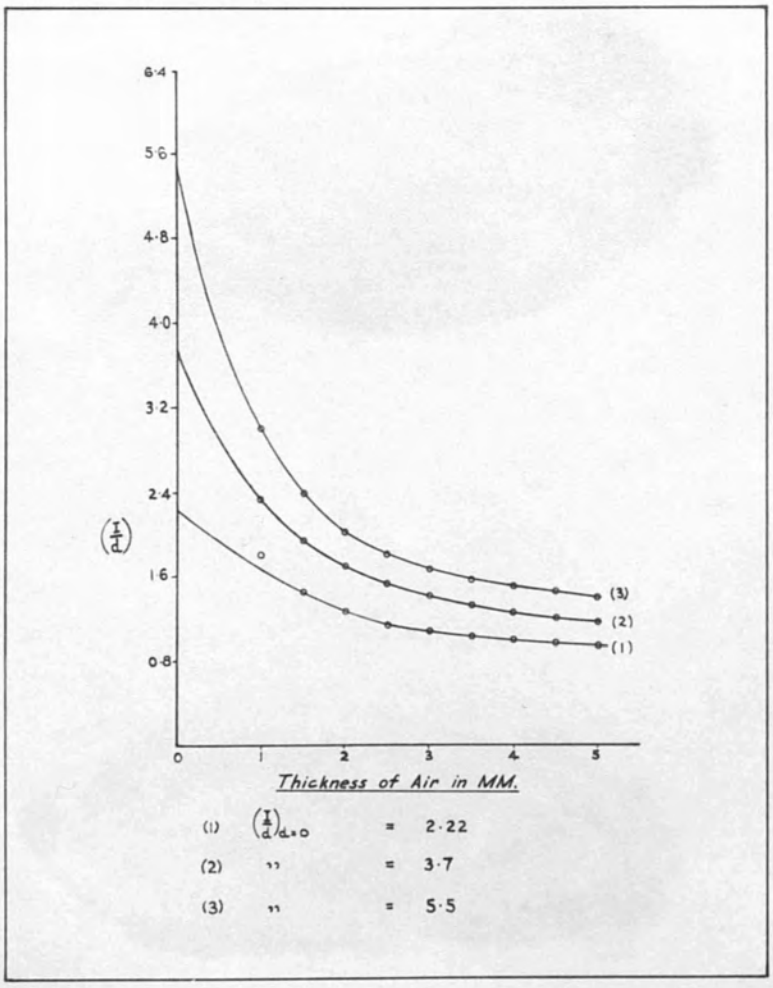

Figure (25).

Ionization per unit spacing - Electrode Spacing Curves.

Effective wavelength = 0.5 A°.

(1) Electrodes:- Pressed mixture of $\bar{Z}$ = 12.84.
(2) " " " " $\bar{Z}$ = 17.04.
(3) " " " " $\bar{Z}$ = 20.84.

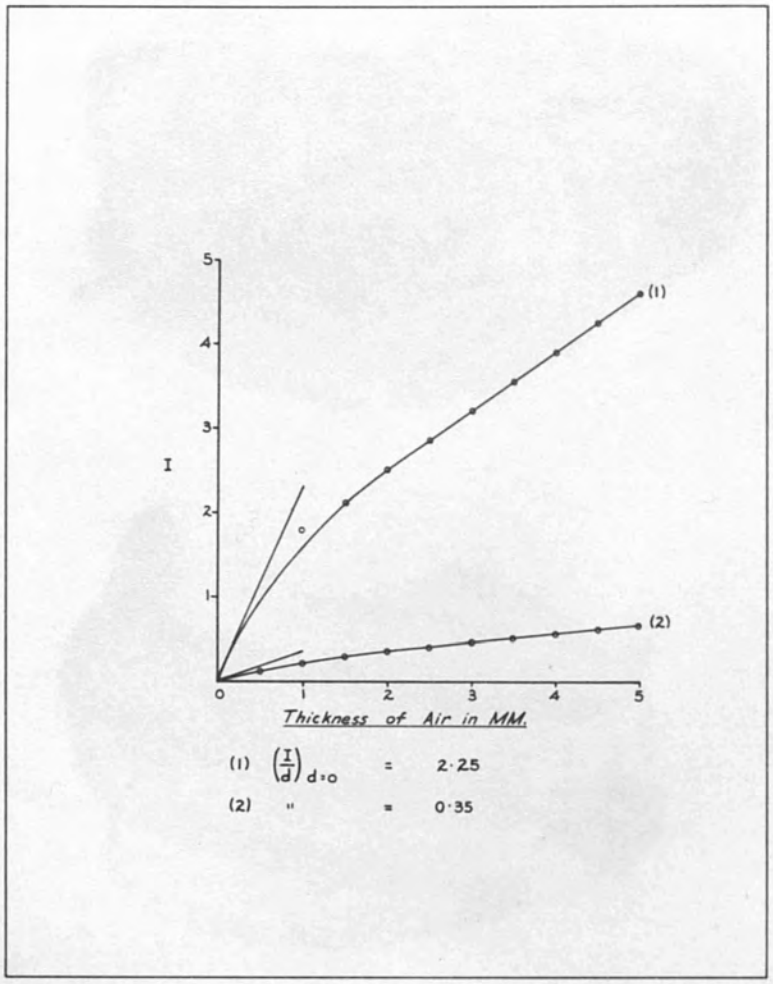

Figure (26).

Ionization - Electrode Spacing Curves.
Electrodes:- Pressed mixture of $\bar{Z}$ = 12.84.

(1) Effective wavelength = 0.5 A°.
(2) " " = 0.328 A°.

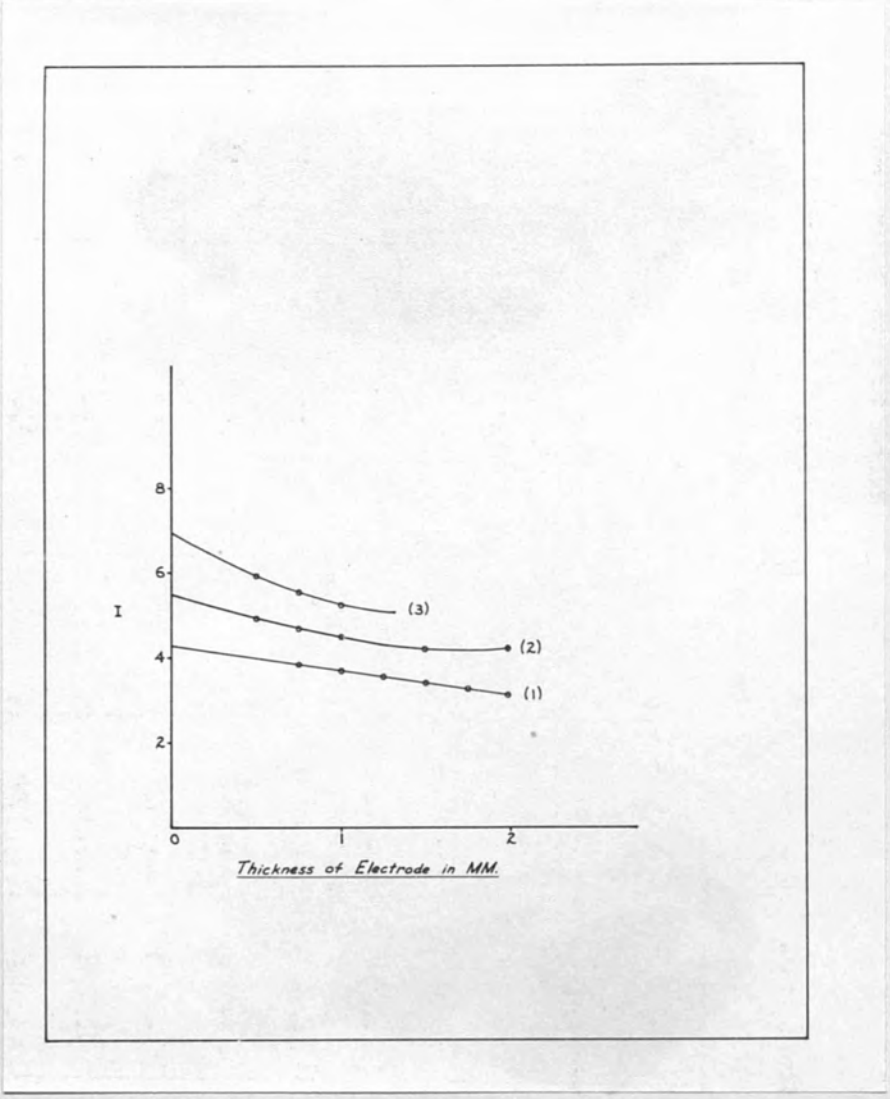

Figure (27).

Extrapolation of I to zero electrode thickness.

Effective wavelength = 0.5 A°.

(1) Electrodes:- Pressed mixture of $\frac{Z}{\bar{Z}}$ = 12.84.
(2) " " " " $\frac{Z}{\bar{Z}}$ = 17.04.
(3) " " " " $\frac{Z}{\bar{Z}}$ = 20.84.

TABLE (23)

60 KVp. 4 m.a.

1 mm. Aluminium (Primary filter)

$\lambda_e = 0.5\ A^o$

Thickness of the upper electrode 0.75 M.M.

($\bar{Z} = 12.84$)

Air thickness in M.M.	Scale Reading	$\frac{1}{I}$	I	$\frac{I}{d}$
1.0	21.5	0.55	1.8	1.8
1.5	87.1	0.47	2.132	1.421
2.0	64.5	0.399	2.506	1.253
2.5	49.9	0.3487	2.867	1.1468
3.0	39.5	0.310	3.225	1.075
3.5	30.9	0.280	3.571	1.020
4.0	24.3	0.2554	3.916	0.979
4.5	18.4	0.235	4.255	0.945
5.0	14.4	0.2179	4.590	0.918

See figures (25 & 26) curves (1 & 1)

TABLE (24)

Extrapolation of I to Zero Electrode Spacing

$\bar{Z} = 12.84$ electrode

(Separation between electrodes 4 M.M.)

$\lambda_e = 0.5\ A^o$

Thickness of electrode in cm.	I
0.075	3.916
0.1	3.637
0.125	3.593
0.15	3.390
0.175	3.290
0.20	3.164

See figure (27) curve (1)

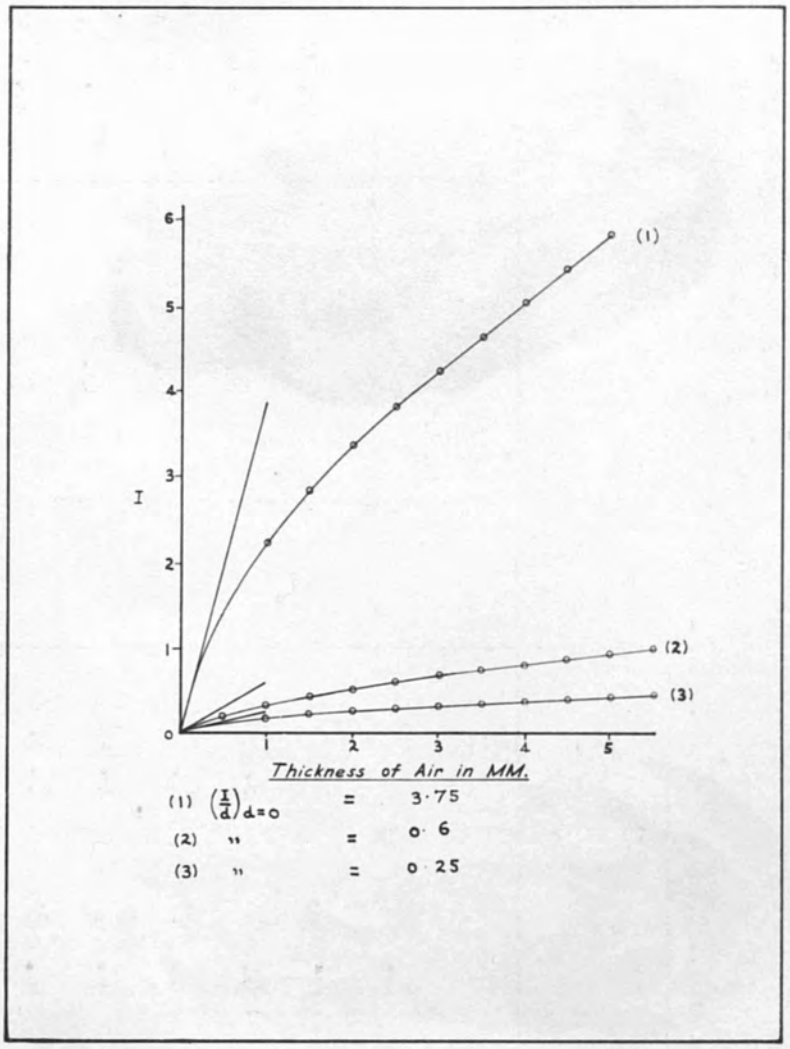

Figure (28).

Ionization - Electrode Spacing Curves.
Electrodes:- Pressed mixture of $\frac{-}{Z}$ = 17.04.

(1) Effective wavelength = 0.5 A°.
(2) " " = 0.328 A°.
(3) " " = 0.256 A°.

TABLE (25)

60 KV_p. 4 m.a.
1 mm. Aluminium (Primary filter)

$\lambda_e = 0.5\ A^o$

Thickness of the upper electrode 0.5 M.M. ($\bar{Z} = 17.04$)

Air thickness in M.M.	Scale Reading	$\frac{1}{I}$	I	$\frac{I}{d}$
1.0	75.0	0.4337	2.300	2.300
1.5	50.5	0.3500	2.857	1.905
2.0	35.5	0.295	3.39	1.695
2.5	25.5	0.260	3.846	1.5384
3.0	19.5	0.2358	4.24	1.413
3.5	14.2	0.2160	4.629	1.322
4.0	9.2	0.1993	5.018	1.254
4.5	5.3	0.1853	5.396	1.199
5.0	2.0	0.1733	5.771	1.1542

See figures (25 & 28) curve (2 & 1)

TABLE (26)

Extrapolation of I to Zero Electrode Spacing

$\bar{Z} = 17.04$ electrode
(Separation between electrodes 4 M.M.)

$\lambda_e = 0.5\ A^o$

Thickness of electrode in cm.	I
0.05	5.018
0.075	4.635
0.10	4.441
0.15	4.227
0.2	4.166

See figure (27) curve (2)

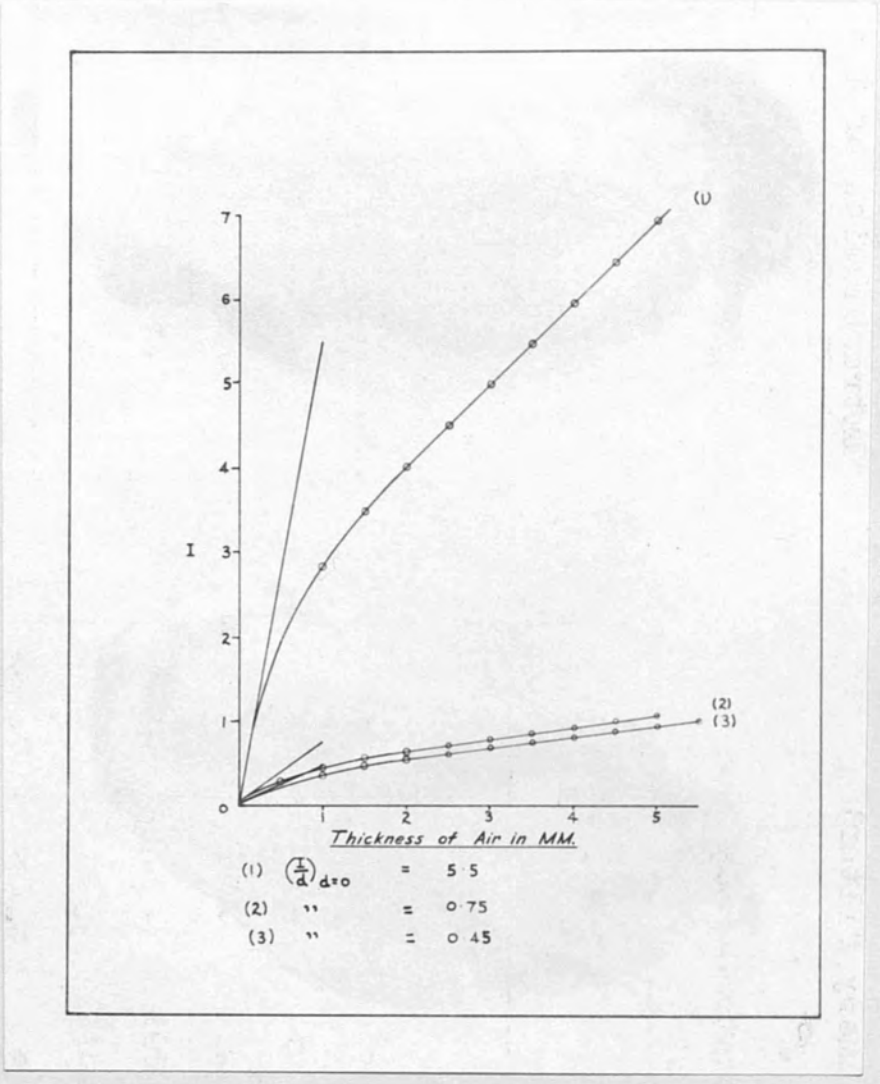

Figure (29).

Ionization - Electrode Spacing Curves.
Electrodes:- Pressed mixture of $\frac{}{Z}$ = 20.84.

(1) Effective wavelength = 0.5 A°.
(2) " " = 0.425 A°.
(3) " " = 0.12 A°.

TABLE (27)

60 KV_p. 4 m.a.

1 mm. Aluminium (Primary filter)

$\lambda_e = 0.5\ A^o$

Thickness of the upper electrode 0.5 M.M.

($\bar{Z} = 20.84$)

Air thickness in M.M.	Scale Reading	$\frac{1}{I}$	I	$\frac{I}{d}$
1.0	46.3	0.328	2.985	2.985
1.5	32.6	0.285	3.51	2.34
2.0	22.5	0.2483	4.027	2.0135
2.5	15.0	0.2201	4.543	1.8172
3.0	34.5	0.198	5.05	1.683
3.5	3.8	0.18	5.479	1.565
4.0	21.6	0.166	6.00	1.5
4.5	16.8	0.154	6.5	1.444
5.0	13.5	0.145	6.9	1.38

See figures (25 & 29) curves (3 & 1)

TABLE (28)

Extrapolation of I to Zero Electrode Spacing

$\bar{Z} = 20.84$ electorde

(Separation between electrodes 4 M.M.)

$\lambda_e = 0.5\ A^o$

Thickness of electrode in cm.	I
0.05	6
0.075	5.455
0.1	5.242

See figure (27) curve (3)

TABLE (29)

80 KV_p. 3 m.a.

2 mm. Aluminium (Primary filter)

$\lambda_e = 0.425\ A^o$

Thickness of the upper electrode 2 M.M. Al.

Air thickness in M.M.	Scale Reading	$\frac{1}{I}$	I	$\frac{I}{d}$
1.0	47.9	0.77	1.299	1.299
1.5	34.9	0.6653	1.503	1.002
2.0	26.3	0.586	1.707	0.853
2.5	18.9	0.5262	1.9	0.76
3.0	13.8	0.4807	2.08	0.693
3.5	77.8	0.4475	2.26	0.646
4.0	68.1	0.4117	2.429	0.607
4.5	60.5	0.385	2.598	0.577
5.0	55.1	0.3664	2.729	0.5458

See figures (18 & 19) curves (2 & 2)

TABLE (30)

Extrapolation of I to Zero Electrode Spacing

Aluminium electrode
(Separation between electrodes 4 M.M.)

$\lambda_e = 0.425\ A^o$

Thickness of electrode in cm.	I
0.075	3.4
0.10	3.125
0.125	2.892
0.15	2.765
0.175	2.547
0.20	2.429

Monitor factor = $\frac{1}{0.3425}$

See figure (20) curve (2)

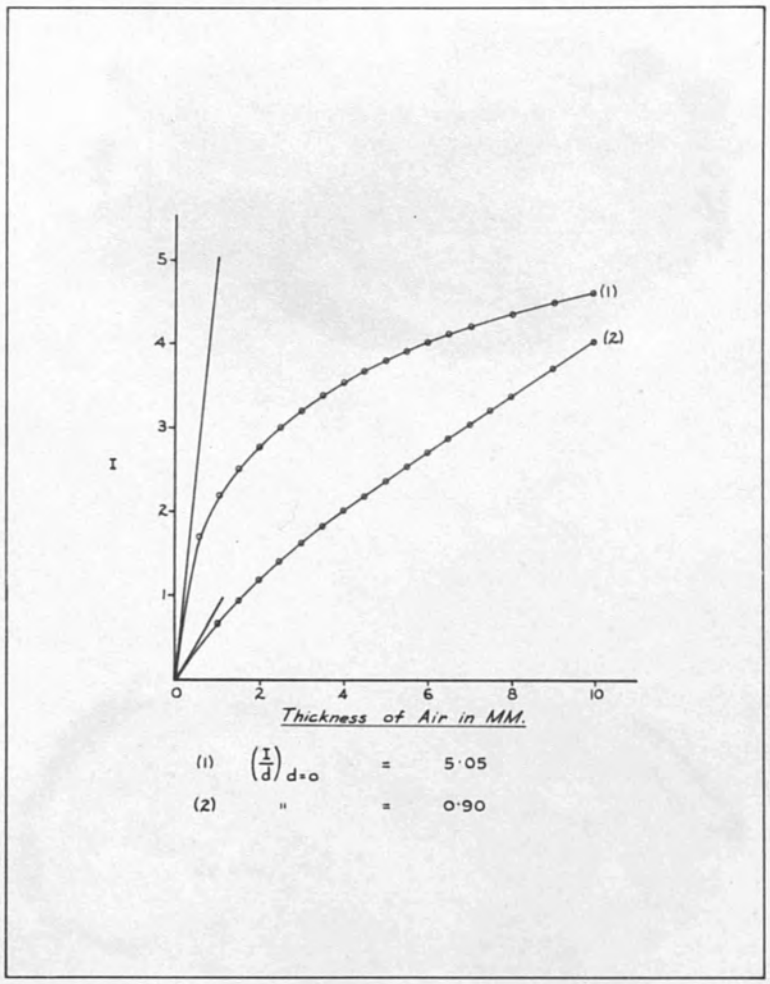

Figure (30).

Ionization - Electrode Spacing Curves.
Electrodes:- Copper.

(1) Effective wavelength = 0.425 A°.
(2) " " = 0.1 A°.

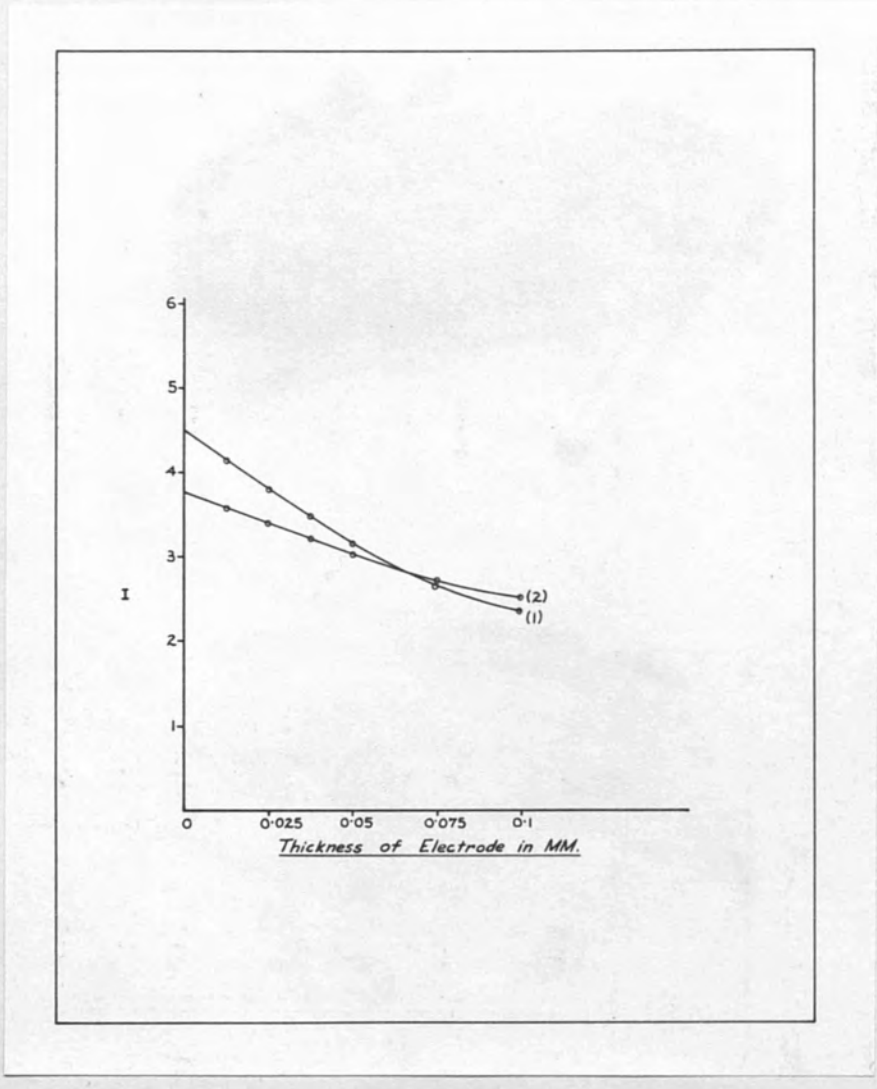

Figure (31).

Extrapolation of I to zero electrode thickness.
Electrodes:- Copper.

(1) Effective wavelength = 0.425 A^{o}.
(2) " " = 0.328 A^{o}.

TABLE (31)

80 KV_p. 3 m.a.

2 mm. Aluminium (Primary filter)

$\lambda_e = 0.425\ A^o$

Thickness of the upper electrode 0.0125 M.M. Copper

Air thickness in M.M.	Scale Reading	$\frac{1}{I}$	I	$\frac{I}{d}$
0.5	25	0.5769	1.734	3.468
1.0	78.5	0.4433	2.256	2.256
1.5	63.6	0.3953	2.530	1.687
2.0	53.9	0.3617	2.765	1.382
2.5	45.9	0.333	3.000	1.200
3.0	40.0	0.3111	3.215	1.071
3.5	35.1	0.2925	3.419	0.977
4.0	31.5	0.2811	3.557	0.889
4.5	28.5	0.2717	3.621	0.818
5.0	25.9	0.2628	3.805	0.7610
5.5	24.3	0.2554	3.916	0.712
6.0	22.5	0.2483	4.027	0.671
6.5	21.0	0.241	4.138	0.637
7	20.0	0.2372	4.216	0.602
8	17.5	0.230	4.348	0.543
9	15.9	0.2231	4.482	0.498
10	14.5	0.2179	4.590	0.4590

See figures (39 & 30) curves (1 & 1)

TABLE (32)

Extrapolation of I to Zero Electrode Spacing

Copper Electrode

(Separation between electrodes 6.5 M.M.)

$\lambda_e = 0.425\ A^o$

Thickness of electrode in cm.	I
0.00125	4.138
0.0025	3.81
0.00375	3.468
0.005	3.12
0.0075	2.63
0.01	2.361

Monitor factor = $\frac{1}{0.0604}$

See figure (31) curve (1)

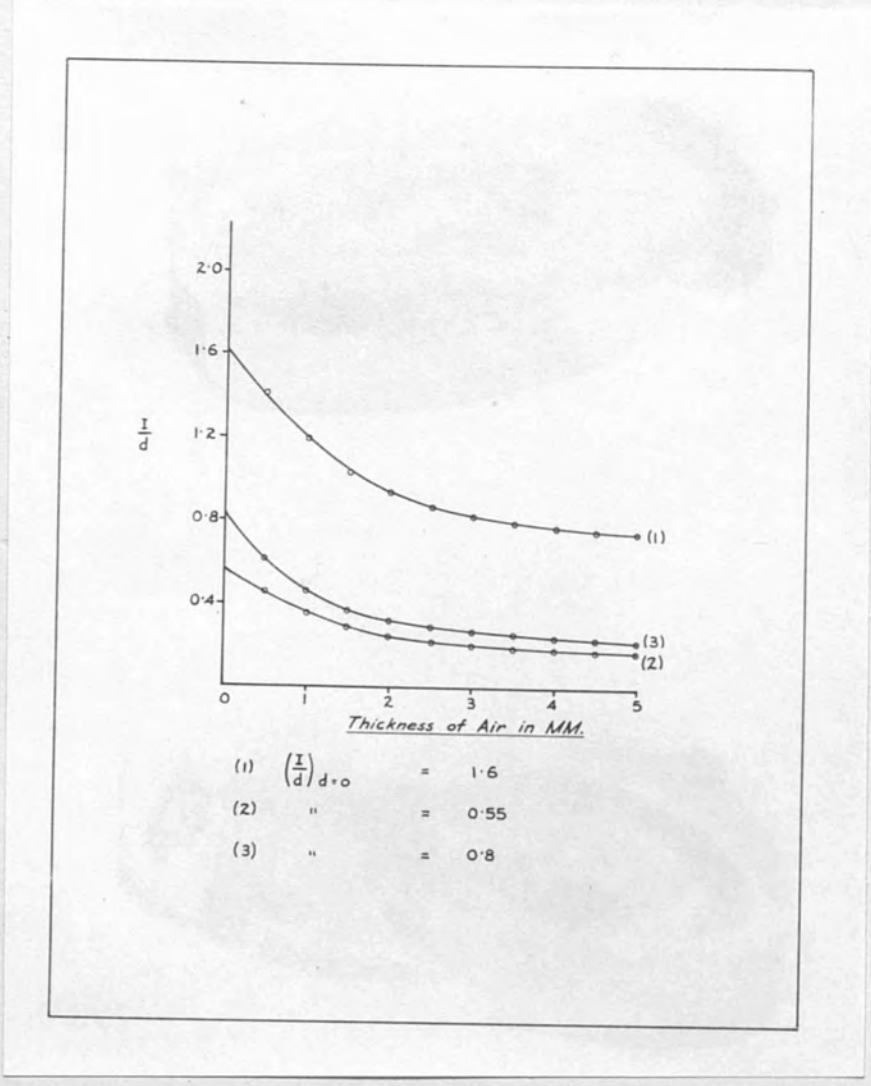

Figure (32).

Ionization per unit spacing - Electrode Spacing Curves.

Effective wavelength = 0.425 A°.

(1) Electrodes:- Pressed mixture of $\frac{I}{Z}$ = 12.84.
(2) " " " " $\frac{I}{Z}$ = 17.04.
(3) " " " " $\frac{I}{Z}$ = 20.84.

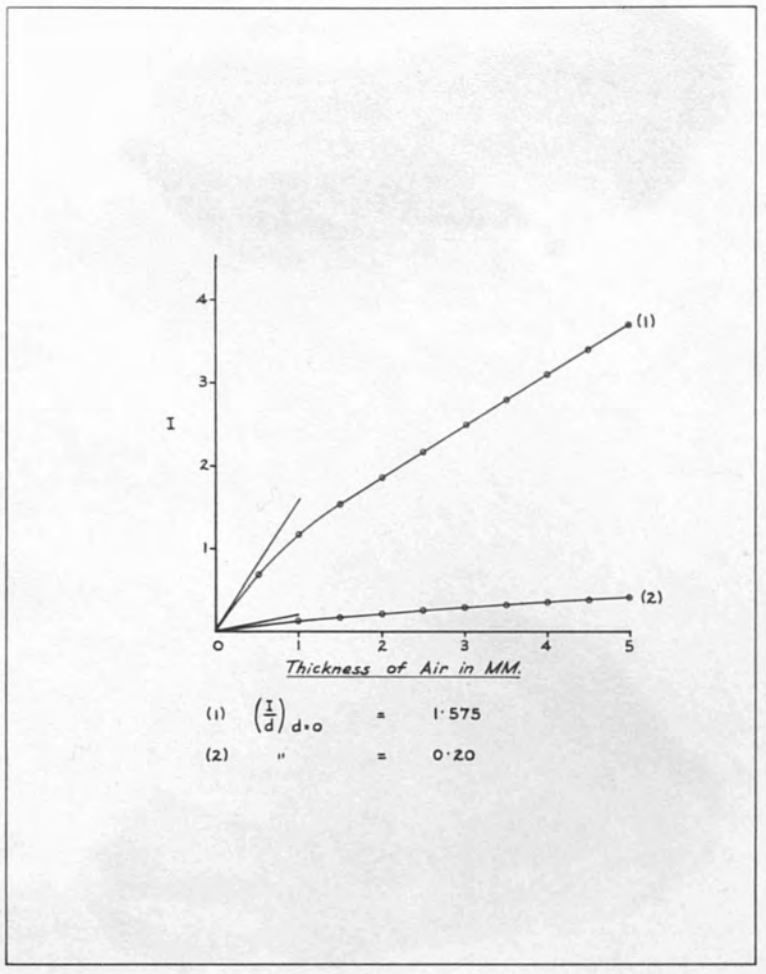

Figure (33).

Ionization - Electrode Spacing Curves.
Electrodes:- Pressed mixture of $\frac{-}{Z}$ = 12.84.

(1) Effective wavelength = 0.425 A°.
(2) " " = 0.172 A°.

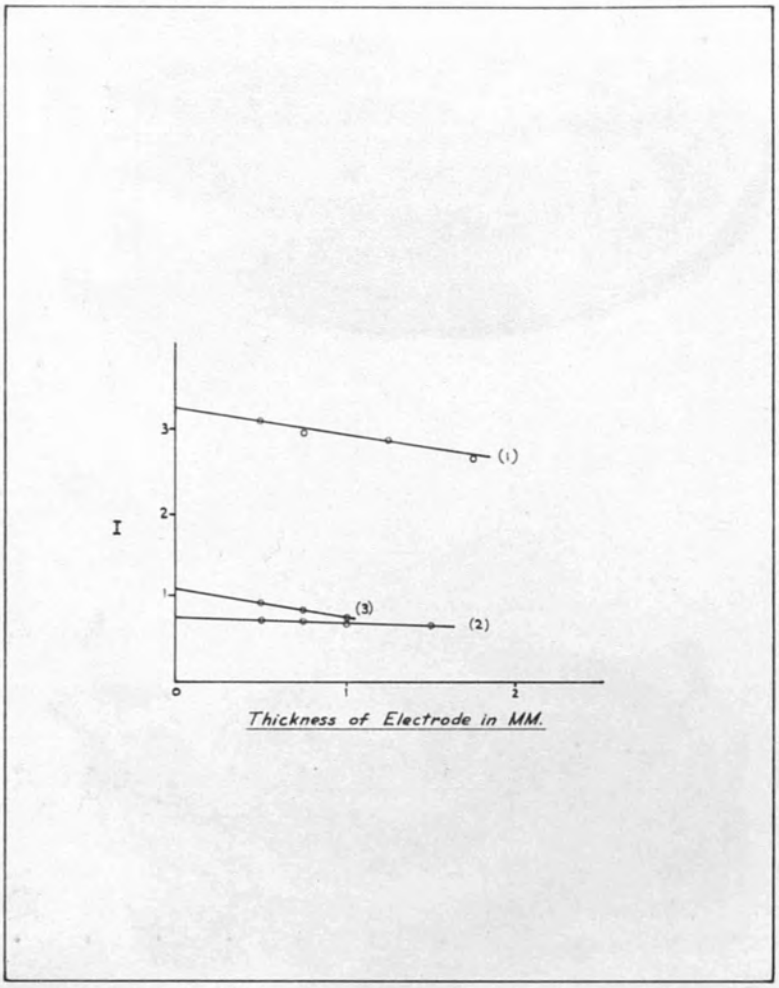

Figure (34).

Extrapolation of I to zero electrode thickness.

Effective wavelength = 0.425 A^{o}.

(1) Electrodes:- Pressed mixture of $\frac{z}{z_1 z_2}$ = 12.84.
(2) " " " " = 17.04.
(3) " " " " = 20.84.

TABLE (33)

80 KVp. 3 m.a.

2 mm. Aluminium (Primary filter)

λ_e = 0.425 A°

Thickness of the upper electrode 0.5 M.M. ($\bar{Z}$ = 12.84)

Air thickness in M.M.	Scale Reading	$\frac{1}{I}$	I	$\frac{I}{d}$
0.5	40.1	-	0.7119	1.4238
1.0	57.5	0.84	1.191	1.191
1.5	35.1	0.6653	1.503	1.002
2.0	20.1	0.5371	1.862	.931
2.9	82.0	0.4567	2.190	0.876
3.0	65.2	0.40	2.50	0.833
3.5	53.0	0.3583	2.797	0.799
4.0	42.9	0.3233	3.093	0.773
4.5	36.0	0.2967	3.370	0.749
5.0	28.5	0.2717	3.681	0.7362

See figures (32 & 33) curve (1 & 1)

TABLE (34)

Extrapolation of I to zero Electrode Spacing

$\bar{Z}$ = 12.84 electrode

(Separation between electrodes 4 M.M.)

λ_e = 0.425 A°

Thickness of electrode in cm.	I
0.5	3.093
7.5	2.926
1.25	2.752
1.75	2.625

See figure (34) curve (1)

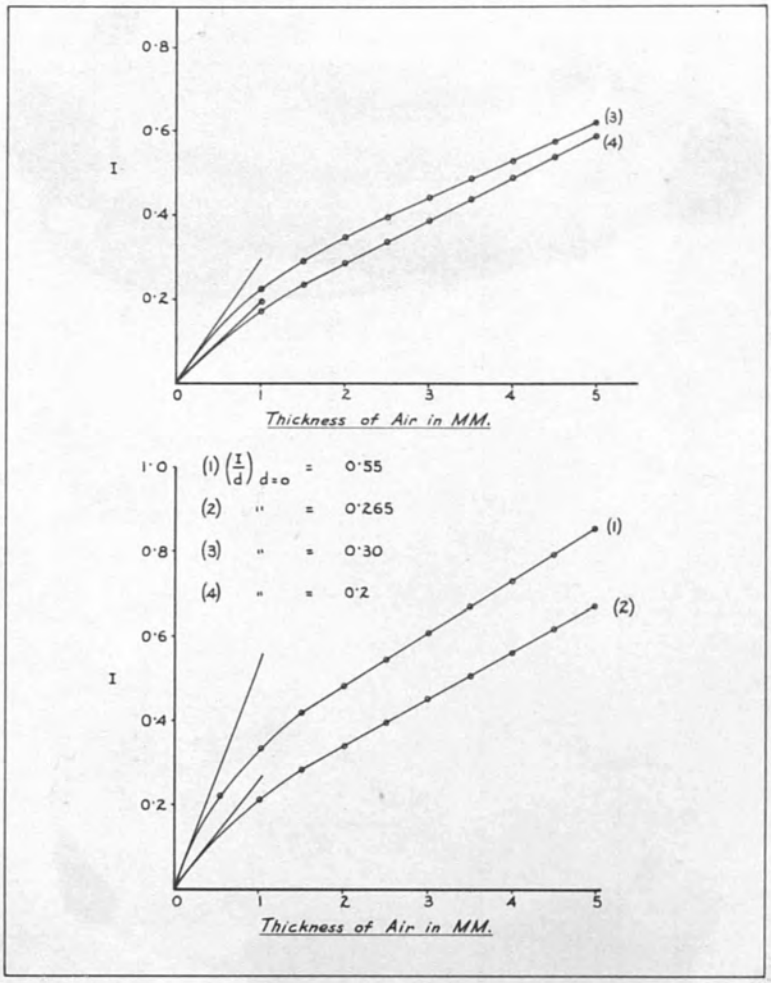

Figure (35).

Ionization - Electrode Spacing Curves.
Electrodes:- Pressed mixture of $\bar{z} = 17.04$.

(1) Effective wavelength = 0.425 A°.
(2) " " = 0.12 A°.
(3) " " = 0.172 A°.
(4) " " = 0.1 A°.

TABLE (35)

80 KV_P. 3 m.a.

2 mm. Aluminium (Primary filter)

λ_e = 0.425 A^o

Thickness of the upper electrode 0.5 M.M.

($\bar{Z}$ = 17.04)

Air thickness in M.M.	Scale Reading	I	$\frac{I}{d}$
0.5	17.5	0.23	0.46
1.0	47.5	0.34	0.34
1.5	6.6	0.42	0.28
2.0	13.8	0.485	0.2425
2.5	21.9	0.550	0.220
3.0	28.9	0.613	0.204
3.5	36.2	0.677	0.193
4.0	44.6	0.74	0.185
4.5	52.8	0.8	0.178
5	59.8	0.86	0.172

See figures (32 & 35) curves (2 & 1)

TABLE (36)

Extrapolation of I to Zero Electrode Spacing

$\bar{Z}$ = 17.04 electrode

(Separation between electrodes 4 M.M.)

λ_e = 0.425 A^o

Air thickness in M.M.	I
0.5	0.74
0.75	0.70
1.0	0.68
1.5	0.66

Monitor factor = $\frac{3.2}{0.6}$

See figure (34) curve (2)

TABLE (37)

80 KVp. 3 m.a.

2 mm. Aluminium (Primary filter)

λ_e = 0.425 A°

Thickness of the upper electrode 0.5 M.M.
($\bar{Z}$ = 20.84)

Air thickness in M.M.	Scale Reading	I	$\frac{I}{d}$
0.5	40.	0.311	0.622
1.0	9.1	0.44	0.44
1.5	20.0	0.537	0.358
2.0	29.8	0.62	0.32
2.5	39.0	0.70	0.28
3.0	49.9	0.777	0.259
3.5	58.9	0.8533	0.2438
4.0	68.1	0.9267	0.2317
4.5	77.5	0.9933	0.2207
5	86.7	1.06	0.212

See figures (32 & 29) curves (3 & 2)

TABLE (38)

Extrapolation of I to Zero Electrode Spacing

$\bar{Z}$ = 20.84 electrode
(Separation between electrodes 4 M.M.)

λ_e = 0.425 A°

Thickness of electrode in cm.	I
0.05	0.9267
0.075	0.86
0.10	0.74

Monitor factor = $\frac{3.2}{0.6}$

See figure (34) curve (3)

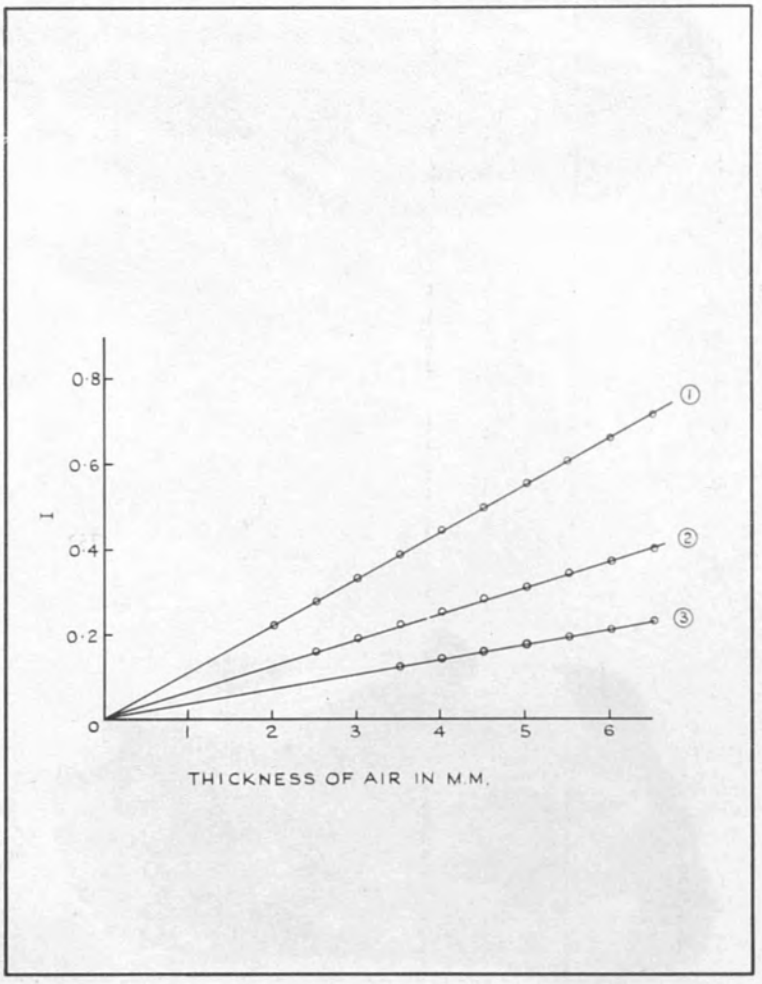

Figure (36).

Ionization - Electrode Spacing Curves.
Electrodes:- Perspex coated with dag.

(1) Effective wavelength = 0.328 A°.
(2) " " = 0.172 A°.
(3) " " = 0.256 A°.

TABLE (39)

100 KV_p. 3 m.a.
4 mm. Aluminium (Primary filter)

$\lambda e = 0.328$ A°.

Upper electrode Perspex coated with dag or
($\bar{Z} = 7.64$)

Air thickness in M.M.	Scale Reading	R´
2.0	15	0.22
2.5	29.5	0.275
3.0	45.2	0.33
3.5	60.7	0.385
4.0	8.0	0.44
4.5	15.6	0.495
5.0	21.8	0.55
5.5	28.0	0.605
6.0	34.5	0.66
6.5	41.0	0.715

The slope of the curve = 0.11

See figure (36) curve (1)

TABLE (40)

170 KV_p. 15 m.a.
Zero filter

$\lambda e = 0.256$ A°.

Upper electrode Perspex coated with dag or
($\bar{Z} = 7.64$)

Air thickness in M.M.	Scale Reading	R´
3.5	5.6	0.1225
4.0	11.5	0.14
4.5	16.0	0.157
5.0	24.5	0.1745
5.5	7.5	0.1917
6.0	12.5	0.210
6.5	17.5	0.2283

The slope of the curve = 0.035

See figure (36) curve (3)

TABLE (41)

150 KVp. 3 m.a.
0.5 mm. copper + 1 mm. Aluminium (Primary filter)

$\lambda_e = 0.172\ A^o$.

upper electrode Perapex coated with dag.

Air thickness in M.M.	Scale Reading	R′
2.5	14.2	0.16
3.0	6.8	0.19
3.5	15.0	0.22
4.0	22.9	0.25
4.5	31.5	0.28
5.0	39.6	0.31
5.5	47.5	0.34
6.0	56.5	0.37
6.5	65.1	0.40

The slope of the curve = 0.06

See figure (36) curve (2)

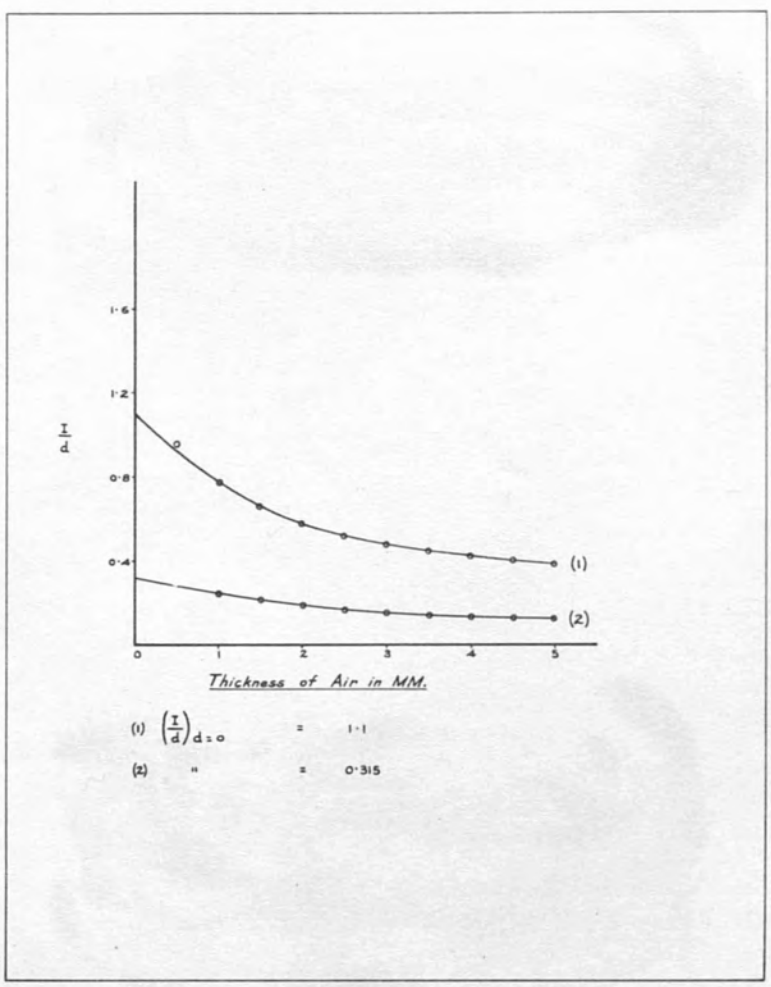

Figure (37).

Ionization per unit spacing - Electrode Spacing Curves.
Electrodes:- Aluminium.

(1) Effective wavelength = 0.328 A°.
(2) " " = 0.256 A°.

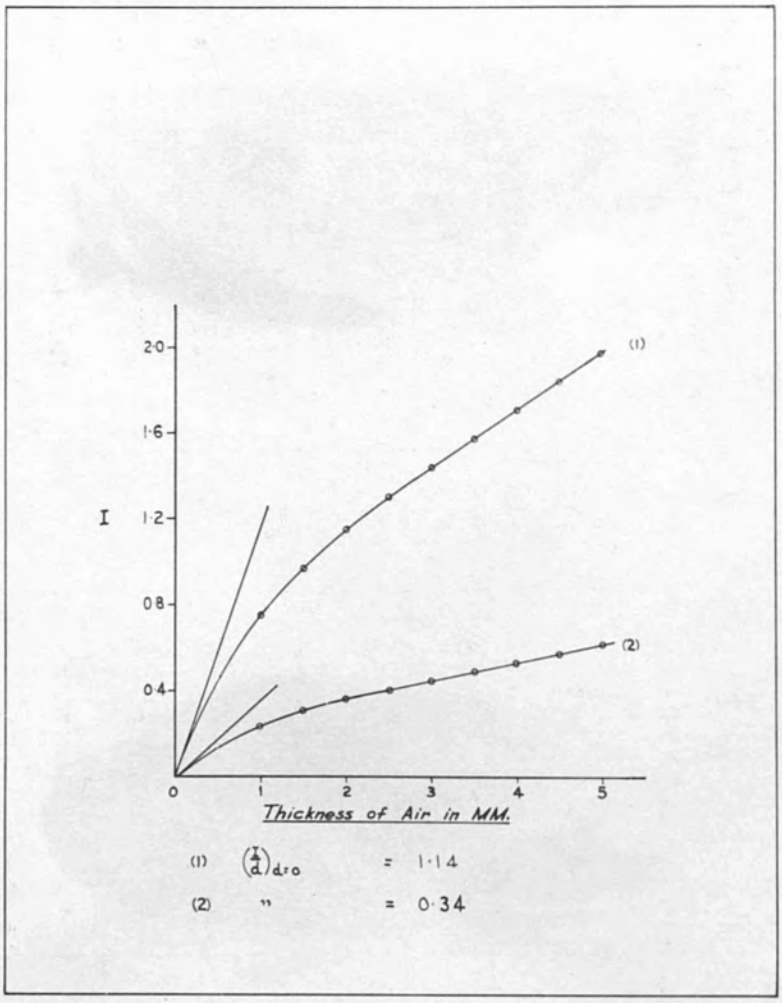

Figure (38).

Ionization - Electrode Spacing Curves.
Electrodes:- Aluminium.

(1) Effective wavelength = 0.328 A°.
(2) " " = 0.256 A°.

TABLE (42)

100 KV_p. 3 m.a.

4 mm. Aluminium (Primary filter)

$\lambda_e = 0.328$ A°

Thickness of the upper electrode 2 M.M. Al.

Air thickness in M.M.	Scale Reading	$\frac{1}{I}$	I	$\frac{I}{d}$
1.0	46.5	-	0.760	0.760
1.5	74.9	-	0.9768	0.6512
2.0	62.0	0.8733	1.145	0.5725
2.5	68.1	0.7667	1.304	0.5216
3.0	37.9	0.6869	1.456	0.485
3.5	31.2	0.6318	1.580	0.451
4.0	26.5	0.5867	1.740	0.432
4.5	21.5	0.5467	1.825	0.405
5.0	18.1	0.5167	1.935	0.3870

See figures (37 & 38) curves (1 & 1)

TABLE (43)

Extrapolation of I to Zero Electrode Spacing

Aluminium electrode
(Separation between electrodes 4 M.M.)

$\lambda_e = 0.328$ A°

Thickness of electrode in cm.	I
0.075	2.013
0.10	1.96
0.125	1.9
0.150	1.825
0.175	1.755
0.2	1.704

See figure (20) curve (3)

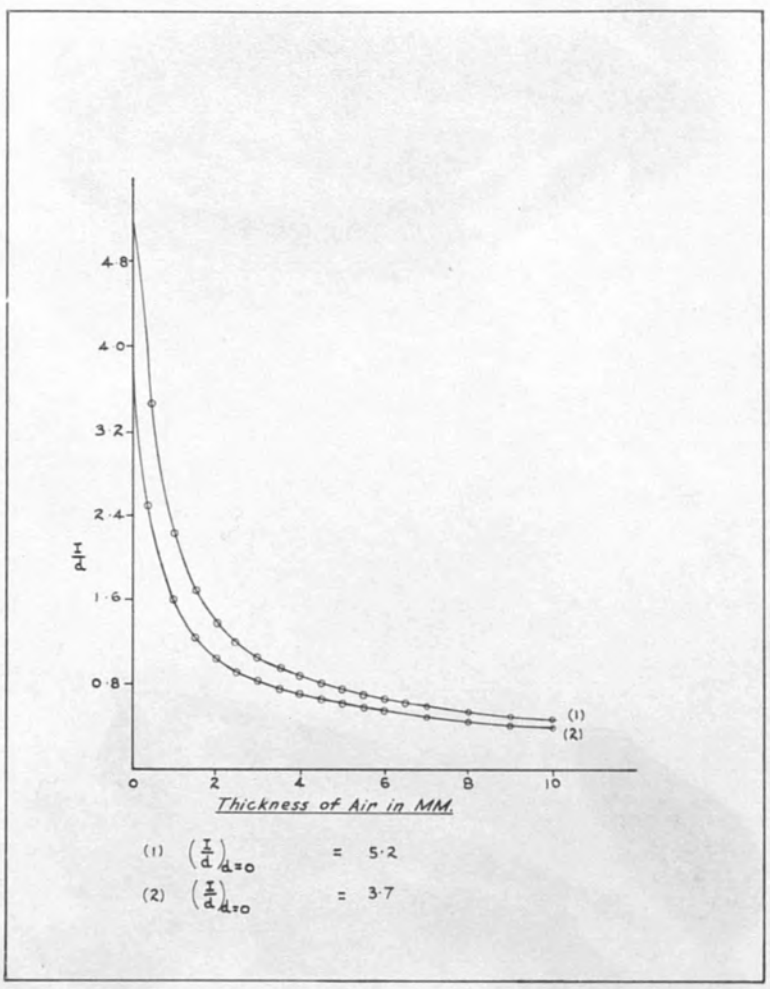

Figure (39).

Ionization per unit spacing - Electrode Spacing Curves.
Electrodes:- Copper.

(1) Effective wavelength = 0.425 A°.
(2) " " = 0.328 A°.

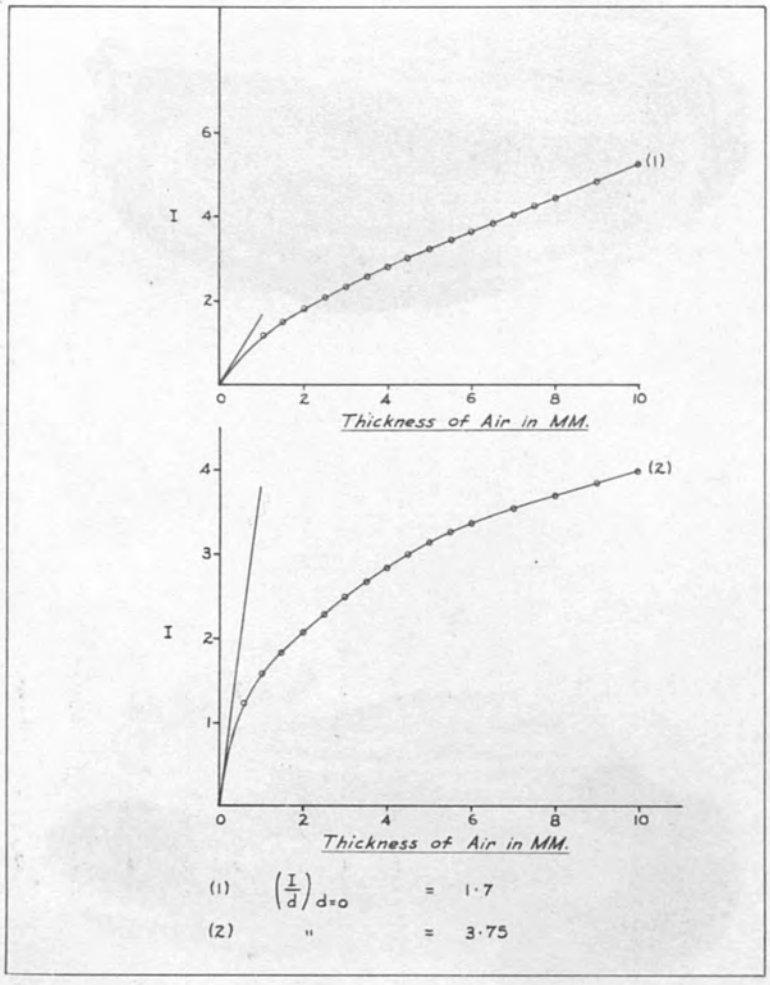

Figure (40).

Ionization - Electrode Spacing Curves.
Electrodes:- Copper.

(1) Effective wavelength = 0.12 A°.
(2) " " = 0.328 A°.

TABLE (44)

100 KV_p. 3 m.a.

4 mm. Aluminium (Primary filter)

$\lambda_e = 0.328$ A°

Thickness of the upper electrode 0.0125 M.M: Copper

Air thickness in M.M.	Scale Reading	$\frac{1}{I}$	I	$\frac{I}{d}$
0.5	51.5	0.7967	1.255	2.510
1.0	30.5	0.6232	1.604	1.604
1.5	19.9	0.537	1.862	1.241
2.0	89.5	0.4792	2.086	1.043
2.5	75.8	0.4350	2.300	0.92
3.0	65.2	0.4	2.500	0.833
3.5	58.5	0.3767	2.655	0.76
4.0	51.9	0.356	2.809	0.702
4.5	47.0	0.3367	2.97	0.66
5.0	42.5	0.32	3.125	0.6250
5.5	38.5	0.3067	3.255	0.592
6.0	36.1	0.2967	3.37	0.561
7.0	31.5	0.2811	3.556	0.508
8	28.1	0.27	3.703	0.463
9	25.5	0.2597	3.85	0.428
10	23.6	0.2517	3.973	0.3973

See figures (39 & 40) curves (2 & 2)

TABLE (45)

Extrapolation of I to Zero Electrode Spacing

Copper Electrode

(Separation between electrodes 7 M.M.)

$\lambda_e = 0.328$ A°

Thickness of electrode in cm.	I
0.00125	3.556
0.0025	3.419
0.00375	3.193
0.005	3.012
0.0075	2.7
0.01	2.511

Monitor factor = $\frac{1}{0.02207}$

See figure (31) curve (2)

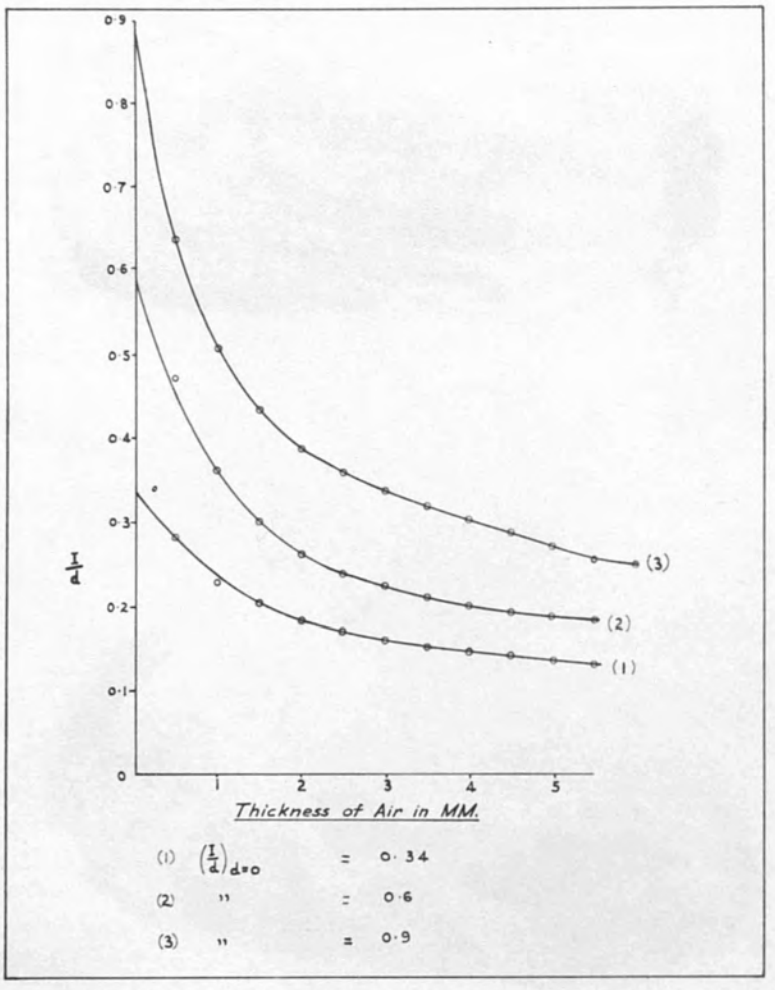

Figure (41).

Ionization per unit spacing - Electrode Spacing Curves.

Effective wavelength = 0.328 A°.

(1) Electrodes:- Pressed mixture of $\bar{z}$ = 12.84.
(2) " " " " $\bar{z}$ = 17.04.
(3) " " " " $\bar{z}$ = 20.84.

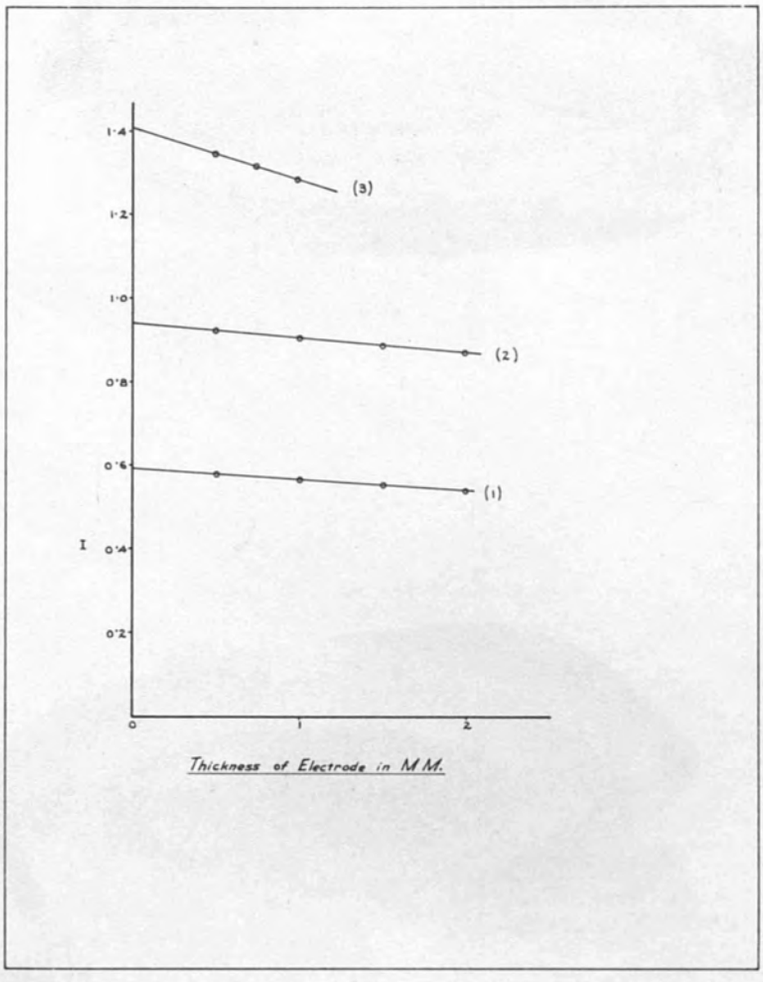

Figure (42).

Extrapolation of I to zero electrode thickness.

Effective wavelength = 0.328 A°.

(1) Electrodes:- Pressed mixture of $\frac{z}{z_2}$ = 12.84.
(2) " " " " $\frac{z}{z_2}$ = 17.04.
(3) " " " " $\frac{z}{z_2}$ = 20.84.

TABLE (46)

100 KVp. 3 m.a.
4 mm. Aluminium (Primary filter)
$\lambda_e = 0.328\ A^o$

Thickness of the upper electrode 0.5 M.M. ($\bar{Z} = 12.84$)

Air thickness in M.M.	Scale Reading	I	$\frac{I}{d}$
0.5	11.6	0.14	0.28
1.0	17.5	0.2283	0.2283
1.5	37.2	0.3008	0.2008
2.0	55.0	0.3664	0.1832
2.9	7.1	0.4250	0.17000
3.0	13.5	0.480	0.160
3.5	19.5	0.530	0.151
4.0	25.2	0.58	0.145
4.5	30.6	0.627	0.139
5.0	35.9	0.673	0.1346
5.5	41.4	0.72	0.131

See figures (41 & 26) curves (1 & 2)

TABLE (47)

Extrapolation of I to Zero Electrode Spacing

$\bar{Z} = 12.84$ electrode (Separate between electrodes 4 M.M.)

$\lambda_e = 0.328\ A^o$

Thickness of electrode in cm.	I
0.05	0.58
0.10	0.565
0.15	0.55
0.20	0.54

See figure (42) curve (1)

TABLE (48)

100 KVp. 3 m.a.

4 mm. Aluminium (Primary filter)

$\lambda_e = 0.328$ A°

Thickness of the upper electrode 0.5 M.M.

($\bar{Z} = 17.04$)

Air thickness in M.M.	Scale Reading	I	$\frac{I}{d}$
0.5	20.0	0.2372	0.4744
1.0	52.6	0.3567	0.3567
1.5	8.9	0.440	0.293
2.0	18.6	0.52	0.26
2.5	27.5	0.60	0.24
3.0	35.7	0.67	0.223
3.5	44.5	0.74	0.211
4.0	52.2	0.803	0.2008
4.5	61.0	0.867	0.193
5.0	68.1	0.9267	0.18534
5.5	75.7	0.980	0.178

See figures (41 & 28) curves (2 & 2)

TABLE (49)

Extrapolation of I to Zero Electrode Spacing

$\bar{Z} = 17.04$ electrode

(Separation between electrodes 5 M.M.)

$\lambda_e = 0.328$ A°

Thickness of electrode in cm.	I
0.05	0.9267
0.1	0.8993
0.15	0.8833
0.2	0.8626

See figure (42) curve (2)

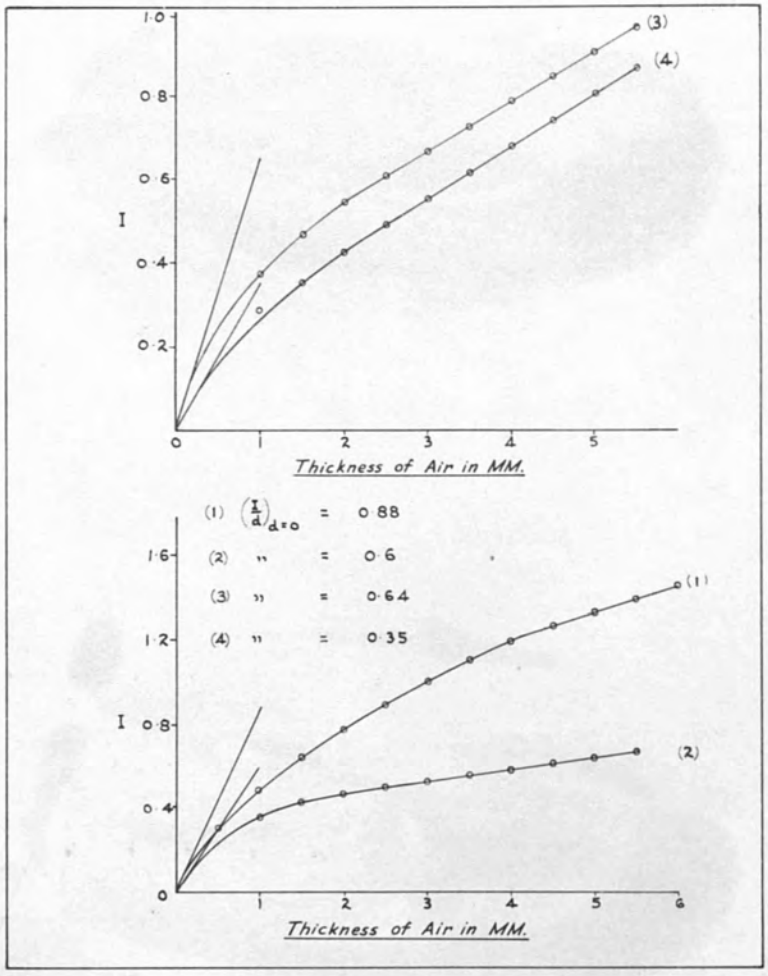

Figure (43).

Ionization - Electrode Spacing Curves.
Electrodes:- Pressed mixture of $\bar{Z}$ = 20.84.

(1) Effective wavelength = 0.328 A°.
(2) " " = 0.256 A°.
(3) " " = 0.172 A°.
(4) " " = 0.1 A°.

TABLE (50)

100 KVp. 3 m.a.

4 mm. Aluminium (Primary filter)

λ_e = 0.328 A°

Thickness of the upper electrode 0.5 M.M.

($\bar{Z}$ = 20.84)

Air thickness in M.M.	Scale Reading	$\frac{1}{I}$	I	$\frac{I}{d}$
0.5	42.2	-	0.32	0.64
1.0	16.1	-	0.50	0.50
1.5	32.2	-	0.64	0.426
2.0	49.5	-	0.78	0.39
2.5	92.5	1.11	0.90	0.36
3.0	76.1	0.9854	1.015	0.338
3.5	64.0	0.89	1.124	0.321
4.0	54.9	0.8256	1.212	0.303
4.5	49.5	0.78	1.282	0.285
5.0	45.0	0.7484	1.337	0.2674
5.5	40.1	0.7119	1.405	0.255
6.0	36.6	0.68	1.471	0.248

See figures (41 & 43) curve (3 & 1)

TABLE (51)

Extrapolation of I to Zero Electrode Spacing

$\bar{Z}$ = 20.84 electrode

(Separation between electrodes 5 M.M.)

λ_e = 0.328 A°

Thickness of electrode in cm.	I
0.05	1.337
0.075	1.316
0.10	1.282

See figure (42) curve (3)

TABLE (52)

170 KV_p. 15 m.a.

Zero filter

λ_e = 0.256 A^o

Thickness of the upper electrode 0.75 M.M. Al.

Air thickness in M.M.	Scale Reading	I	$\frac{I}{d}$
1.0	20.9	0.2417	0.2417
1.5	40.0	0.311	0.207
2.0	0	0.360	0.180
2.5	4.7	0.405	0.1620
3.0	10.0	0.448	0.149
3.5	15.0	0.49	0.14
4.0	19.5	0.530	0.132
4.5	24.0	0.5687	0.126
5.0	28.1	0.605	0.1210

See figures (37 & 38) curves (2 & 2)

TABLE (53)

Extrapolation of I to Zero Electrode Spacing

Aluminium electrode

(Separation between electrode 4 M.M.)

λ_e = 0.256 A^o

Thickness of electrode in cm.	I
0.075	0.530
0.125	0.5133
0.2	0.4912

See figure (20) curve (4)

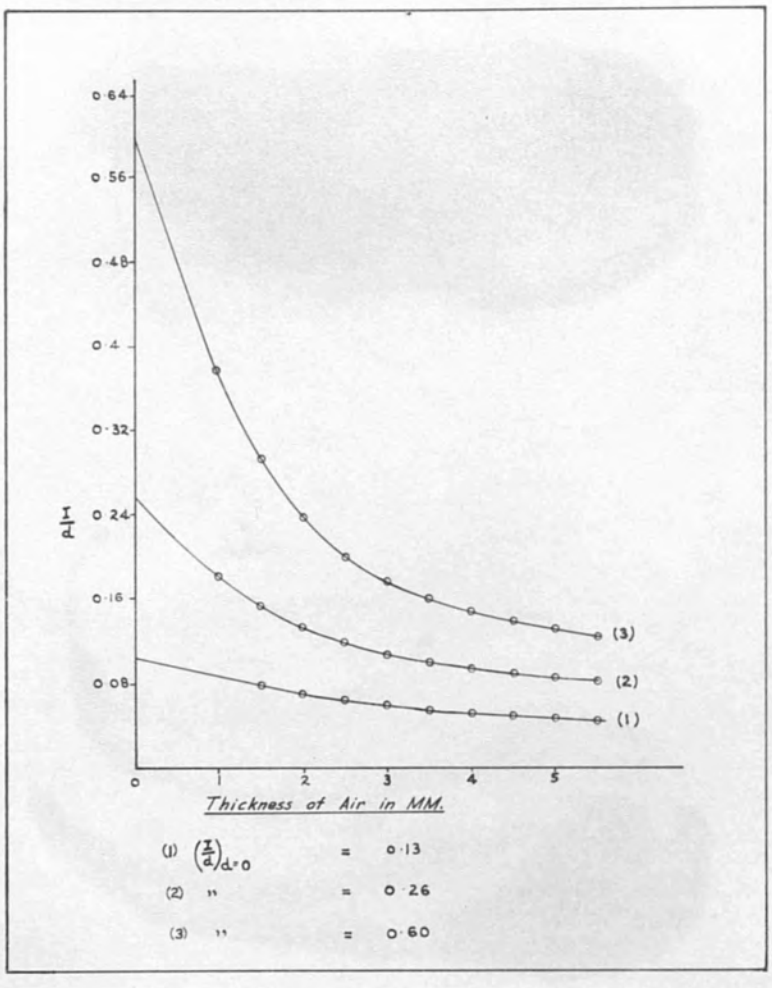

Figure (44).

Ionization per unit spacing - Electrode Spacing Curves.

Effective wavelength = 0.256 A°.

(1) Electrodes:- Pressed mixture of $\frac{Z}{Z} = 12.84.$
(2) " " " " $\frac{Z}{Z} = 17.04.$
(3) " " " " $\frac{Z}{Z} = 20.84.$

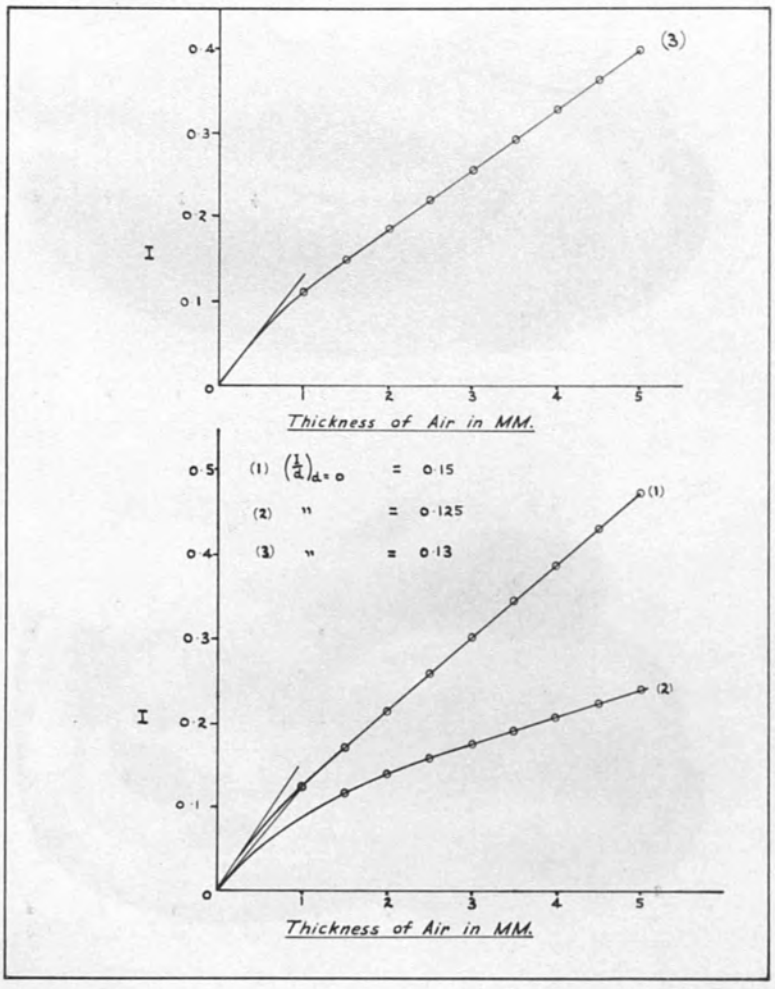

Figure (45).

Ionization - Electrode Spacing Curves.
Electrodes:- Pressed mixture of $\frac{-}{z}$ = 12.84.

(1) Effective wavelength = 0.12 A°.
(2) " " = 0.256 A°.
(3) " " = 0.1 A°.

TABLE (54)

170 KVp. 15 m.a.
Zero filter

λ_e = 0.256 A°

Thickness of the upper electrode 0.5 M.M.
($\bar{Z}$ = 12.84)

Air thickness in M.M.	Scale Reading	I	$\frac{I}{d}$
1.5	4.6	0.12	0.08
2.0	11.5	0.141	0.0705
2.5	20.2	0.161	0.0644
3.0	3.0	0.177	0.059
3.5	7.6	0.1933	0.0553
4.0	11.4	0.209	0.0522
4.5	16.3	0.225	0.05
5.0	20.5	0.240	0.048
5.5	24.2	0.255	0.0463

See figures (44 & 45) curves (1 & 2)

TABLE (55)

170 KVp. 15 m.a.
Zero filter

λ_e = 0.256 A°

Thickness of the upper electrode 0.5 M.M.
($\bar{Z}$ = 17.04)

Air thickness in M.M.	Scale Reading	I	$\frac{I}{d}$
1.0	3.8	0.180	0.18
1.5	17.5	0.230	0.153
2.0	28.1	0.270	0.135
2.5	37.0	0.30	0.12
3.0	43.5	0.325	0.108
3.5	50.4	0.350	0.1
4.0	58.1	0.375	0.09375
4.5	65.0	0.400	0.0889
5.0	72.5	0.425	0.0850
5.5	80.0	0.4487	0.0816

Monitor factor = $\frac{0.21}{0.265}$

See figures (44 & 28) curves (2 & 3)

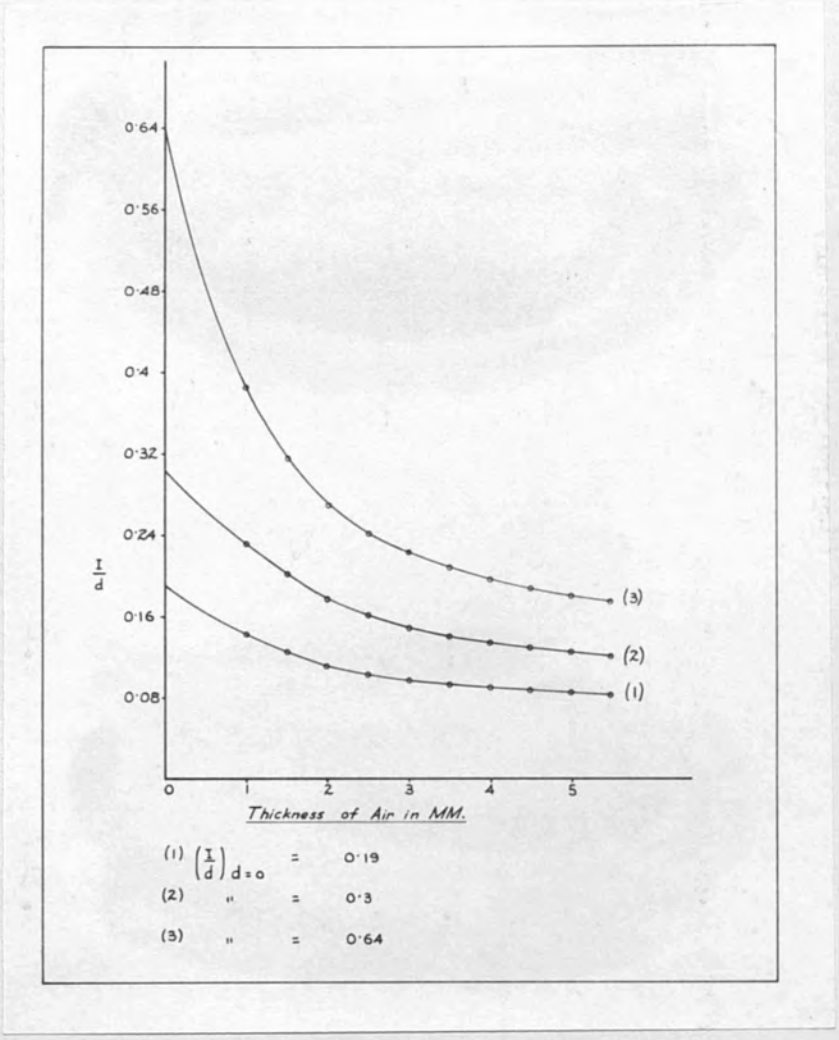

Figure (46).

Ionization per unit spacing - Electrode Spacing Curves.

Effective wavelength = 0.172 A^{o}.

(1) Electrodes:- Pressed mixture of $\frac{Z}{Z}$ = 12.84.
(2) " " " " $\frac{Z}{Z}$ = 17.04.
(3) " " " " $\frac{Z}{Z}$ = 20.84.

TABLE (56)

170 KV_p. 15 m.a.

Zero filter

$\lambda_e = 0.256\ A^o$

Thickness of the upper electrode 0.5 M.M.

($\bar{Z} = 20.84$)

Air thickness in M.M.	Scale Reading	I	$\frac{I}{d}$
1.0	59.3	0.38	0.38
1.5	74.1	0.43	0.287
2.0	86.5	0.47	0.235
2.5	16.1	0.50	0.20
3.0	19.5	0.53	0.177
3.5	23.0	0.56	0.16
4.0	27.0	0.59	0.147
4.5	29.8	0.62	0.138
5.0	33.2	0.65	0.130
5.5	36.7	0.68	0.124

Monitor factor = $\frac{0.21}{0.265}$

See figures (44 & 43) curves (3 & 2)

TABLE (57)

150 KV_p. 15 m.a.

0.5 mm. Cu + 1 mm. Al.

(Primary filter)

$\lambda_e = 0.172\ A^o$

Thickness of the upper electrode 0.5 M.M.

($\bar{Z} = 12.84$)

Air thickness in M.M.	Scale Reading	I	$\frac{I}{d}$
1.0	13.9	0.146	0.146
1.5	5.0	0.1833	0.1232
2.0	15.0	0.220	0.110
2.5	24.3	0.255	0.1020
3.0	34.0	0.290	0.0967
3.5	43.5	0.325	0.0929
4.0	53.0	0.3583	0.0891
4.5	3.2	0.39	0.0867
5.0	6.5	0.42	0.084
5.5	10.0	0.448	0.0814

See figures (46 & 33) curves (1 & 2)

TABLE (58)

150 KV_p. 15 m.a.

0.5 mm. Cu + 1 mm. Al. (Primary filter)

λ_e = 0.172 A°

Thickness of the upper electrode 0.5 M.M. ($\bar{Z}$ = 17.04)

Air thickness in M.M.	Scale Reading	I	$\frac{I}{d}$
1.0	19.5	0.2358	0.2358
1.5	35.1	0.2925	0.1950
2.0	50.0	0.3487	0.1743
2.5	4.2	0.4	0.16
3.0	10.2	0.450	0.15
3.5	15.4	0.495	0.141
4.0	20.4	0.5383	0.1346
4.5	25.5	0.5816	0.1292
5.0	30.0	0.624	0.1248
5.5	35.1	0.6653	0.1209

See figures (46 & 35) curves (2 & 3)

TABLE (59)

150 KV_p. 15 m.a.

0.5 mm. Cu + 1 mm. Al. (Primary filter)

λ_e = 0.172 A°

Thickness of the upper electrode 0.5 M.M. ($\bar{Z}$ = 20.84)

Air thickness in M.M.	Scale Reading	I	$\frac{I}{d}$
1.0	60.6	0.385	0.385
1.5	12.5	0.470	0.313
2.0	21.1	0.545	0.272
2.5	28.7	0.61	0.244
3.0	35.6	0.67	0.223
3.5	43.0	0.73	0.209
4.0	50.7	0.79	0.198
4.5	58.7	0.85	0.190
5.0	66.5	0.91	0.182
5.5	73.5	0.965	0.175

See figures (46 & 43) curves (3 & 3)

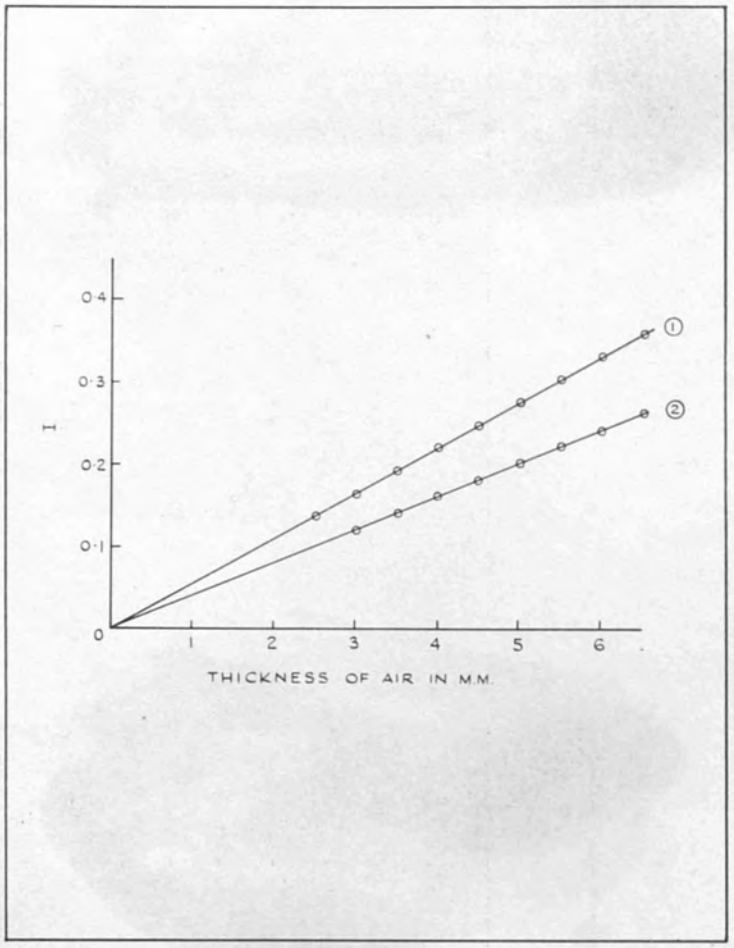

Figure (47)

Ionization - Electrode Spacing Curves.
Electrodes:- Perspex coated with dag.

(1) Effective wavelength = 0.12 A°.
(2) " " = 0.1 A°.

TABLE (60)

200 KV_p. 15 m.a.

1.5 mm. Cu. + 1 mm. Al. (Primary filter)

$\lambda e = 0.12\ A^{\circ}$.

Upper electrode perspex coated with dag.

Air thickness in M.M.	Scale Reading	R´
2.5	9.7	0.135
3.0	20.3	0.1625
3.5	6.5	0.19
4.0	14.6	0.2175
4.5	21.7	0.245
5.0	28.8	0.2725
5.5	36.9	0.300
6.0	44.4	0.3275
6.5	52.0	0.355

The slope of the curve = 0.055

See figure (44) curve (1)

TABLE (61)

220 KV_p. 15 m.a.

2 mm. Cu. + 1 mm. Al. (Primary filter)

$\lambda e = 0.1\ A^{\circ}$.

Upper electrode perspex coated with dag.

Air thickness in M.M.	Scale Reading	R´
3.0	9.5	0.12
3.5	11.5	0.14
4.0	19.5	0.16
4.5	3.8	0.18
5.0	9.8	0.20
5.5	14.9	0.22
6.0	20.5	0.24
6.5	25.5	0.26

The slope of the curve = 0.04

See figure (44) curve (2)

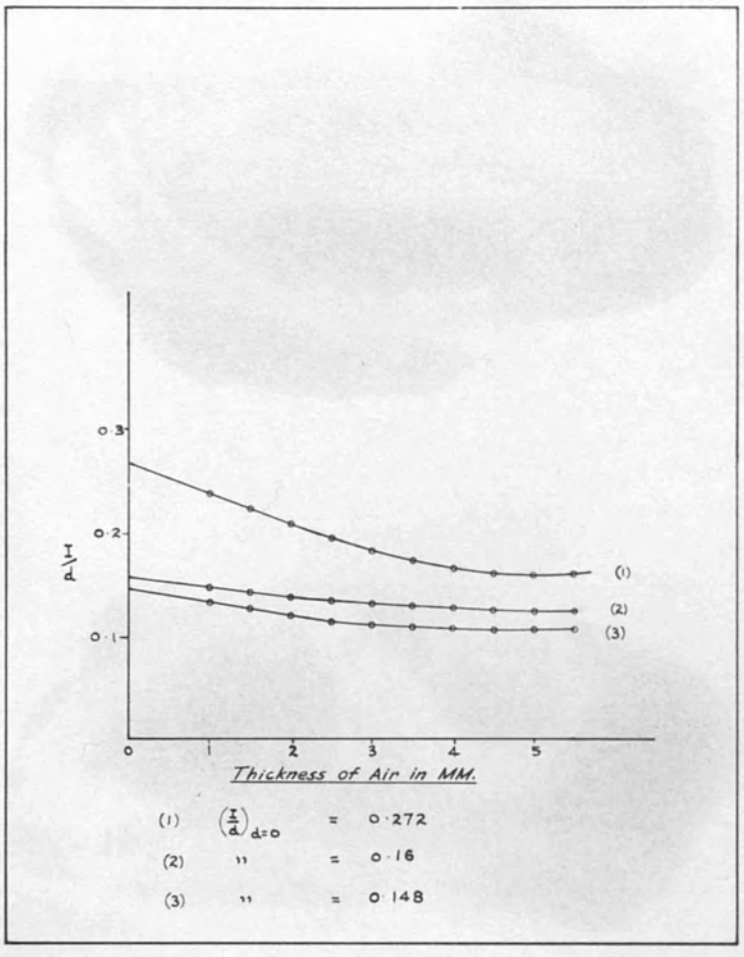

Figure (48).

Ionization per unit spacing - Electrode Spacing Curves.
Electrodes:- Aluminium.

(1) Effective wavelength = 0.172 A°.
(2) " " = 0.12 A°.
(3) " " = 0.1 A°.

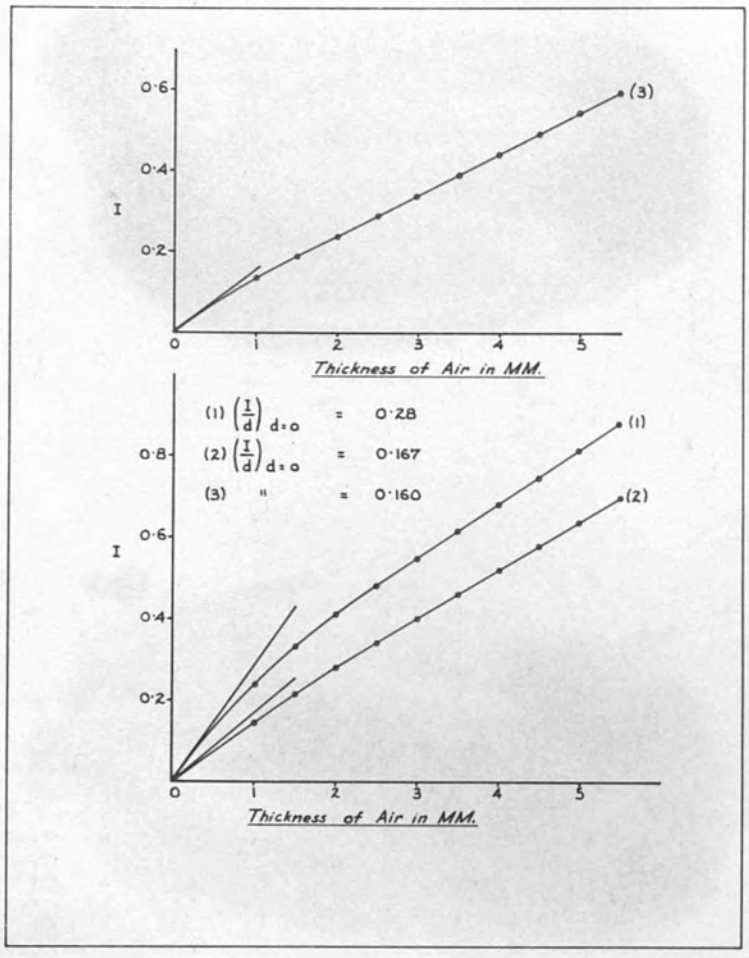

Figure (49).

Ionization - Electrode Spacing Curves.
Electrodes:- Aluminium.

(1) Effective wavelength = 0.172 A°.
(2) " " = 0.120 A°.
(3) " " = 0.1 A°.

TABLE (62)

150 KV_p. 15 m.a.

0.5 mm. Cu + 1 mm. Al.
(Primary filter)

λ_e = 0.172 A^o

Thickness of the upper electrode 0.75 M.M. Al.

Air thickness in M.M.	Scale Reading	I	$\frac{I}{d}$
1.0	20.5	0.24	0.24
1.5	45.0	0.3295	0.219
2.0	69.2	0.4153	0.2076
2.5	92.5	0.4867	0.19468
3.0	22.0	0.5533	0.184
3.5	29.7	0.6193	0.177
4.0	37.2	0.6853	0.171
4.5	45.7	0.750	0.1667
5.0	53.7	0.8150	.16300
5.5	62.5	0.88	0.16

See figures (48 & 49) curves (1 & 1)

TABLE (63)

200 KV_p. 15 m.a.

0.5 mm. Cu + 1 mm. Al.
(Primary filter)

λ_e = 0.12 A^o

Thickness of the upper electrode 0.75 M.M. Al.

Air thickness in M.M.	Scale Reading	I	$\frac{I}{d}$
1.0	15.5	0.15	0.15
1.5	14.7	0.217	0.144
2.0	31.0	0.280	0.140
2.5	47.5	0.341	0.1364
3.0	65.3	0.402	0.134
3.5	84.5	0.463	0.132
4.0	18.7	0.523	0.1307
4.5	25.7	0.583	0.129
5.0	32.0	0.640	0.128
5.5	38.1	0.697	0.126

See figures (48 & 49) curves (2 & 2)

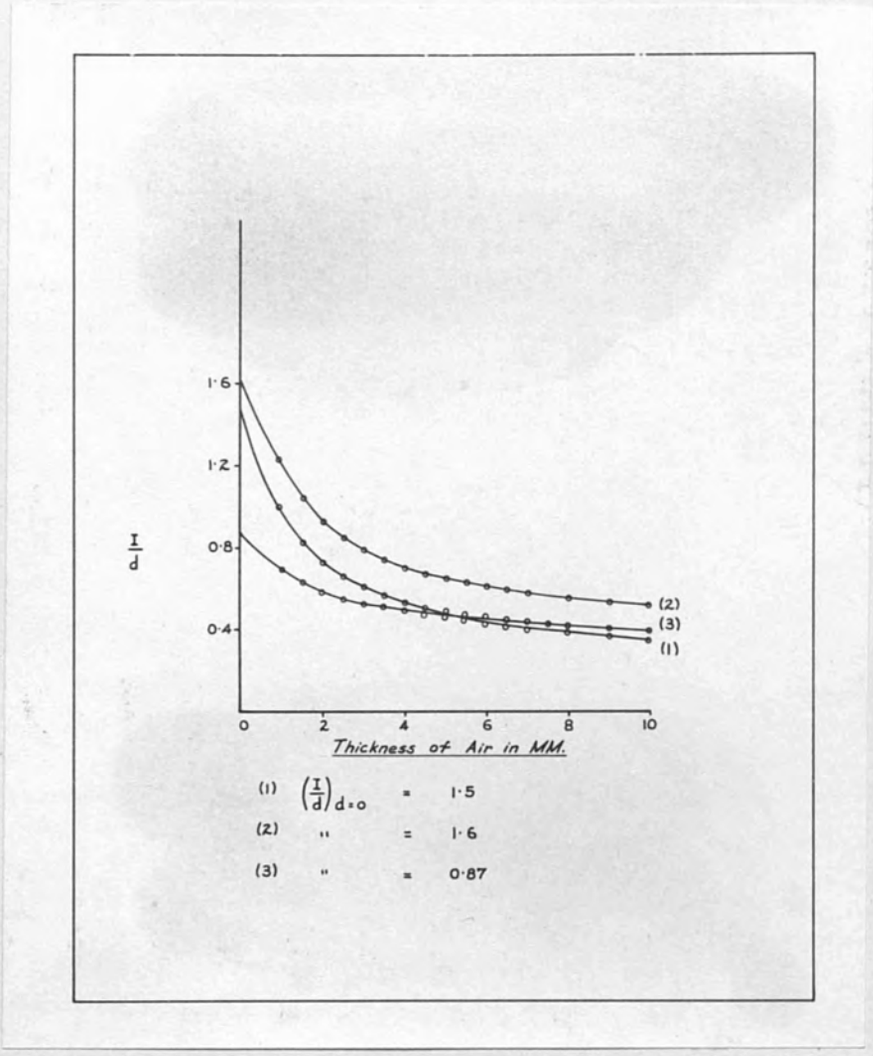

Figure (50).

Ionization per unit spacing - Electrode Spacing Curves.
Electrodes:- Copper.

(1) Effective wavelength = 0.172 A°.
(2) " " = 0.120 A°.
(3) " " = 0.1 A°.

TABLE (64)

220 KVp. 15 m.a.

2 mm. Cu + 1 mm. Al
(Primary filter)

λ_e = 0.1 A°

Thickness of the upper electrode
0.75 M.M. Al.

Air thickness in M.M.	Scale Reading	I	$\frac{I}{d}$
1.0	11.5	0.14	0.14
1.5	6.5	0.19	0.1267
2.0	20.5	0.24	0.12
2.5	34.0	0.29	0.116
3.0	47.5	0.34	0.113
3.5	62.0	0.39	0.111
4.0	9.1	0.44	0.11
4.5	14.9	0.49	0.109
5.0	20.5	0.54	0.108
5.5	27.0	0.59	.107

See figures (48 & 49) curves (3 & 3)

TABLE (65)

150 KVp. 15 m.a.

0.5 mm. Cu + 1 mm. Al.
(Primary filter)

λ_e = 0.172 A°

Thickness of the upper electrode
0.0125 M.M. Copper

Air thickness in M.M.	Scale Reading	$\frac{1}{I}$	I	$\frac{I}{d}$
1.0	76.1	0.9854	1.015	1.015
1.5	53.2	0.81	1.234	0.823
2.0	38.1	0.6933	1.445	0.7225
2.5	28.2	0.6066	1.648	0.6592
3.0	22.1	0.5533	1.807	0.602
3.5	17.0	0.510	1.96	0.56
4.0	12.8	0.4733	2.113	0.528
4.5	9.0	0.4417	2.264	0.503
5.0	69.5	0.4167	2.40	0.48
5.5	63.8	0.3953	2.53	0.46
6.0	58.5	0.3767	2.655	0.444
6.5	53.5	0.36	2.778	0.427
7	49.1	0.345	2.898	0.414
8	42.8	0.322	3.106	0.388
9	37.5	0.303	3.310	0.37
10	32.5	0.285	3.510	0.351

See figures (50 & 22) curves (1 & 2)

TABLE (66)

200 KV_p. 15 m.a.

1.5 mm. Cu + 1 mm. Al. (Primary filter)

λ_e = 0.12 A^o

Thickness of the upper electrode 0.0125 M.M. Copper

Air thickness in M.M.	Scale Reading	$\frac{1}{I}$	I	$\frac{I}{d}$
1.0	50.0	0.7838	1.276	1.276
1.5	32.3	0.6390	1.565	1.043
2.0	20.9	0.5433	1.841	0.9205
2.5	88.1	0.474	2.11	0.844
3.0	72.5	0.4255	2.35	0.783
3.5	60.8	0.386	2.59	0.74
4.0	52.0	0.355	2.817	0.704
4.5	44.9	0.3295	3.035	0.674
5.0	38.1	0.3033	3.248	0.6496
5.5	33.8	0.2896	3.454	0.628
6.0	28.8	0.2725	3.657	0.609
6.5	25.2	0.2590	3.860	0.594
7.0	22.3	0.2462	4.061	0.580
7.5	18.4	0.235	4.255	0.566
8.0	16.2	0.2247	4.45	0.556
9.0	11.5	0.2067	4.838	0.537
10.0	7.1	0.1917	5.217	0.5217

See figures (50 & 40) curves (2 & 1)

TABLE (67)

220 KV_p. 15 m.a.

2 mm. Cu + 1 mm. Al. (Primary filter)

λ_e = 0.1 A^o

Thickness of the upper electrode 0.0125 M.M. Copper

Air thickness in M.M.	Scale Reading	$\frac{1}{I}$	I	$\frac{I}{d}$
1.0	39	-	0.7	0.7
1.5	71.6	-	0.95	0.633
2.0	59.4	0.8547	1.17	0.585
2.5	41.5	0.720	1.389	0.5556
3.0	29.8	0.6234	1.604	0.535
3.5	21.9	0.55	1.818	0.519
4.0	15.5	0.4967	2.013	0.503
4.5	81.2	0.4533	2.2	0.49
5.0	70.5	0.420	2.38	0.476
5.5	62.5	0.3917	2.553	0.464
6.0	55.5	0.367	2.725	0.454
6.5	49.1	0.3458	2.893	0.445
7.0	43.9	0.3267	3.060	0.437
7.5	39.5	0.31	3.225	0.430
8.0	35.5	0.295	3.39	0.424
9.0	28.5	0.27	3.703	0.411
10.0	22.5	0.2487	4.021	0.4021

Monitor factor = $\frac{14}{19}$

See figures (50 & 30) curves (3 & 2)

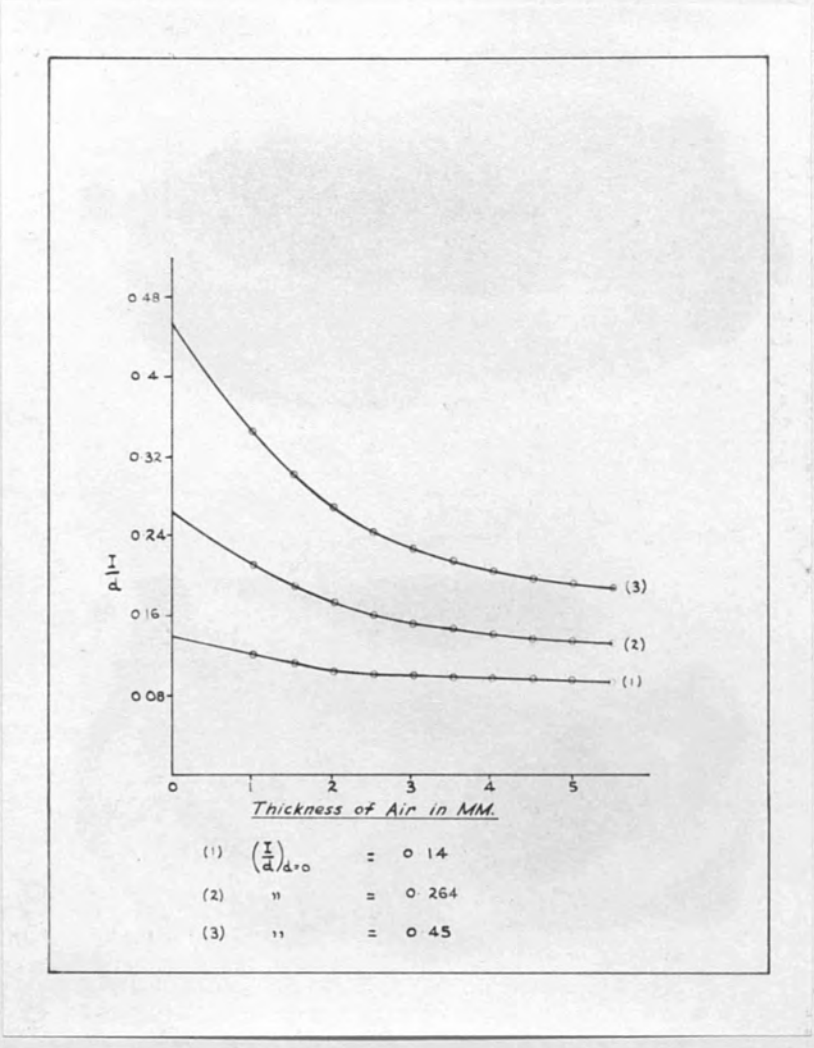

Figure (51).

Ionization per unit spacing - Electrode Spacing Curves.

Effective wavelength = 0.12 A°.

(1) Electrodes:- Pressed mixture of $\frac{Z_2}{Z_1}$ = 12.84.
(2) " " " " $\frac{Z_2}{Z_1}$ = 17.04.
(3) " " " " $\frac{Z_2}{Z_1}$ = 20.84.

TABLE (68)

200 KV_p. 15 m.a.

1.5 mm. Cu + 1 mm. Al
(Primary filter)

λ_e = 0.12 A^o

Thickness of the upper electrode
0.5 M.M. ($\bar{Z}$ = 12.84)

Air thickness in M.M.	Scale Reading	I	$\frac{I}{d}$
1.0	6.3	0.125	0.125
1.5	22.7	0.170	0.113
2.0	13.6	0.215	0.1075
2.5	25.5	0.260	0.104
3.0	37.5	0.303	.101
3.5	49.7	0.347	0.099
4.0	3.3	0.390	0.0975
4.5	7.9	0.433	0.0962
5.0	13.0	0.475	0.0950
5.5	17.8	0.515	0.0936

See figures (51 & 45) curves (1 & 1)

TABLE (69)

200 KV_p. 15 m.a.

1.5 mm. Cu + 1 mm. Al.
(Primary filter)

λ_e = 0.12 A^o

Thickness of the upper electrode
0.5 M.M. ($\bar{Z}$ = 17.04)

Air thickness in M.M.	Scale Reading	I	$\frac{I}{d}$
1.0	46.1	0.216	0.216
1.5	33.3	0.2873	0.1915
2.0	48.7	0.3446	0.1723
2.5	65.0	0.4	0.16
3.0	82.1	0.4567	0.1522
3.5	17.5	0.5133	0.1466
4.0	24.0	0.57	0.142
4.5	30.0	0.624	0.138
5.0	36.3	0.678	0.1356
5.5	42.9	0.730	0.133

See figures (51 & 35) curve (2 & 2)

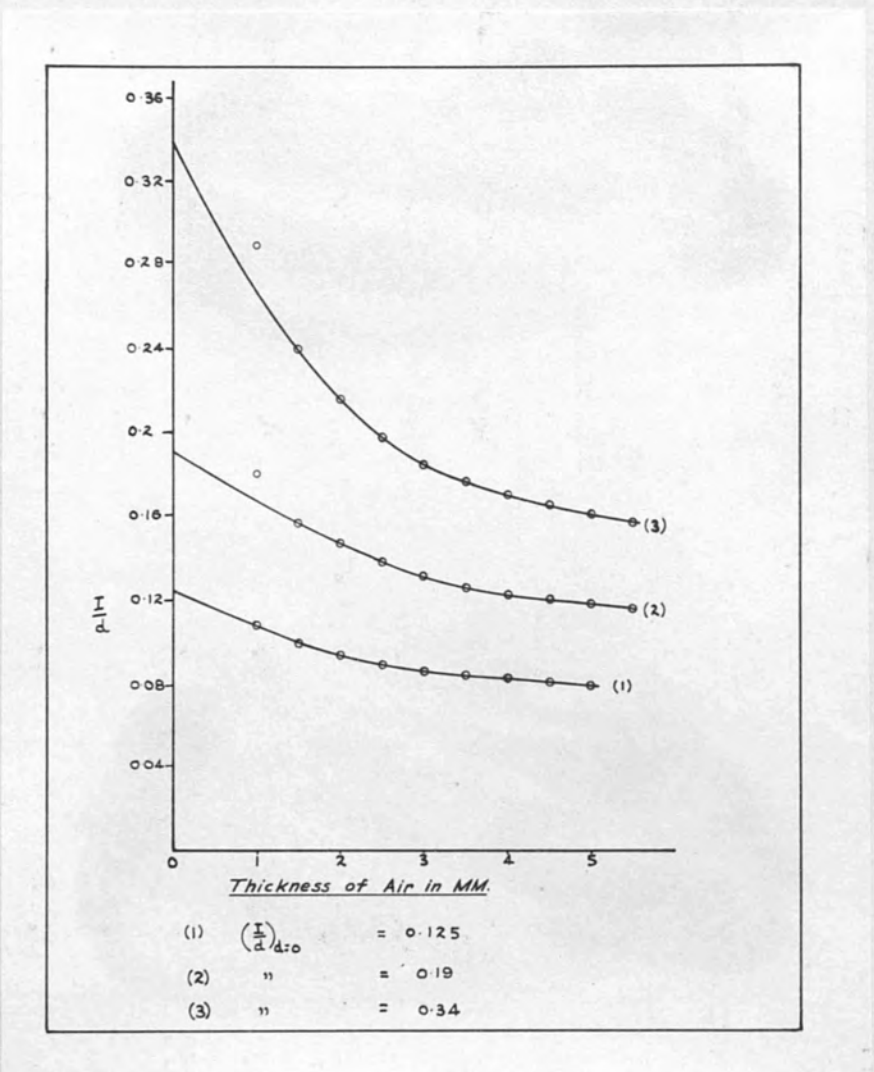

Figure (52).

Ionization per unit spacing - Electrode Spacing Curves.

Effective wavelength = 0.1 A°.

(1) Electrodes:- Pressed mixture of $\frac{Z}{Z}$ = 12.84.
(2) " " " " $\frac{Z}{Z}$ = 17.04.
(3) " " " " $\frac{Z}{Z}$ = 20.84.

TABLE (70)

200 KV_p. 15 m.a.

1.5 mm. Cu + 1 mm. Al.
(Primary filter)

λ_e = 0.12 A^o

Thickness of the upper electrode
0.5 M.M. ($\bar{Z}$ = 20.84)

Air thickness in M.M.	Scale Reading	I	$\frac{I}{d}$
1.0	50.4	0.350	0.350
1.5	10.0	0.448	0.299
2.0	20.1	0.537	0.268
2.5	28.7	0.610	0.244
3.0	37.2	0.6833	0.228
3.5	45.7	0.75	0.214
4.0	54.5	0.82	0.205
4.5	63.5	0.8867	0.197
5.0	72.2	0.953	0.1906
5.5	80.0	1.016	0.185

See figures (51 & 29) curves (3 & 3)

TABLE (71)

220 KV_p. 15 m.a.

2 mm. Cu + 1 mm. Al.
(Primary filter)

λ_e = 0.1 A^o

Thickness of the upper electrode
0.5 M.M. ($\bar{Z}$ = 12.84)

Air thickness in M.M.	Scale Reading	I	$\frac{I}{d}$
1.0	1.0	0.11	0.11
1.5	14.1	0.147	0.098
2.0	28.8	0.185	0.0925
2.5	18.3	0.223	0.0892
3.0	25.0	0.2583	0.0861
3.5	35.3	0.294	0.084
4.0	45.0	0.3295	0.0824
4.5	54.7	0.365	0.081
5.0	65.2	0.40	0.08
5.5	8.1	0.435	0.0790

Monitor factor 0.8

See figures (52 & 45) curves (1 & 3)

TABLE (72)

220 KV_p. 15 m.a.

2 mm. Cu + 1 mm. Al.
(Primary filter)

λ_e = 0.1 A^o

Thickness of the upper electrode
0.5 M.M. ($\bar{Z}$ = 17.04)

Air thickness in M.M.	Scale Reading	I	$\frac{I}{d}$
1.0	5.0	0.18	0.18
1.5	19.7	0.2360	0.157
2.0	33.7	0.2883	0.1441
2.5	47.5	0.340	0.136
3.0	61.9	0.3897	0.1299
3.5	9.1	0.440	0.1257
4.0	15.0	0.490	0.1225
4.5	20.5	0.540	0.12
5.0	26.5	0.590	0.118
5.5	32.3	0.639	0.116

Monitor factor = $\frac{14}{19}$

See figures (52 & 35) curves (2 & 4)

TABLE (73)

220 KV_p. 15 m.a.

2 mm. Cu + 1 mm. Al.
(Primary filter)

λ_e = 0.1 A^o

Thickness of the upper electrode
0.5 M.M. ($\bar{Z}$ = 20.84)

Air thickness in M.M.	Scale Reading	I	$\frac{I}{d}$
1.0	35.3	0.29	0.29
1.5	54.7	0.3650	0.242
2.0	7.6	0.43	0.215
2.5	15.3	0.493	0.1972
3.0	22.3	0.555	0.185
3.5	29.5	0.617	0.176
4.0	36.3	0.678	0.1695
4.5	44.6	0.74	0.164
5.0	52.0	0.80	0.160
5.5	59.8	0.86	0.156

Monitor factor = $\frac{14}{19}$

See figures (52 & 43) curves 3 & 4)

IV. DISCUSSION AND CONCULSIONS

The ionization current produced in the chamber by a certain quality of radiation is due to the following groups of electrons:-

1. The photo and recoil electrons arising from the air in the chamber.
2. The recoil electrons arising from the wall of the chamber.
3. The photoelectrons from the wall of the chamber.
4. The Auger electrons.

Therefore, in an infinitely small cavity in a homogeneous medium placed in a uniform field of X-rays or γ-rays, there is an atmosphere of fast electrons, made up of recoil and photoelectrons from air, recoil and photoelectrons from the wall and Auger electrons.

Since the scattering absorption coefficient per electron ($_e\sigma_a$) for the wall is independent of the nature of the walls, which are also the electrodes, we may conclude that a change in the material of the electrodes will cause a change only in the photoelectron and Auger electron atmosphere (3) and (4).

In the case of photoelectrons two factors affect their number and energy.

(a) The number of photoelectrons increases with atomic number of wall material.

(b) The energy of photoelectrons changes with the quality of incident radiation. (The change is slight for radiations of long wavelengths but rapid for radiations of short wavelengths such as hard X-rays and γ rays.)

In the case of Auger electrons it has been found that [39] the length of the Auger tracks is independent of the wavelength of the incident radiation while it increases as the atomic number increases.

a. <u>The Ionization - Volume Curves</u>.

When the electrodes are of graphite, in every case examined the curves obtained are very closely straight lines indicating that the ionization I_o is proportional to air volume (V) and that graphite is a close approximation to air-wall material,

$$I_o = m_o V \qquad \ldots\ldots (1)$$

The slope of the curve (m_o) in any particularly case thus gives the corresponding value of the ionization per unit volume and this value is independent of the air volume iteslf (See Fig. 17). This is a result already observed in the case of X-rays of 200 kv. by Failla and Quimby (10, 11 & 12).

When the electrodes are of higher atomic number extra ionization is produced in excess of that when the electrodes are air walled. This is produced essentially

by the extra photoelectron emission from the electrodes of higher atomic number. But the amount of extra ionization produced is a function of the electrode psacing.

Considering the previous data, the amount of extra ionization per unit spacing increases with decrease in electrode spacing (Fig. 18), (The increase is slight at large separation but rapid at small separation) and it is because of this dependence of the extra ionization upon chamber dimensions that the observations of previous workers proved difficult to interpret.

b. <u>The Ionization per Unit Spacing as The volume tends to Zero</u> $\left(\frac{I}{d}\right)_{d=o}$

It is evident that at zero spacing the ionization must be zero, but the ionization per unit spacing $\left(\frac{I}{d}\right)$ of air has a definite value even when the air space is vanishingly small.

Therefore, it seems that we may interpret our data, and obtain the $\left(\frac{I}{d}\right)_{d=o}$ values in two ways. For reasons that will be pointed out, both methods have their advantages and disadvantages. For the present purpose, therefore, it has been considered desirable to use both methods and to compare the results obtained by them.

(i) First Method

Firstly, and most simply, we may draw, at the origin, a tangent to the ionization - spacing curve. The slope of this gives a measure of the quantity we need, i.e. $\left(\frac{I}{d}\right)_{d=o}$. This method has the advantage of being most direct, but, unfortunately, it would not seem possible to define the tangent with very great precision because in most cases the ionization is changing so very rapidly with electrode spacing or air volume. We have however, determined the values obtained by this procedure.

(ii) Second Method

Secondly, it is possible, from the original curves (or the tabulated results), to calculate values of ionization per unit spacing corresponding to each separation (or volume used). New curves can now be drawn as shown before which show the variation of ionization per unit spacing with spacing. From these it is seen that as the spacing decreases towards zero so the ionization per unit spacing increases, in some cases very rapidly. Extrapolation of these

curves back to zero spacing (From the minimum spacing used) should lead to the quantity we need, i.e. $\left(\frac{I}{d}\right)_{d=o}$. In fact it aids in two ways.

(a) It gives a reading for the conditions in which an infinitesimal air volume is completely surrounded by the same electrode material.

(b) It eliminates the contribution to the ionization due to particles originating in the air volume.

This method has the disadvantage of being less direct but the advantage that these curves do emphasise one of the points that this work sets out to examine, viz. that if the dimensions of the chamber are made smaller and smaller, the ionization per unit volume will increase steadily towards a limiting value whereas previous observations with rather large non-air wall chambers have not taken this into account.

The extrapolation it is necessary to make is not so accurate a procedure as is desirable chiefly because of the rather large rate of change of ionization per unit volume as the origin is approached*. We have

* The situation would have been easier if some even smaller spacings had been used and in any further work upon these lines this fact should be borne in mind. Our apparatus, conditioned as it was by the use of X-ray machines in a hospital department would hardly have permitted this in any case.

attempted it nevertheless. This fact serves again to emphasise how very small the dimensions of the non-air wall chamber may have to be if the full ionization due to 100 - 220 KV_p. X-rays is to be observed in it.

c. The Absorption Factor (f)

From each experiment with a certain electrode material and certain wavelength of radiation it is possible to plot the results obtained with various thickness of upper electrode and by extrapolation to zero wall thickness, obtain values which should correspond to no absorption in the wall. In some cases, where the absorption was almost linear for the small range of wall thickness used, it was possibly simple to find a correction factor (f) which allowed for the absorption in the thinnest wall used.

d. The Ratio of Ionization between chambers of high atomic Number and Air walled material

Our chief interest centres upon "R", the ratio of the ionizations (as $V \rightarrow o$) for a high atomic number wall and for graphite (an approximately air equivalent wall) for each wavelength.

Now the theoretical considerations (see p. 13) express the ratio of ionization as,

$$R = \frac{J_2}{J_1}$$

Since, for a strictly air wall material,

$$J_1 = \frac{m_o}{A} \quad (\text{i.e. } m_o = \frac{I_o}{d})$$

and,

$$J_2 = \frac{1}{A}\left(\frac{I}{d}\right)_{d=o} \times f \qquad \ldots\ldots \quad (2)$$

where f is the correction for absorption in the thickness of the chamber wall and A is the area of the collecting electrode.

Therefore,

$$R = \frac{\left(\frac{I}{d}\right)_{d=o}}{m_o} \times f \qquad \ldots\ldots \quad (3)$$

Therefore if $\left(\frac{I}{d}\right)_{d=o}$ is known by the two previous methods and also m_o and f the values of R can be deduced in two ways and compared with the calculated values.

It must be noted that the value of R obtained in this manner from the experimental results, is deduced for the limiting condition of zero air volume, and therefore, it should strictly be comparable to the conditions envisaged theoretically, when it is assumed that the air volume is so small as to allow the photo-electrons from the walls to contribute their maximum possible ionization density. In chambers of finite size, as previously used, this condition is never fulfilled.

e. Comparison between Theoretical and Practical Values

In view of the fact that at very short wavelengths, the photoelectric absorption is negligible while the absorption coefficient ${}_e\sigma_a$ is predominant it is legitimate to consider that,

For hard rays $R \longrightarrow 1^*$ ..... (1)
(Theoretical)

It is also known that this is experimentally true. As the wavelength increases τ_e becomes the important factor. Since (according to Walter's formula) this coefficient is proportional to $Z^{2.94}$, we have:

$$R \longrightarrow \frac{Z_2^{2.94}}{Z_1^{2.94}} \quad \text{..... (2)}$$

where Z_1 and Z_2 are the atomic numbers of the air wall and heavy materials respectively.

Therefore the increase of "R" is chiefly according to this relation. Thus we conclude that the amount of increase depends on the values of Z_2.

For longer wavelengths the factor governing the ratio is the absorption in the walls and as in our experiments we extrapolated to zero wall thickness this factor is eliminated.

In the case of cerium mixtures, for wavelengths longer than 0.3 A^o. the photoelectrons from the K shell

*a correction must be made for the stopping power.

are not ejected. This has the effect of causing "R" to decrease. The amount of diminution depends on the amount of cerium in the mixture. Therefore a maximum should be expected in the intermediate region of wavelengths and this maximum should be more pronounced as the amount of cerium in the mixture increases.

The final data obtained for the ionization ratios by following the above procedures are tabulated below (Tables 74, 75, 76, 77, 78 and 79) Tables (75 & 78) show the ratio values obtained by drawing tangents to the curves at the origin, tables (74 & 77) those values obtained by the other method. In tables (76 & 79), the ratio obtained by the two methods are retabulated together with the theoretical values for comparison.

Experimental data 1.

Summary of Results using Method whereby $\frac{I}{d}$ for Simple Elements is Extrapolated to zero volume (i.e. zero spacing)

TABLE (74)

λ_e in A°	(A) $\frac{I}{d}$ for carbon	Al.		Cu.	
		(B) $\left(\frac{I}{d}\right)_{d=o} \times f$	$R_P = \frac{B}{A}$	(B) $\left(\frac{I}{d}\right)_{d=o} \times f$	$R_P = \frac{B}{A}$
0.5	0.8	12.98	16.23	98.51	123.1
0.425	0.6	9.016	15.03	93.63	150.05
0.328	0.11	1.42	12.91	17.7	160.9
0.256	0.035	0.3269	9.34	-	-
0.172	0.06	0.272	4.53	3.253	54.2
0.12	0.055	0.16	2.909	1.6	29.09
0.10	0.04	0.109	2.725	0.6409	16.02

Experimental data II

Summary of Results Using Method Whereby Tangents are drawn at Origin (i.e. zero spacing) of (I - d) curves for Simple Elements.

TABLE (75)

λ_e in A°	(A) $\frac{I}{d}$ for carbon	Al. (B) $\left(\frac{I}{d}\right)_{d=o} \times f$	Al. $R_P = \frac{B}{A}$	Cu. (B) $\left(\frac{I}{d}\right)_{d=o} \times f$	Cu. $R_P = \frac{B}{A}$
0.5	0.8	13.25	16.6	99.49	124.4
0.425	0.6	9.243	15.4	90.93	155.1
0.328	0.11	1.472	13.39	17.92	162.9
0.256	0.035	0.3529	10.08	-	-
0.172	0.06	0.280	4.667	3.253	54.2
0.120	0.055	0.167	3.036	1.7	30.9
0.10	0.04	0.1179	2.94	0.6630	16.58

Experimental Data III

Comparison between Experimental and Theoretical For Simple Elements

TABLE (76)

λ_e in A°	Aluminium			Copper		
	R_T	R_P Extrapol-ation Method	R_P Tangent Method	R_T	R_P Extrapolation Method	R_P Tangent Method
0.5	15.51	16.23	16.6	268.1	123.1	124.4
0.425	14.4	15.03	15.4	265	156.05	155.1
0.328	11.8	12.91	13.39	236.25	160.9	162.9
0.256	8.4	9.34	10.08	-	-	-
0.172	3.9	4.53	4.667	78.75	54.2	54.2
0.120	2.1	2.909	3.036	26.25	29.09	30.9
0.10	1.7	2.725	2.94	15.0	16.02	16.58

Experimental data IV

Summary of Results using Method whereby $\frac{I}{d}$ for Cerium mixtures is Extrapolated to zero volume (i.e. zero spacing).

TABLE (77)

λ_e in A^o	(A) $\frac{I}{d}$ for carbon	$\bar{Z}$ = 12.84		$\bar{Z}$ = 17.04		$\bar{Z}$ = 20.84	
		(B) $\left(\frac{I}{d}\right)_{d=o} \times f$	$R_P = \frac{B}{A}$	(B) $\left(\frac{I}{d}\right)_{d=o} \times f$	$R_P = \frac{B}{A}$	(B) $\left(\frac{I}{d}\right)_{d=o} \times f$	$R_P = \frac{B}{A}$
0.5	0.8	2.438	3.045	4.056	5.070	6.416	8.021
0.425	0.6	1.681	2.802	3.052	5.087	5.064	8.439
0.328	0.11	3.459	3.145	6.087	5.534	9.488	8.626
0.256	0.035	0.13	3.714	2.061	5.887	4.755	13.58
0.172	0.06	0.19	3.166	0.30	5.00	0.64	10.67
0.120	0.055	0.14	2.545	0.264	4.799	0.45	8.181
0.10	0.04	0.100	2.500	0.140	3.50	0.2505	6.26

Experimental data V

Summary of Results using Method whereby Tangents are drawn at Origin (i.e. zero spacing) of (I - d) curves for Cerium Mixtures.

TABLE (78)

λ_e in A^o	(A) $\frac{I}{d}$ for carbon	$\bar{Z}$ = 12.84		$\bar{Z}$ = 17.04		$\bar{Z}$ = 20.84	
		(B) $\left(\frac{I}{d}\right)_{d=o} \times f$	$R_P = \frac{B}{A}$	(B) $\left(\frac{I}{d}\right)_{d=o} \times f$	$R_P = \frac{B}{A}$	(B) $\left(\frac{I}{d}\right)_{d=o} \times f$	$R_P = \frac{B}{A}$
0.5	0.8	2.471	3.088	4.111	5.139	6.416	8.021
0.425	0.6	1.655	2.758	3.052	5.087	4.747	7.912
0.328	0.11	3.563	3.240	6.087	5.534	9.279	8.435
0.256	0.035	0.125	3.572	1.981	5.659	4.755	13.58
0.172	0.06	0.20	3.333	0.30	5.00	0.64	10.67
0.120	0.055	0.150	2.727	0.265	4.817	0.45	8.181
0.10	0.04	0.104	2.60	0.1474	3.684	0.2578	6.445

Experimental Data VI

Comparison between Experimental and Theoretical for Cerium Mixtures

TABLE (79)

λ_e in A°		$\bar{Z}$ = 12.84		$\bar{Z}$ = 17.04			$\bar{Z}$ = 20.84		
	R_T	R_P Extra-polation Method	R_P Tangent Method	R_T	R_P Extra-polation Method	R_P Tangent Method	R_T	R_P Extra-polation Method	R_P Tangent Method
0.5	3.1	3.045	3.088	8.31	5.07	5.139	16.04	8.021	8.021
0.425	3.1	2.802	2.758	8.25	5.087	5.087	15.5	8.439	7.912
0.328	16.0	3.145	3.240	43.25	5.534	5.534	83.5	8.626	8.435
0.256	12.1	3.714	3.572	32.0	5.887	5.659	61.5	13.58	13.58
0.172	5.7	3.166	3.333	14.5	5.00	5.00	24.5	10.67	10.67
0.12	3.0	2.545	2.727	5.75	4.799	4.817	10.0	8.181	8.181
0.10	2.4	2.500	2.6	3.8	3.50	3.684	6.5	6.26	6.445

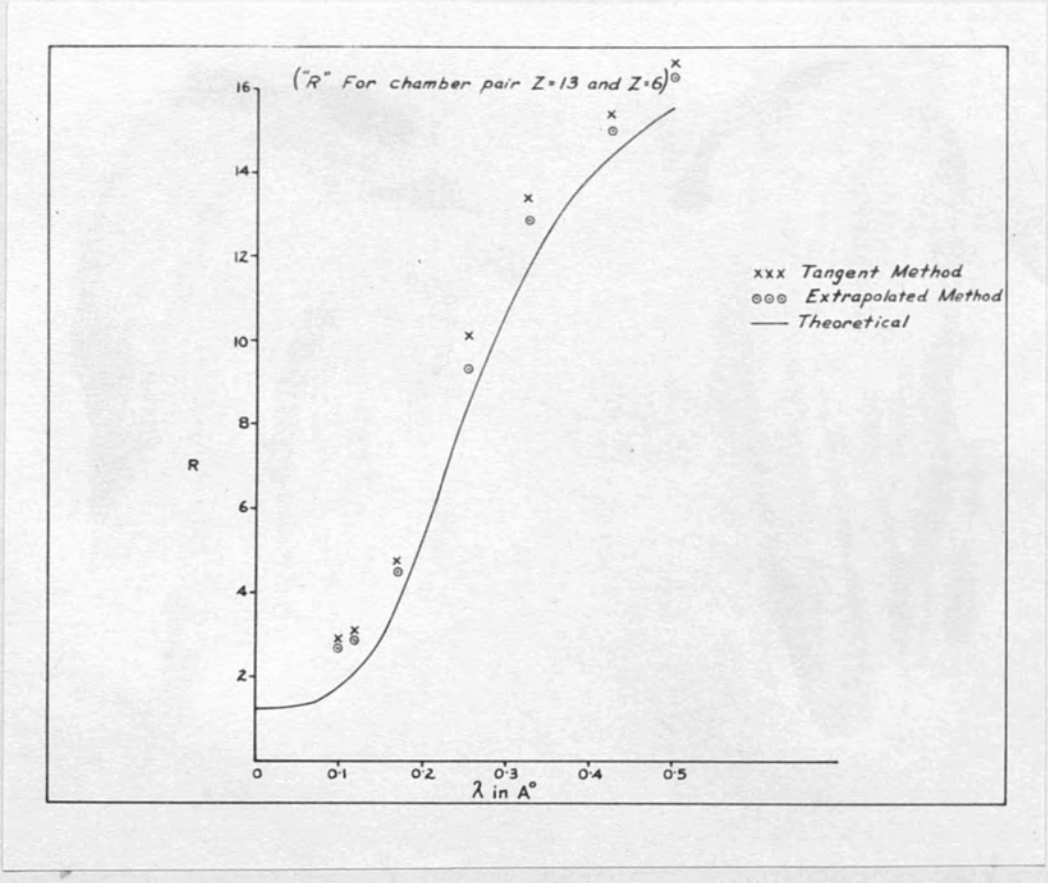
("R" For chamber pair Z=13 and Z=6)
16
14
12
10
8
6
4
2
R
0
0·1
0·2
0·3
0·4
0·5
λ in A°
xxx Tangent Method
⊙⊙⊙ Extrapolated Method
—— Theoretical

Figure (53).

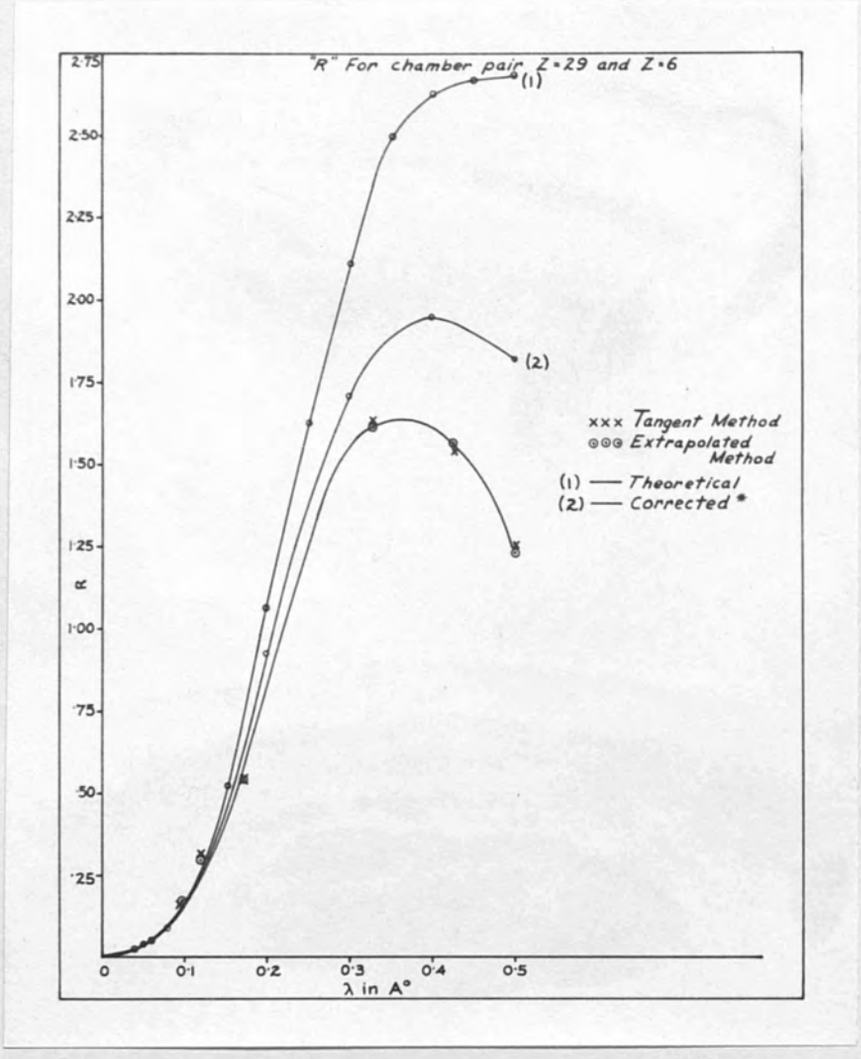

Figure (54).

* See page (126).

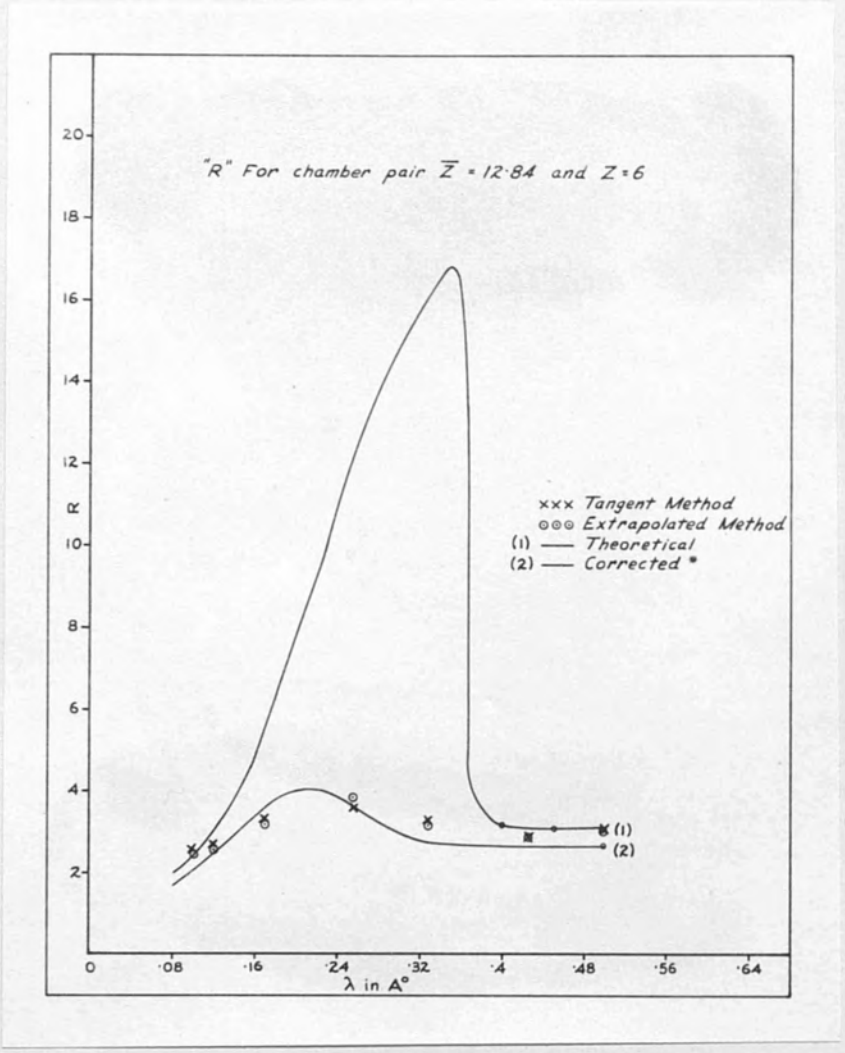

Figure (55).

* See page (126).

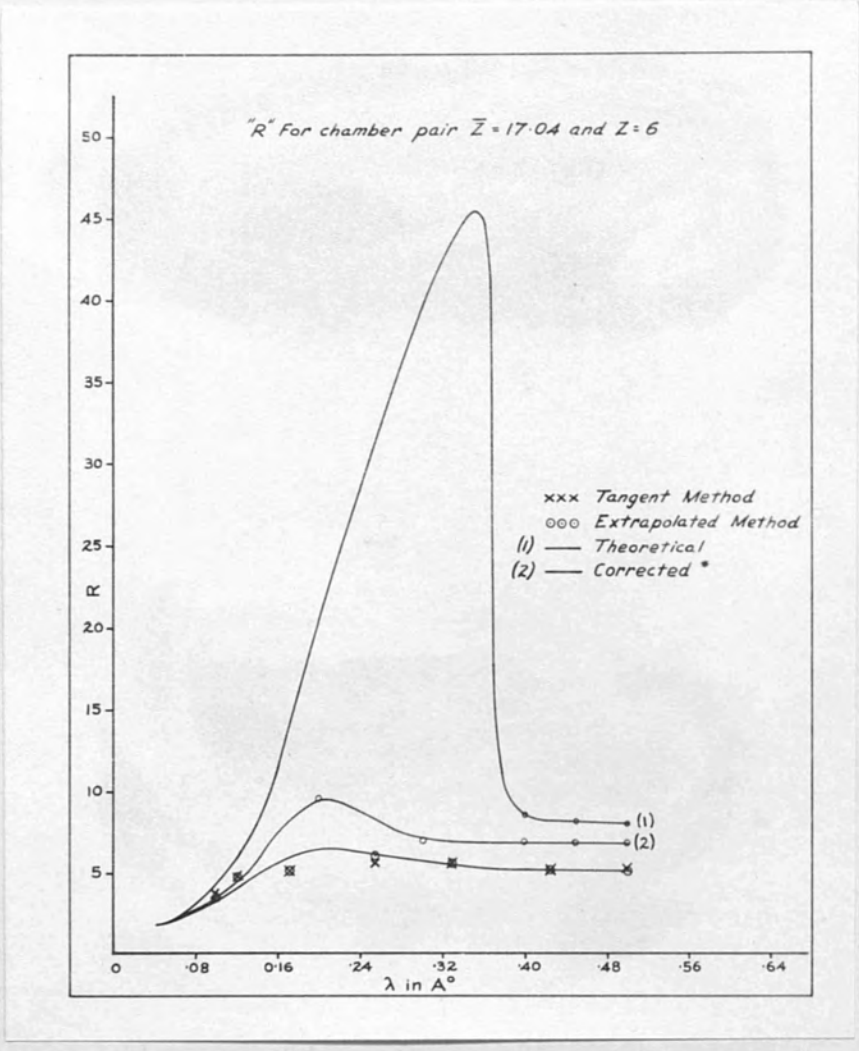

Figure (56).

* See page (126).

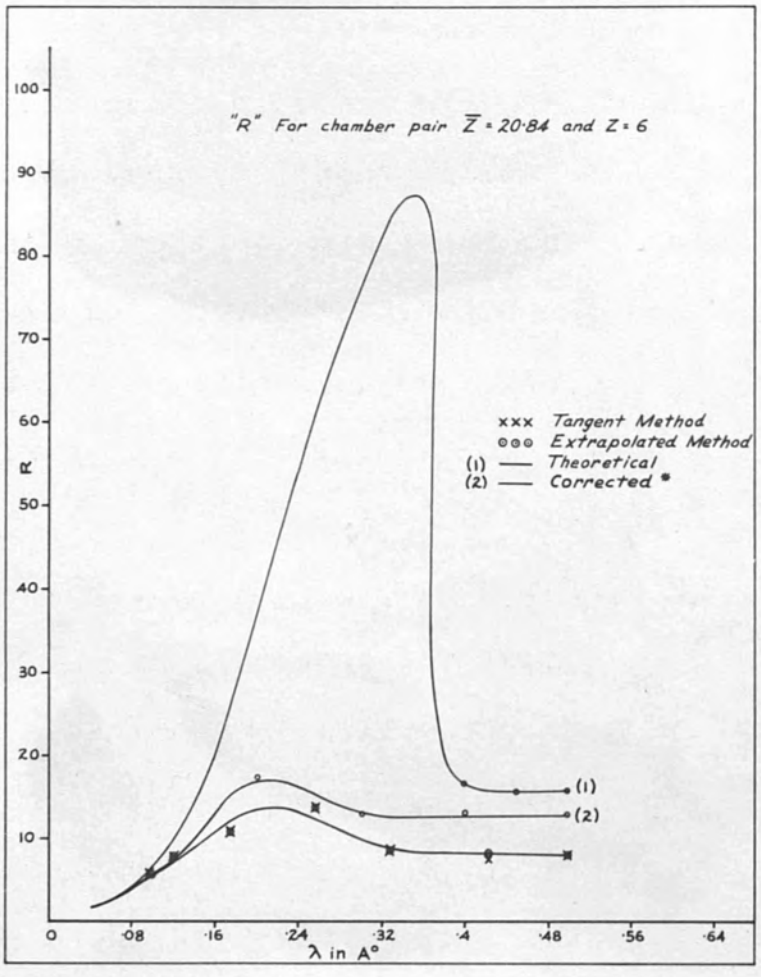

Figure (57).

* See page (126).

From tables (76 & 79) and graphs (53, 54, 55, 56 & 57) we see that for aluminium the experimental results agree approximately* with the theoretical values for qualities ranging from 0.5 A^{o}., to 0.1 A^{o}. In the case of copper a considerable difference between the experimental and theoretical values occurs, especially for longer wavelengths. The theoretical value at 0.5 A^{o}. is two times the experimental value as seen from figure (54). This difference decreases as the wavelength decreases until they seem to agree approximately in the region of 0.12 A^{o} or less.

For cerium mixtures (see fig. 55, 56, & 57) the experimental values are near minimum for short wavelengths, then increase till they attain a maximum at about 0.2 A^{o}., then decrease as the wavelength increases. It is also noticed, as was predicted theoretically, that the values of the maxima vary with the composition of the material to be compared with the air wall chamber. The greatest maximum value of R is for $\bar{Z} = 20.84$ and least for $\bar{Z} = 12.84$. It may be seen also that the right hand branch of the curves is flat but the difference between theory and experiment increases as the atomic number of the mixture increases.

* This may be because we use a spectrum of radiation and not a monochromatic one.

Quantitatively we find considerable differences between the experimental and theoretical values for the pressed mixtures, especially for the longer wavelengths. They seem to agree approximately in all mixtures in the region of 0.08 A°. or less (c.f. Aly and Wilson) and then begin to differ considerably.

Considering our results in general, it appears likely that there is agreement between theory and experiment for walls of elements of atomic number up to about 13, even up to a wavelength of the order of 0.5 A°, In the absence of more data it is not possible to say for what atomic number disagreement first appears i.e. the disagreement here is not sharp. Also, it is probable, particularly in the light of theoretical considerations put forward later, that for materials of different atomic number in this range, disagreement will first occur at different wavelengths. For copper (Z = 29) the theory and experiment agree for a wavelength of about 0.12 A°.

For cerium mixtures, however, the agreement occurs in the region of 0.08 A°. and beyond that the degree of difference increases very rapidly with the increase of wavelength.

The experiments of various workers who have made measurements of the ionization produced by high voltage radiation in ionization chambers having walls of various atomic number, indicate differences between theory and experimental results, the latter being less. In general this difference increased with the increase of wavelength. In most of these experiments the situation was confusing because of the effect of the dimensions of the chambers used and absorption of radiation in the chamber walls. The experimental method used in the present work has attempted to eliminate these factors, but discrepancies still exist between the experimentally observed and theoretically calculated results when the wavelengths used are sufficiently great, and the atomic number of the chamber, or of constituents of the chamber, is sufficiently high.

When the quantum energy of the incident radiation is great compared with the binding energy of the photo-electron removed the theory holds; the discrepancy appears as the binding energy rises or becomes a significant fraction of the quantum energy.

For the range of wavelengths investigated in our

experiments (0.5 A°. to 0.1 A°.) the energies of the incident quanta range from about 25 to 125 eKV. When these quanta act photoelectrically on the material of the copper chamber, resulting quanta of copper K radiation appear which have an energy of about 9 eKV. Thus about 36% to 7% of the energy photoelectrically removed from the primary beam reappears as secondary X - radiation. This radiation may act photoelectrically on another (L or M probably) electron in the same atom to eject it (Auger effect)(40, 41, 42, 43) or may be absorbed in other parts of the chamber.

Also, in the case of cerium mixtures, for wavelengths above 0.35 A°. the K electrons are not ejected and the L radiation has a critical potential of about 5 eKV. Below 0.35 A°. the K electron is ejected having critical potential of about 40 eKV. Thus we expect more energy to be photoelectrically removed in this case and that is probably why the agreement with theory in this case is at a shorter wavelength than in the case of copper.

A point of comparison which is also of interest in this respect is as follows. The bakelite - graphite

mixture loaded with 1.6 per cent cerium oxide is approximately equivalent to aluminium as regards energy absorption but it is not equivalent to it in respect of energy of secondary electron emission (see fig 53 & 55) because the critical voltage for the cerium K electron is about 40 eKV. The photoelectrons from the cerium will thus have much lower energies than those from aluminium. Over the wavelength range 0.1 A°. to 0.3 A°. the cerium K - electrons will be ejected with energies ranging approximately from 80 eKV. to zero, whereas those for aluminium will have nearly the full quantum energies of 120 eKV. - 40 eKV.

Moreover, a discontinuity in the response of the cerium loaded chamber might be expected at $\lambda = 0.34$ A°., the wavelength of the cerium K absorption edge and the curves in fig (55, 56 & 57) show distinct evidence of this effect (see also Spiers) (9)

In addition (44, 45, 46) the photoelectrons are not ejected in the direction of the incident radiation, but at an angle θ to it; the component of range of the electrons in the direction of the radiation is proportional to $\cos\theta$. For higher atomic number θ increases while

$\cos\theta$ decreases and so also the component of the range of the electron. The effect of greatly reduced ranges of the photoelectrons will be to lower the photoelectric contribution to the ionization of the chamber. This point could be studied by varying the angle of incidence of the beam of radiation with respect to the plane walls of the chamber.

Finally, although the surfaces of the electrodes used were clean they were not especially prepared so that we cannot disregard entirely the possible effects of surface conditions on the velocities of the electrons.

These considerations may, to a certain extent, account for the discrepancies between the measured values of the ionization and those calculated simply from the Bragg-Gray theory. These discrepancies have been noticed at all steps of our investigation with various chamber materials (simple elements and cerium mixtures covering the same range of atomic number) and wavelengths ranging from 0.5 A^{o} to 0.1 A^{o}. For elements in the lower range of atomic numbers, certainly up to Z = 13, it would seem that for wavelengths up to at least 0.5 A^{o}., the Bragg-Gray theory leads to results which are quite compatible with

experiment. It should thus be quite satisfactory to use this theory for calculation of the energy absorbed from radiation by media in this range of quality and atomic number. For each higher atomic number it is possible that there is some wavelength below which the theory is still a reliable statement of the facts.

f - Electron Range and Ionization - Electrode - Spacing Curve.

It was thought that a point of interest in this study might be the determination of the mean energy and the mean range in air of the secondary electrons emitted from the walls of the different materials used, since they should be related to the results obtained.

For the determination of the mean range of the electrons it is necessary to know the relative numbers and absolute ranges of photoelectrons and recoil electrons.

i - Relative numbers of Recoil and Photoelectrons

Since one quantum is scattered in the production of each recoil electron and one quantum is involved in each photoelectric emission the proportion of the total

number of electrons which are recoil electrons is given by (47)

$$N_r = \frac{e^{\sigma}}{e^{\tau} + e^{\sigma}} \qquad \ldots\ldots \qquad (1)$$

where e^{σ} is the scattering absorption coefficient and e^{τ} is the photoelectric coefficient.

Also, the relative number of photoelectrons is given by

$$N_p = \frac{e^{\tau}}{e^{\tau} + e^{\sigma}} \qquad \ldots\ldots \qquad (2)$$

This relationship has been tested experimentally for air and found to be correct at least within experimental error (48, 49, 50, 51)

In the case of scattering materials such as carbon and aluminium all the photoelectrons are from the K shell. In the case of heavy scattering elements such as copper and cerium some of the photoelectrons are from the K shell and the others from the L shell. The fraction of the total number of ejected photoelectrons which come from the K shell (52) is,

$$\frac{r_K - 1}{r_K}$$

where r_K is the K absorption jump ratio (53, 54, 55)

Therefore the relative numbers of the photoelectrons which come from the K and L orbit are respectively

$$N_P^K = \frac{e^{\tau}}{e^{\tau} + e^{\sigma}} \frac{r_K - 1}{r_K} \qquad \ldots\ldots \quad (3)$$

and,

$$N_P^L = \frac{e^{\tau}}{e^{\tau} + e^{\sigma}} \frac{1}{r_K} \qquad \ldots\ldots \quad (4)$$

We have calculated the relative numbers of recoil and photoelectrons by this means for the different materials used in our investigation.

It must be remembered that in general the photoelectrons have far greater energies than the recoil electrons and therefore the relatively few photoelectrons which are produced by short wavelength radiation are of more importance in the production of ionization than their numbers would lead one to suppose. The relative energies of the two sets of electrons may be found from the following.

$$\left.\begin{aligned} A_P &= \frac{e^{\tau}}{e^{\sigma_a} + e^{\tau}} \\ \text{and,} \quad A_r &= \frac{e^{\sigma_a}}{e^{\sigma_a} + e^{\tau}} \end{aligned}\right\} \qquad \ldots\ldots \quad (5)$$

where A_P and A_r are the relative energies of the photoelectrons and the recoil electron.

(ii) - The absolute value of the range

The absolute values of the range of the secondary electrons have been calculated using Wilson's data. The values are not very accurate but intended to give an approximate idea of the magnitudes involved. According to Wilson's formula we have

$$\left.\begin{aligned} R_P^K &= \frac{(E_P^K)^2}{440} \\ R_P^L &= \frac{(E_P^L)^2}{440} \\ \text{and,}\quad R_r &= \frac{(E_r)^2}{440} \end{aligned}\right\} \quad \ldots\ldots \quad (6)$$

where R_P^K, R_P^L and R_r are the ranges in air in cm. of the photoelectrons from the K shell, the L shell and the recoil electrons respectively, also,

$$\left.\begin{aligned} E_P^K &= h\,(\nu - \nu_K) \\ E_P^L &= h\,(\nu - \nu_L) \end{aligned}\right\} \quad \ldots\ldots \quad (7)$$

and,

$$E_r = mc^2 \frac{\alpha^2}{1 + 2\alpha}$$

where m is the mass of the electron, c is the velocity of light, h is Planck's constant, ν is the frequency of incident radiation*, ν_K is the critical frequency of the K shell and ν_L is that of the L shell

* We have assumed ν to be that corresponding to the effective frequency of the radiation although, of course, in actual fact, a whole range of ν values are present.

Most of the photoelectrons are ejected at a large angle θ to the direction of the x - ray beam. The length of the path in the forward direction is then proportional to the cosine of this angle. On this basis the previous equations become.

$$\left.\begin{aligned} R_P^K &= \frac{(E_P^K)^2}{440} \cos\theta_K \\ R_P^L &= \frac{(E_P^L)^2}{440} \cos\theta_L \end{aligned}\right\} \quad \ldots\ldots \quad (8)$$

where,(see ref. 40)

$$\left.\begin{aligned} \cos\theta_K &= \frac{1}{c} \sqrt{\frac{h(\nu - \nu_K)}{2m}} \\ \text{and,} \quad \cos\theta_L &= \frac{1}{c} \sqrt{\frac{h(\nu - \nu_L)}{2m}} \end{aligned}\right\} \quad \ldots\ldots \quad (9)$$

(iii)- <u>The mean Range of the electrons in air</u>

The mean energy of the photoelectrons for the materials in our investigation was calculated from the following formula

$$E_P^m = E_P^K \; N_P^K + E_P^L \; N_P^L \quad \ldots\ldots \quad (10)$$

while for recoil electrons

$$E_r^m = E_r N_r \qquad \ldots\ldots \qquad (11)$$

was used.

Thus in the case of graphite or aluminium i.e. materials of low atomic number, the following formula was used for the range of the electrons in air.

$$R_m = \frac{(E_p)^2}{440} N_p \cos\theta + \frac{(E_r)^2}{440} N_r \qquad \ldots\ldots \qquad (12)$$

while for materials of high atomic number.

$$R_m = \frac{(E_p^K)^2}{440} N_p^K \cos\theta_K + \frac{(E_p^L)^2}{440} N_p^L \cos\theta_L + \frac{E_r^2}{440} N_r \qquad (13)$$

The results obtained from these calculations are listed in tables (80, 81 & 82)

TABLE (80)

Relative number and mean energy of electrons originating from mixture of effective atomic number

$\bar{Z} = 7.64$

in λ A°.	E_p	E_r	N_p	N_r	E_p^m	cos θ	R_pN_p	R_rN_r	R_m
0.5	19.86	1.12	0.619	0.381	12.29	0.139	0.0773	0.001	0.078
0.45	22.61	1.345	0.548	0.452	12.39	0.149	0.0945	0.002	0.096
0.40	26.05	1.681	0.464	0.537	12.08	0.16	0.114	0.0034	0.1176
0.35	30.45	2.221	0.372	0.628	11.33	0.173	0.1356	0.007	0.1426
0.30	36.39	2.882	0.278	0.722	10.13	0.189	0.158	0.014	0.1717
0.25	44.76	4.041	0.175	0.825	7.82	0.209	0.166	0.031	0.1965
0.20	57.09	6.064	0.11	0.89	6.275	0.236	0.1924	0.075	0.2672
0.15	77.76	10.12	0.052	0.948	4.071	0.276	0.1986	0.221	0.4192
0.12	98.45	14.91	0.37	0.963	3.616	0.310	0.2511	0.487	0.7378
0.08	150.2	29.32	0.01	0.99	1.477	0.383	0.193	1.934	2.127

TABLE (81)

The mean ranges are calculated in the same manner described before for chambers of effective atomic number as stated.

λ in A°.	R_m in cm. for $\bar{Z} = 12.84$	R_m in cm for $\bar{Z} = 17.04$	R_m in cm for $\bar{Z} = 20.84$
0.5	0.0543	0.099	0.1109
0.45	0.0907	0.1283	0.147
0.40	0.1485	0.1653	0.1968
0.35	0.0472	0.0537	0.0561
0.30	0.072	0.082	0.0916
0.25	0.1283	0.1637	0.18
0.20	0.2503	0.355	0.429
0.15	0.5223	0.804	1.016
0.12	0.8867	1.328	1.781
0.08	2.421	3.149	4.019

TABLE (82)

The mean ranges are calculated in the same manner described before for chambers of simple elements as stated.

λ in A°.	R_m in cm. for graphite.	R_m in cm. for aluminium	R_m in cm. for copper
0.5	0.068	0.163	0.0977
0.45	0.07	0.209	0.139
0.40	0.072	0.261	0.2038
0.35	0.077	0.3322	0.309
0.30	0.08	0.4316	0.5899
0.25	0.098	0.5394	0.8243
0.20	0.1236	0.646	1.507
0.15	0.2328	0.7542	3.308
0.12	0.5053	0.9061	4.969
0.08	1.954	1.954	8.789

TABLE (83)

The threshold electrode - spacing "d" for mixtures and simple element.

λ in A^{o}	"d" in M.M. for Al.	"d" in M.M. for Cu.	"d" in M.M. for $\bar{Z}$ = 12.84	"d" in M.M. for $\bar{Z}$ = 17.04	"d" in M.M. for $\bar{Z}$ = 20.84
0.5	2.5	5.0	1.5	2.0	2.0
0.425	2.5	6.0	1.5	1.5	2.0
0.328	2.75	6.0	3.0	3.5	4.0
0.256	2.5	-	2.0	2.0	2.0
0.172	2.0	6.0	2.0	2.0	2.0
0.12	2.0	4.0	1.5	1.5	1.5
0.1	5.0	4.0	1.0	1.5	1.5

If the character of the Ionization per unit spacing - Electrode spacing curve is to be attributed to the character of the mean ranges of the electrons emitted from the walls the following interpretation might be suitable.

It is evident from the previous data that the rate of change of ionization with spacing is approximately constant up to a certain threshold spacing below which it increases rapidly as the spacing decreases.

With the elements aluminium and copper the threshold spacing appears approximately to decrease with decrease of wavelength, the spacings being very much greater for copper than for aluminium. This possibly may be attributed to the fact that the mean range of electrons increases rapidly at short wavelengths.

In the case of cerium mixtures the threshold spacing decreases with decrease of wavelength, then increases to a pronounced maximum value at 0.328 A^{o}.; with further decrease in wavelength below 0.328 A^{o}. the threshold spacing decreases, this may be due to the fact that the mean range of the electrons increases.

decreases and then increases again as the wavelength of the incident radiation decreases. Also, since about 90% of the mixture is of air wall materials this may be a contributary factor in the occurrence of the threshold spacing at smaller value than for simple elements; as the amount of cerium in the mixture increases the threshold spacing increases.

g. A modification to Gray's Theorem

From the previous results and investigations it seems necessary to modify Gray's equation for the energy absorption in an attempt to correct for the disagreement between theory and practice for materials of high atomic number.

According to Gray (see p. 11 equ. 4.)

$$E_1 = n_1 \left(e^{\sigma_a} + e^{\tau_2}\right) I$$

Since $$I = n\, h\nu$$

where n is the number of incident quanta per second per unit area perpendicular to the beam.

$$\therefore \quad E_1 = n_1\, n\, h \left[e^{\sigma_a \nu} + e^{\tau_2 \nu}\right]$$

In the case of recoil electrons no energy is removed for their ejection because they are free electrons but in the case of photoelectrons a certain energy $h\nu_K$ (where ν_K is the critical frequency of the K shell) is removed in ejecting an electron from its orbit.

$$\therefore \quad E_1 = n_1\, n\, h\nu \left[e^{\sigma_a} + e^{\tau_2} \frac{\nu - \nu_K}{\nu} \quad *\right]$$

and,

$$R = \frac{e^{\sigma_a} + e^{\tau_2} \frac{\nu - \nu_K}{\nu}}{e^{\sigma_a} + e^{\tau_1}} \frac{S_1}{S_2}$$

*In a paper recently published by Gray (56) a correction analogous to this was made to the factor representing the contribution due to pair production.

We have applied this correction and the results of doing this are shown in figs. (54, 55, 56 and 57.)

From figure (55) we see that for cerium mixture of $\bar{Z} = 12.84$ the experimental results approximately agree with the modified theoretical values, this may be due to the fact that the variation of ionization with spacing does not change very rapidly at spacing below 0.5 mm. (the lowest separation used) and the extrapolated value are most reliable.

In the case of copper and of cerium mixtures of $\bar{Z} = 17.04$ and $\bar{Z} = 20.84$ (See fig. 54, 57 & 57) a difference between the modified theory and experiment still exists, this may be attributed to the rapid change of ionization with spacing below 0.5 mm. spacing so that the extrapolated results are possibly not so reliable. The extrapolated values are approximate and this difference may disappear if some smaller spacings could be used to obtain the extrapolated value more accurately.

ACKNOWLEDGMENT

The Author is greatly indebted and wishes to express gratitude:- to Professor H.T. Flint for his general guidance, great interest and advice; to Dr. C.W. Wilson of the physics department, Westminster Hospital (in whose laboratory the work was done) for his suggestion of this field of research, for provision of facilities, for most helpful discussions and interest in this work. The help of Mr. N.H. Pierce and his staff in the construction of the apparatus is also gratefully acknowledged.

REFERENCES.

(1) Bragg, W.H. "Studies in Radioactivity" London: Macmillan 1912.

(2) Gray, L.H. "Proc. Roy. Soc.", A, vol. 122, P.648 (1928)

(3) Mayneord, W.V. "Proc. Roy. Soc.", A, vol. CXXX P.63 (1930)

(4) Clarkson, J.R. & Mayneord, W.V. "Brit. Journ. Rad." vol. XII, No. 135, P.168 (1939)

(5) Wilson, C.W. "Brit. Journ. Rad.", vol. XII, No.136, p. 231 (1939)

(6) Clarkson, J.R. "Phil. Mag." ser. 7, vol XXXI, P.437 (1941)

(7) Aly, M.S. & Wilson, C.W. "Brit. Journ. Rad.", vol XXII No. 257, P. 243 (1949).

(8) British Empire Cancer Campaign, 23rd. Annual Report, P.59 (1946)

(9) Spiers, F.W. "Brit. Journ. Rad." vol XXII, No. 261 P. 521.

(10) Failla, G. "Radiology" vol. 29, No. 2, P. 202 (1937)

(11) Quimby, E.H., Marinelli, L.D., and Farrow, J.H ."Am.J. Reontgenol", 1938, 39, 799 - 815.

(12) Quimby, E.H., and Focht, E.F. "Am. J. Reontgenol" and Rad. Therapy, (1941), 46, 376-399.

(13) Buzau, "Dissertation", Paris (1928)

(14) Eisl., "Ann. physik", vol. 3, P. 227 (1929)

(15) Williams, "Proc. Roy. Soc.", A, vol. 135, P.117 (1932)

(16) Gray, L.H., "Proc. Roy. Soc.", A, vol. 156, P.581 (1936)

(17) Fricke, Glasser. "Amer. Journ. Reont", 138, 453 (1925).

(18) Walter, B. Forts. a.d. Geb. d. Reontgen 35, 929, 1308 (1927).

(19) Wilson, C.W. "Brit. Journ. Rad". vol XVIII No. 215, 344 (1945).

(20) Aly, S.M., "Thesis", London (1948) P. 75.

(21) Chao, C.W. "Nat. Acad. Sci", 16, 431 (1930), Phys Rev. 36, 1519 (1930).

(22) Read, J. & Lauristen, C. "Phys. Rev." 45, 433, (1934)

(23) Cukendall, J.R. "Phys. Rev." 1,105 (1936)

(24) Klein & Nishina "Zeit. phys". 52, 852 (1928)

(25) Siegbain,M. "Physik Zeits", 15, 733, (1914)

(26) Hull, A.W. & Rice, M. "Phys. Rev." 37, 1238 (1931)

(27) Dershem, E.& Skein, M."Phys. Rev". 37, 1238 (1931)

(28) Richtmayer, F.K. "Phys. Rev", XVIII 13, (1921)

Richtmayer, F.K. & Warbuston F.W. "Phys. Rev" VI 539, (1923)

(29) Victoreen, J.A. "Journ. App. phys", 14, No. 295 (1943)

(30) Compton & Allison "x-Rays in theory and experiment" New York (1935)

(31) Madgwick, "Phil. Mag.", vol. 30, P.627 (1915)

(32) Gray, L.H. "Proc. Roy. Soc" A., vol CLVI. P. 578, (1936)

(33) Bethe, "Ann. Physik", vol. 5, P.325 (1930)

(34) Kemp, L.A.W. "Brit. Journ. Rad" vol XIX, No. 222. P.233 (1936.)

(35) Kemp, L.A.W. "Brit. Journ. Rad", vol. XVIII. No. 208, P.1075 (1945).

(36) Lindemann, F.A. and Kerley, T.C. "Phil. Mag" 47, 577 (1924)

(37) Grimmett, L.G. 1 "Proc. Phys. Soc." vol. 45, Part I No. 246 p. 47 (1933)

(38) Greening, J.R. Unpublished work.

(39) Compton, A.H. and Allison, S.K. "x-Rays in theory and experiment" P. 480 D. Van Nostrand Inc, New York (1935)

(40) Auger, P."Compt. rend"180, 65 (1925)

(41) Auger, P."Journal de physique"6, 205 (1925)

(42) Auger, P."Compt. rend." 182, 773, 215 (1926)

(43) Wilson C.T.R.,"Proc. Roy. Soc." 104, 192 (1923)

(44) Compton, A.H. and Allison, S.K. "x-Rays in theory and experiment" P. 574 D. Van Nostrand Inc. New York (1935)

(45) Allgemeine physik der Rontgenstrahlen, Akademische Verlagsgesells chaft, Leipzig (1930)

(46) Compton, A.H. and Allison, S.K. "x-Rays in theory and Experiment" p. 570. D. Van Nostrand Inc. New York (1935)

(47) Mayneord, W.V."Brit. Journ. Rad." Vol II No 20, P. 371 (1929)

(48) Compton, A.H. and Simon A.W."Phys. Rev"25, 309 (1925)

(49) Nuttall, J.M. and Williams E.J."Phil. Mag." 1, 1217 (1926)

(50) Hewlett, C.W."Phys. Rev," 17, 284 (1921)

(51) Compton, A.H. and Allison, S.K. "x-Rays in theory and experiment" pp 212 - 214. D. Van Nostrand Inc. New York (1935).

(52) Compton, A.H. and Allison, S.K. "x-rays in theory and experiment" P. 542. D. Van Nostrand Inc, New York (1935)

(53) Jonson, "Diss. Uppsola"(1928)

(54) Martin and Lang,"Proceeding, Roy. Soc." Lond. A 137, 199 (1931)

(55) Compton, A.H. and Allison, S.K. "x-Rays in theory and experiment P. 538. D. Van Nostrand Inc. New York (1935)

(56) Gray, L.H. "Brit. Journ. Rad.," vol. XXII, No. 264 P. 677 (1949).